Gabriel André Homsi

# Ship routing and speed optimization with heterogeneous fuel consumption profiles

## DISSERTAÇÃO DE MESTRADO

DEPARTAMENTO DE INFORMÁTICA
Programa de Pós-Graduação em Informática

Rio de Janeiro
February 2018

Pontifícia Universidade Católica
do Rio de Janeiro

**Gabriel André Homsi**

# Ship routing and speed optimization with heterogeneous fuel consumption profiles

**Dissertação de Mestrado**

Dissertation presented to the Programa de Pós-Graduação em Informática of the Departamento de Informática, PUC-Rio as partial fulfillment of the requirements for the degree of Mestre em Informática.

Advisor: Prof. Thibaut Victor Gaston Vidal

Rio de Janeiro
February 2018

Pontifícia Universidade Católica
do Rio de Janeiro

**Gabriel André Homsi**

# Ship routing and speed optimization with heterogeneous fuel consumption profiles

Dissertation presented to the Programa de Pós-Graduação em Informática of PUC-Rio in partial fulfillment of the requirements for the degree of Mestre em Informática. Approved by the Undersigned Examination Committee.

**Prof. Thibaut Victor Gaston Vidal**
Advisor
Departamento de Informática — PUC-Rio

**Prof. Rafael Martinelli Pinto**
Departamento de Engenharia Industrial — PUC-Rio

**Prof. Eduardo Uchoa Barboza**
Departamento de Engenharia de Produção — UFF

**Prof. Márcio da Silveira Carvalho**
Vice Dean of Graduate Studies
Centro Técnico Científico — PUC-Rio

Rio de Janeiro, February $8^{th}$, 2018

**Gabriel André Homsi**

Bachelor's in Computer Science at the Rio de Janeiro State University (2016).



Bibliographic data

Homsi, Gabriel André

Ship routing and speed optimization with heterogeneous fuel consumption profiles / Gabriel André Homsi ; advisor: Thibaut Victor Gaston Vidal. — 2018.
67 f. : il. ; 30 cm

Dissertação (Mestrado em Informática)-Pontifícia Universidade Católica do Rio de Janeiro, Rio de Janeiro, 2018.
Inclui bibliografia

1. Informática – Teses. 2. Transportes;. 3. Roteamento de navios;. 4. Meta-heurísticas;. 5. Branch-and-price;. 6. Otimização de velocidade;. 7. Otimização convexa;. I. Vidal, Thibaut Victor Gaston. II. Pontifícia Universidade Católica do Rio de Janeiro. Departamento de Informática. III. Título.

CDD: 004

## Acknowledgments



I devote this space to acknowledge the big influence that the following teachers had on my computer science career: Thibaut Vidal, Rafael Martinelli, Ricardo Costa, and Daniel Fleischman.

This research project was made possible thanks to funds provided by CNPq and CAPES.

## Abstract

Homsi, Gabriel André; Vidal, Thibaut Victor Gaston (advisor). **Ship routing and speed optimization with heterogeneous fuel consumption profiles**. Rio de Janeiro, 2018. 67p. Dissertação de Mestrado — Departamento de Informática, Pontifícia Universidade Católica do Rio de Janeiro.

The shipping industry is essential for international trade. However, in the wake of the 2008 financial crisis, this industry was severely hit. In these times, transportation companies can only obtain profit if their fleet is routed effectively. In this work, we study a class of ship routing problems related to the Pickup and Delivery Problem with Time Windows. To solve these problems, we introduce a heuristic and an exact method. The heuristic method is a hybrid metaheuristic with a set-partitioning-based large neighborhood, while the exact method is a branch-and-price algorithm. We conduct experiments on a benchmark suite based on real-life shipping segments. The results obtained show that our algorithms largely outperform the state-of-the-art methodologies. Next, we adapt the benchmark suite to model a ship routing problem where the speed on each sailing leg is a decision variable, and fuel consumption per time unit is a convex function of the ship speed and payload. To solve this new ship routing problem with speed optimization, we extend our metaheuristic to find optimal speed decisions on every local search move evaluation. Our computational experiments demonstrate that such approach can be highly profitable, with only a moderate increase in computational effort.



## Keywords

Transportation; Ship routing; Metaheuristics; Branch-and-price; Speed optimization; Convex optimization;

## Resumo

Homsi, Gabriel André; Vidal, Thibaut Victor Gaston. **Roteamento de navios e otimização de velocidade com perfis de consumo de combustível heterogêneos**. Rio de Janeiro, 2018. 67p. Dissertação de Mestrado — Departamento de Informática, Pontifícia Universidade Católica do Rio de Janeiro.

A indústria de transporte marítimo é essencial para o comércio internacional. No entanto, no despertar da crise financeira de 2008, essa indústria foi severamente atingida. Nessas ocasiões, empresas de transporte só são capazes de obter lucro se suas frotas forem roteadas de forma eficaz. Neste trabalho, nós estudamos uma classe de problemas de roteamento de navios relacionados ao *Pickup and Delivery Problem with Time Windows*. Para resolver esses problemas, nós introduzimos um método heurístico e um exato. O método heurístico é uma meta-heurística híbrida com uma vizinhança larga baseada em *set partitioning*, enquanto o método exato é um algoritmo de *branch-and-price*. Nós conduzimos experimentos em um conjunto de instâncias baseadas em rotas de navios reais. Os resultados obtidos mostram que nossos algoritmos superam as metodologias estado da arte. Em seguida, nós adaptamos o conjunto de instâncias para modelar um problema de roteamento de navios no qual a velocidade em cada segmento de rota é uma variável de decisão, e o consumo de combustível por unidade de tempo é uma função convexa da velocidade e carga do navio. A fim de resolver esse novo problema de roteamento de navios com otimização de velocidade, nós estendemos nossa meta-heurística para encontrar decisões de velocidade ótimas em toda avaliação de solução vizinha de uma busca local. Nossos experimentos demonstram que essa abordagem pode ser altamente rentável, e que requer apenas um aumento moderado de recursos computacionais.



## Palavras-chave

Transportes; Roteamento de navios; Meta-heurísticas; Branch-and-price; Otimização de velocidade; Otimização convexa;

# Contents

# List of Figures

# List of Tables

# 1
# Introduction

International trade depends heavily on ship transportation, as it is the only cost-effective mode of transportation of large volumes over long distances. It is common to distinguish between three main modes of operation in maritime transportation: liner, industrial, and tramp shipping. Liner shipping, which includes container shipping, has similarities to a bus service: fixed schedules and itineraries must be followed. In industrial shipping, the operator owns the cargoes and controls the fleet, trying to minimize the cost of transporting all its cargoes. Finally, a tramp shipping operator follows the availability of cargoes in the market, often transporting a mix of mandatory and optional cargoes with the goal of maximizing profit.

In this work, we focus on heuristic and exact methodologies for a class of Industrial and Tramp Ship Routing and Scheduling Problems (ITSRSPs), along with problem extensions where the sailing speed of ships is a decision variable and the fuel consumption is a convex function of speed and payload. In this class of problems, a shipping company has a mix of mandatory and optional cargoes for transportation. Each cargo in the given planning period must be picked up at its given loading port within a specified time window, transported, and then delivered at its corresponding unloading port, also within a given time window. The shipping company controls a heterogeneous fleet of ships to transport the cargoes, each ship with a given initial position and time for when it becomes available for new transportation tasks. Compatibility constraints between ships and cargoes may restrict which cargoes a ship can transport (e.g. due to draft limits in the ports). The shipping company sometimes also has the possibility to charter ships from the spot market to transport some of the cargoes. The planning objective in the ITSRSP is to construct routes and schedules, decide which spot cargoes to transport and which cargoes to be transported by a spot charter, so that all mandatory cargoes are transported while maximizing profit or minimizing costs. The ITSRSP extends the Pickup and Delivery Problem with Time Windows (PDPTW) with a heterogeneous fleet, compatibility constraints, different ship starting points and starting times, and service flexibility with penalties. The interplay of these complex attributes requires to jointly optimize multiple

decision sets.

These problems typically arise in the shipping of bulk products, such as crude oil, chemicals and oil products (wet bulk), and iron ore, grain, coal, bauxite, alumina and phosphate rock (dry bulk). In 2016, these product types constituted more than 60% of the weight transported in international seaborne trade. Yet, in the wake of the financial crisis in 2008, the freight rates in the dry bulk shipping segment dropped dramatically: the Baltic Dry Index dropped more than 80%, remained low since then, and experienced record lows in 2016. Additionally, for the fifth year in a row, world fleet growth has been decelerating. Despite this decline, the supply of shipping capacity still increased faster than demand, leading to a continued situation of shipping overcapacity and downward pressure on freight rates (UNCTAD, 2017). In such times, a shipping company can only obtain profit if its fleet is routed effectively.

This work is organized as follows: in Chapter 2, a formal statement is given for the ITSRSP and its extension, the Industrial and Tramp Ship Routing and Scheduling Problem with Speed Optimization (ITSRSPSO). A literature review is conducted in Chapter 3. The solution methodologies for the ITSRSP are studied in Chapter 4, and the solution methodologies for the ITSRSPSO are studied in Chapter 5. Final remarks are presented in Chapter 6.

# 2
# Problem Statement

We now provide a formal definition for the ITSRSP and its extension, the ITSRSPSO.

## 2.1
## The ITSRSP

The ITSRSP is defined on a complete graph $G = (V, A)$, where $V$ is the union of a set of pickup nodes $P = \{1, \ldots, n\}$, delivery nodes $D = \{n + 1, \ldots 2n\}$, and starting locations $\{0_1, \ldots, 0_m\}$. A tramp or industrial shipping operator owns a fleet of $m$ ships, and $n$ cargoes are available for transportation. Each cargo $i \in \{1, \ldots, n\}$ is characterized by a load $q_i$ and must be transported from a pickup $i \in P$ to a corresponding delivery location $n + i \in D$. Therefore, $q_i \geq 0$ for $i \in P$, and $q_i = -q_{n+i}$. Every node $i \in P \cup D$ is associated with a time window of allowable visit times $[a_i, b_i]$. Each ship $k \in \{1, \ldots, m\}$ becomes available at a time $s^{\mathrm{D}}_{0k}$, at a location $0_k$. It has a capacity $Q_k$ and can traverse any arc $(i, j) \in A$ for a cost $c^k_{ij}$ (counting fuel and canal costs) and duration $\delta^k_{ij}$. For every ship $k$ and node $i \in P \cup D$, there is an associated port service cost $s^{\mathrm{C}}_{ik} \geq 0$ and duration $s^{\mathrm{D}}_{ik} \geq 0$. There might be incompatibilities between ships and cargoes (e.g. due to draft limits in the ports). For each $i$ and $k$, the boolean $I_{ik}$ defines whether cargo $i$ can be serviced by ship $k$. Finally, a penalty $s^{\mathrm{C}}_{i0}$ is paid if a cargo $i$ is not transported by the fleet. This penalty corresponds either to the associated charter price, or the loss revenue due to not transporting an optional cargo.

The objective of ITSRSP is to form routes that minimize the sum of total travel cost and possible penalties in the case where charter ships are used or some cargoes are not transported. The routes begin at their respective starting points but have no specified endpoint, as ships operate around the clock. Every route must be feasible: ships cannot exceed their capacity, cargoes should be serviced only within their prescribed time windows, and ships cannot transport incompatible cargoes. Furthermore, routes must respect pairing and precedence constraints. The pairing constraint states that any pair $(i \in P, n+i \in D)$ must belong to the same route, and the precedence constraint states that any pickup $i \in P$ must be serviced before its delivery $n + i \in D$.

**Set partitioning formulation.** A simple Set Partitioning (SP) formulation of the ITSRSP is given in Eqs. (2-1) to (2-5). Let $\Omega_k$ be the set of all feasible routes for ship $k \in \{1, \ldots, m\}$. This formulation uses a binary variable $\lambda_r^k \in \Omega_k$ to indicate whether route $r$ of vehicle $k$ is used or not in the current solution for a cost of $c_r^k$. Moreover, $a_{ri}^k$ is a binary constant valued to 1 if and only if the route $r$ of ship $k$ transports cargo $i$, and 0 otherwise. Each variable $y_i$ is valued to 1 if and only if the cargo $i$ is allowed to be transported by a charter instead of being included in a route.

$$\text{Minimize} \quad \sum_{k=1}^{m} \sum_{r \in \Omega_k} c_r^k \lambda_r^k + \sum_{i \in P} s_{i0}^{\mathrm{C}} y_i \tag{2-1}$$

$$\text{subject to} \quad \sum_{r \in \Omega_k} \lambda_r^k \leq 1 \qquad k = \{1, \ldots, m\} \tag{2-2}$$

$$\sum_{k=1}^{m} \sum_{r \in \Omega_k} a_{ri}^k \lambda_r^k + y_i = 1 \qquad i \in \{1, \ldots, n\} \tag{2-3}$$

$$\lambda_r^k \in \{0, 1\} \qquad k = \{1, \ldots, m\}, r \in \Omega_k \tag{2-4}$$

$$y_i \in \{0, 1\} \qquad i \in \{1, \ldots, n\}. \tag{2-5}$$

Objective (2-1) minimizes routing and charter costs. Constraint (2-2) ensures that each ship is used at most once, and Constraint (2-3) guarantees that each cargo is either transported in a route or chartered. This formulation clearly contains an exponential number of variables due to the definition of the sets $\Omega_k$. To circumvent this issue, it is necessary to use heuristics such as the Hybrid Genetic Search (HGS), presented in Section 4.1, or exact methods such as the Branch-and-Price (B&P), presented in Section 4.2. Moreover, the SP formulation can also be used inside the HGS to find new high-quality solutions, as we explain in Section 4.1.5.

## 2.2 The ITSRSPSO

The ITSRSPSO is an extension of the ITSRSP where sailing speeds are a decision variable, and travel costs depend on the ship sailing speed and payload. A ship $k \in \{1, \ldots, m\}$ can traverse an arc $(i, j)^k \in A$ at any speed $v$ (in knots) within a feasible range $[v_{\min}^k, v_{\max}^k]$, for a cost of $F_c f_{ij}^k(v, w)$. The fuel cost per tonne is represented as $F_c$, $w$ is the proportion of maximum load on board the ship before arriving node $j$, and $f_{ij}^k(v, w)$ is the amount of fuel (in tonnes) consumed. The objective of the ITSRSPSO remains the same as the ITSRSP objective.

# 3
# Literature Review

Early studies about ship routing and scheduling optimization date back from the 1970-80s. In a seminar study, Ronen (1983) discusses the differences between classical vehicle routing and ship routing and lists possible explanations for the scarcity of the research at the time. The author also provides a comprehensive classification scheme for various types of ship routing and scheduling problems. Since the inception of this article, research on ship routing has flourished, as highlighted by the general survey about maritime transportation by Christiansen et al. (2007), as well as dedicated recent reviews on routing and scheduling by Christiansen et al. (2013), and Christiansen & Fagerholt (2014).

Many variations of ship routing and scheduling problems have been formulated and investigated, and these problems have generally grown in richness, complexity and accuracy over the years. To name a few, Brown et al. (1987) introduced an elastic SP model to solve a full-shipload routing and scheduling problem for a fleet of crude oil tankers. Fagerholt & Christiansen (2000*b*) proposed a dynamic programming algorithm to solve a traveling salesman problem with applications to ship scheduling subproblems. The same algorithm was later exploited by Fagerholt & Christiansen (2000*a*) to solve subproblems for a multi-ship PDPTW. A maritime PDPTW with split loads was studied by Andersson et al. (2011). The authors proposed two alternative path-flow models and an exact algorithm that generates single ship schedules a priori. Vilhelmsen et al. (2014) presented a solution method based on Column Generation (CG) to solve a tramp ship routing and scheduling problem with integrated bunker optimization.

Heuristics and metaheuristics were also applied to solve several variants of ship routing problems. Some notable examples are the multi-start local search of Brønmo et al. (2007), the unified tabu search of Korsvik et al. (2009), the large neighborhood searches of Korsvik et al. (2011) and Hemmati et al. (2014), and the HGS of Borthen et al. (2017). In the latter article, hybrid genetic algorithms were used with great success to solve a multi-period supply vessel planning problem for offshore installations. Beyond this, the Unified Hybrid Genetic Search (UHGS) methodology of Vidal et al. (2012, 2014) has led to

highly accurate solutions for a considerable number of Vehicle Routing Problem (VRP) variants, including the classical Capacitated Vehicle Routing Problem (CVRP), the Vehicle Routing Problem with Time Windows (VRPTW) (Vidal et al., 2013), several prize-collecting VRPs with profits and service selections (Vidal et al., 2016; Bulhões et al., 2018), among others. Nevertheless, this methodology has neither been extended to this date to heterogeneous fixed fleet problems, nor to pickup-and-delivery problem variants, due to the necessity of designing drastically different neighborhood search operators and ensuring proper precedence and pairing between pickups and deliveries in the crossover and split operators.

A set of publicly available benchmark instances for ITSRSPs is proposed by Hemmati et al. (2014). The authors propose a mixed-integer programming model and an Adaptive Large Neighborhood Search (ALNS) metaheuristic to solve these instances. Later, Hemmati & Hvattum (2016) evaluated the effect of randomization of ALNS components on the same benchmark instances.

The effect of oil price on the optimal speed of ships was studied by Ronen (1982). The author discussed how changes in price may lead to different routing patterns (e.g. *slow steaming*). Different speed models were surveyed by Psaraftis & Kontovas (2013). A shortest path algorithm with discretized port arrival times was introduced by Fagerholt et al. (2010) to optimize the speed of fixed shipping routes. Later, an $\mathcal{O}(n^2)$ Recursive Smoothing Algorithm (RSA) was proposed by (Norstad et al., 2011) to solve the Speed Optimization Problem (SOP) inside every move evaluation of a multi-start local search heuristic for an ITSRSPSO. However, the RSA usage is limited, as it only works if the fuel consumption functions are the same for all sailing legs. Hence, it cannot be used when fuel consumption also depends on the ship payload. Wang & Meng (2012) used piecewise linear functions to approximate a fuel consumption function on a mixed-integer nonlinear programming model. Wen et al. (2016) studied a full shipload problem with load-dependent fuel consumption and proposed a three-index mixed-integer linear programming formulation and a set packing formulation for a B&P algorithm. Fukasawa et al. (2016) adapted the ITSRSP benchmark instances of Hemmati & Hvattum (2016) and proposed a SP formulation and a branch-and-cut-and-price algorithm to solve a joint routing and speed optimization problem.

# 4
# Hybrid and Exact methods for the ITSRSP

In a recent study, Hemmati et al. (2014) have defined a broad class of ship routing and scheduling problems, and made available a benchmark suite based on real shipping segments. Due to their combination of size, variety of decision sets and constraints, the instances obtained from this suite pose considerable challenges for heuristic and exact methods. To solve these problems, we introduce a hybrid metaheuristic and an exact branch-and-price algorithm.

## 4.1
## Hybrid Genetic Search



To solve the Industrial and Tramp Ship Routing and Scheduling Problem (ITSRSP), we propose a Hybrid Genetic Search (HGS), a non-trivial extension of the Unified Hybrid Genetic Search (UHGS) of Vidal et al. (2014). The proposed HGS includes a set-partitioning-based large neighborhood and uses problem-tailored crossover and local search operators to cover multiple ITSRSP attributes which were not included in the original framework. Being a hybrid metaheuristic, the HGS combines the exploration capabilities of genetic algorithms with efficient local search improvement procedures. Several components of the HGS ensure a balance between solution quality and population diversity, and the local search procedure also employs granular search techniques to reduce the size of the neighborhoods. Similar heuristics were widely used to successfully solve many vehicle routing problem variants (Vidal et al., 2012, 2013, 2014; Borthen et al., 2017).

The behavior of the HGS is summarized in Algorithm 4.1.1. The HGS jointly evolves a feasible and an infeasible subpopulation. At each iteration, two parents are selected. A crossover operator is applied to these parents, generating a new offspring. This offspring is improved with local search and inserted into a subpopulation, according to its feasibility. If the offspring is infeasible, a repair procedure is executed on a copy of it aiming to reach feasibility, finally inserting the resulting offspring into its subpopulation. Whenever a subpopulation reaches a maximum size, survivor selection removes individuals according to their fitness. If no improving solution is found after

a fixed number of iterations, new individuals are added to the population in order to diversify it. Penalty coefficients are periodically adjusted to control the proportion of feasible individuals generated.

**Algorithm 4.1.1:** HGS

```
Initialize population;
while number of iterations without improvement < It_NI and
 time < T_max do
    Select parent solutions P_1 and P_2;
    Generate offspring C from P_1 and P_2 (crossover);
    Educate offspring C (local search);
    Insert C into respective subpopulation;
    if C is infeasible then
        With probability p_rep, repair C (local search) and
        insert it into respective subpopulation;
    end
    if maximum subpopulation size reached then
        Select survivors;
    end
    if best solution not improved for It_DIV iterations then
        Diversify population;
    end
    if best solution not improved for It_SP iterations then
        Run set partitioning;
    end
    Adjust penalty coefficients for infeasibility;
end
Return best feasible solution;
```



### 4.1.1 Search space

The search space of the HGS includes penalized infeasible solutions. Previous work demonstrates that the use of penalized infeasible solutions enhances the search towards high-quality feasible solutions (Glover & Hao, 2009; Vidal et al., 2015*a*). A solution is infeasible if either (a) the current load of a ship exceeds its capacity at any point in the route, (b) some cargoes are not picked up or delivered within their respective time windows, or (c) a ship transports incompatible cargoes. Infeasibility (a) is penalized according to the excess of peak load in the trip. To allow time window infeasible solutions, we use the approach of Nagata et al. (2010) where time precedence constraints are relaxed. Then, the infeasibility (b) penalty is proportional to the amount of returns in time in the trip. Finally, infeasibility (c) is penalized according to the number of incompatible cargoes in the trip. No component of the HGS

allows solutions that break precedence and pairing constraints. A route $r$ with ship $k$ is characterized with:

$$\textit{Travel cost: } C_k(r) = \sum_{i=1}^{|r|-1} (c^k_{r_i,r_{i+1}} + s^{\mathrm{C}}_{r_i}) \tag{4-1}$$

$$\textit{Peak load: } Q^{\max}_k(r) = \max_{1\le i\le j\le |r|} \sum_{l=i}^{j} q_{r_l} \tag{4-2}$$

$$\textit{Time warp use: } TW_k(r) = \sum_{i=2}^{|r|} \max\{t^k_{r_{i-1}} + s^{\mathrm{D}}_{r_{i-1}} + \delta^k_{r_{i-1},r_i} - t^k_{r_i}, 0\} \tag{4-3}$$

$$\textit{Incompatibilities: } I_k(r) = \sum_{i=1}^{|r|} I_{r_i,k}, \tag{4-4}$$

where $t^k_{r_i}$ represents the start-of-service time at the $i$th node of route $r$ with ship $k$, defined as

$$t^k_{r_i} = \begin{cases} a_{r_i} \ \textit{if } i = 1, \\ \max\{a_{r_i}, \min\{t_{r_{i-1}} + s^{\mathrm{D}}_{r_{i-1}} + \delta^k_{r_{i-1},r_i}, b_{r_i}\}\} \ \textit{otherwise.} \end{cases} \tag{4-5}$$

The cost of a route $r$ with ship $k$ equals to its travel cost $C_k(r)$. As we penalize violated constraints, we define the penalized cost this route as

$$\phi(r) = C_k(r) + \omega^{Q^{\max}} \max\{0, Q^{\max}_k(r) - Q_k\} + \omega^{TW} TW_k(r) + \omega^I I_k(r), \tag{4-6}$$

where $\omega^{Q^{\max}}$, $\omega^{TW}$ and $\omega^I$ are the respective penalty coefficients for peak load, time window, and incompatibility constraints violations. The penalized cost of a solution $S$ is the sum of the penalized cost of all its routes, that is, $\phi(S) = \sum_{r\in\mathcal{R}^S} \phi(r)$. Penalty coefficients are adjusted during the execution of the HGS as described in Section 4.1.5.

### 4.1.2 Solution representation and evaluation

A solution $S$ is represented as a giant tour $\pi^S$ that holds a permutation of nodes $P \cup D$. We use a polynomial Split algorithm to obtain the routes $\mathcal{R}^S$ from $\pi^S$ after crossover. Split is a dynamic programming algorithm that finds a minimum cost segmentation of a giant tour (Prins, 2004). Split was originally conceived for the Capacitated Vehicle Routing Problem (CVRP), but is flexible enough to be adapted to problem variants with pickups-and-deliveries (Velasco et al., 2009), fixed fleet size (Vidal, 2016), and heterogeneous fleet (Prins, 2009).

When dealing with vehicle routing problems with heterogeneous fleets,

several previous authors have assumed that the SPLIT algorithm should jointly optimize the giant tour segmentation and the choice of ship for each route (Duhamel et al., 2011, 2013). This extension, unfortunately, leads to a special case of a resource constrained shortest path problem, and only pseudo-polynomial algorithms are known to this date. To avoid this issue, we fix the sequence of ships and restrict the use of the SPLIT algorithm to the segmentation of the tours, in which case the ships are considered one by one in their order of appearance. To avoid any potential bias from the input instance, we shuffle the order of the ships in the solution representation. The decisions related to the use of spot charter or to not transport optional cargoes are integrated into the HGS with a dummy ship $k = 0$ that accounts for the associated penalties. This ship is the last one in the SPLIT ship permutation.

The SPLIT graph is defined as follows. Let $G^S$ be a directed acyclic graph with nodes $V^S = \{v_0^0, \ldots, v_{2n}^0, v_0^1, \ldots v_{2n}^1, \ldots, v_0^m, \ldots, v_{2n}^m\}$ and arcs $A^S = \{(v_i^k, v_j^{k+1}) : 0 \leq i \leq j \leq 2n, 0 \leq k \leq m+1\}$ An arc $(v_i^k, v_j^{k+1}) \in A^S$ represents the route

$$r_{i+1,j}^k = (0_k, \pi_{i+1}^S, \pi_{i+2}^S, \ldots, \pi_{j-1}^S, \pi_j^S), \tag{4-7}$$

with ship $k$. If $i = j$, then $r_{i+1,j}^k = (0_k)$, that is, an empty route. The arc $(v_i^k, v_j^{k+1})$ has cost $\phi(r_{i+1,j}^k)$. If $r_{i+1,j}^k$ is not pairing or precedence feasible, then the cost of $(v_i^k, v_j^{k+1})$ is $+\infty$. The optimal segmentation of the giant tour is given by the shortest path between nodes $v_0^0$ and $v_{2n}^m$. The full algorithm can be implemented with time complexity $\mathcal{O}(mn^2)$ and space complexity $\mathcal{O}(mn)$.

**Individual evaluation.** The quality of an individual $S$ is measured as a combination of its solution quality and diversity contribution to the subpopulation. This combination is referred to as the *biased fitness* of $S$ in its subpopulation $\mathcal{P}$, and is defined as

$$f_{\mathcal{P}}(S) = f_{\mathcal{P}}^{\phi}(S) + \left(1 - \frac{\mu^{ELITE}}{|\mathcal{P}|}\right) f_{\mathcal{P}}^{DIV}(S), \tag{4-8}$$

where $f_{\mathcal{P}}^{\phi}(S)$ is the penalized cost rank of $S$ in $\mathcal{P}$, and $f_{\mathcal{P}}^{DIV}(S)$ is the diversity contribution rank of $S$ in $\mathcal{P}$. Both ranks are relative to the subpopulation size. A parameter $\mu^{ELITE}$ balances the weight of each rank. The diversity contribution of $S$ in $\mathcal{P}$ is defined as the average distance to its $\mu^{CLOSE}$ closest individuals. The distance metric used is the *broken pairs* distance (Campos et al., 2005; Prins, 2004): it is the proportion of arcs $(i,j)^k \in A^+$ that are in $\mathcal{R}^S$ but are not in $\mathcal{R}(S')$, where $A^+ = \{(i,j)^k \in A, k \neq 0\}$.

### 4.1.3 Parent selection and crossover

Two parents $P_1$ and $P_2$ are selected for crossover. Each one is obtained by a binary tournament: two individuals are selected randomly from the union of the feasible and infeasible subpopulations, and the one with smaller biased fitness is kept. We generate an offspring $C$ using a one-point crossover operator between giant tours $\pi^{P_1}$ and $\pi^{P_2}$ Velasco et al. (2009).

**The one-point crossover.** Our one-point crossover is defined as follows: a cutting point $s \in \{1, \ldots, 2n\}$ is randomly selected, and the offspring giant tour $\pi^C$ is initialized as an empty sequence. Then, nodes $\pi_1^{P_1}, \ldots, \pi_s^{P_1}$ are inserted at the end of $\pi^C$. Afterwards, the sequence of missing deliveries in $\pi_1^C, \ldots, \pi_s^C$ is inserted at the end of $\pi^C$. Finally, $\pi^{P_2}$ is swept left to right, inserting missing nodes at the end of $\pi^C$. This crossover operator never generates a giant tour with a delivery before its respective pickup. After crossover, routes $\mathcal{R}^S$ are generated by Split and are optimized through education and repair. Fig. 4.1 illustrates our one-point crossover with a cutting point $s = 4$. The nodes that were copied from $\pi^{P_1}$ have a gray background, missing deliveries that were inserted have a dashed background, and the remaining nodes copied from $\pi^{P_2}$ have a white background.

Figure 4.1: One-point crossover illustration with a cutting point $s = 4$.

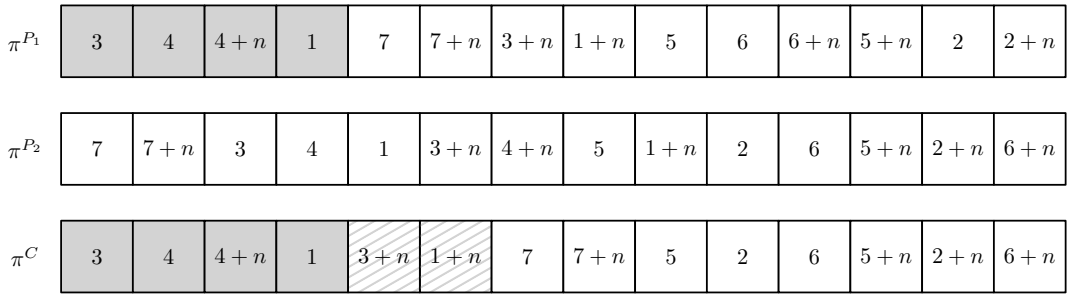


### 4.1.4 Education and repair

The HGS educates and repairs individuals with a first improvement local search procedure with constant time move evaluations. Routes are initially obtained with Split on a giant tour $\pi^S$, and are improved with a set of neighborhood structures evaluated in random order. When the search terminates, $\pi^S$ is updated with the concatenation of all routes in $\mathcal{R}^S$. As a penalized search space is considered, solutions may be infeasible at the end of a local search. If an infeasible solution is obtained, it undergoes a *repair* phase with probability $p_{rep}$. Repair consists of temporarily multiplying the

base penalty coefficients by 10 and running a local search. If the resulting solution still is not feasible, then the base coefficients are multiplied by 1000 and the local search is run again.

**Neighborhood structures.** We use the following neighborhood structures, with size $\mathcal{O}(n^2)$:

- $\mathcal{N}_1$ (relocate pickup, intra-route only) relocate a pickup $i \in P$ after a node $j \in V$.
- $\mathcal{N}_2$ (relocate delivery, intra-route only) relocate a delivery $i \in D$ after a node $j \in V$.
- $\mathcal{N}_3^{\Delta}$ (relocate pair) relocate a pair $(i, n+i)$ placing $i$ after a node $j \in V$ and placing $n+i$ $\Delta$ nodes after $i$. Restricted to $\Delta \in \{0, 1, 2\}$.
- $\mathcal{N}_4$ (swap pair) given two pairs $(i, n+i)$ and $(j, n+j)$, swap $i$ with $j$ and $n+i$ with $n+j$.
- $\mathcal{N}_5$ (swap ships, inter-route only) exchange the ship types between two routes.

Except for $\mathcal{N}_1$ and $\mathcal{N}_2$, the solutions found in these neighborhoods never violate pairing and precedence constraints. The remaining scenarios that break these constraints are always ignored during the local search.

**Move evaluations.** We perform move evaluations in $\mathcal{O}(1)$. This is possible because we represent moves as the concatenation of a constant number of route subsequences with preprocessed information. These concepts are formalized in Kindervater & Savelsbergh (1997); Irnich (2008), and Vidal et al. (2015*b*).

The subsequence resources are expressed in Table 4.1, both for subsequences with a single node ($\sigma^0$), and the concatenation of two subsequences $\sigma$ and $\sigma'$, according to a ship $k$. Given a solution $S$, for every subsequence $\sigma = (r_i^k, \ldots, r_j^k), 1 \leq i \leq j \leq |r^k|$ of any route $r^k \in \mathcal{R}^S$, we preprocess all resources for $\sigma$ with ship $k$. Then, for every prefix $\sigma^p = (0^k, \ldots, r_j^k), 1 \leq j \leq |r^k|$ and suffix $\sigma^s = (r_i^k, \ldots, r_{|r^k|}^k), 1 \leq i \leq |r^k|$ subsequence of any route $r^k \in \mathcal{R}^S$, we preprocess all resources for $\sigma^p$ and $\sigma^s$, for all $m$ ships.

**Memories.** The HGS avoids redundant move evaluations by checking the last-modified time of a route and the last-evaluated time for each move. This constant-time check avoids the computational effort of evaluating moves that will not render an improvement.

**Granular search.** Our HGS follows similar granular search principles as Toth & Vigo (2003); Vidal et al. (2012), and Vidal et al. (2013), restricting move evaluations to those that create at least one directed arc $(i, j)$ such that

Table 4.1: Subsequence resources.

| Resource name | Base case | Concatenation |
|---|---|---|
| Travel cost | $C_k(\sigma^0) = s^{\mathrm{c}}_{ik}$ | $C_k(\sigma \oplus \sigma') = C_k(\sigma) + C_k(\sigma') + c^k_{\sigma_{\lvert\sigma\rvert}\sigma'_1}$ |
| Load | $Q_k(\sigma^0) = q_i$ | $Q_k(\sigma \oplus \sigma') = Q_k(\sigma) + Q_k(\sigma')$ |
| Peak load | $Q^{\max}_k(\sigma^0) = q_i$ | $Q^{\max}_k(\sigma \oplus \sigma') = \max\{Q^{\max}_k(\sigma), Q_k(\sigma) + Q^{\max}_k(\sigma')\}$ |
| Time warp use | $TW_k(\sigma^0) = 0$ | $TW_k(\sigma \oplus \sigma') = TW_k(\sigma) + TW_k(\sigma') + \Delta^k_{TW}$ |
| Earliest possible completion time | $E_k(\sigma^0) = a_i$ | $E_k(\sigma \oplus \sigma') = \max\{E_k(\sigma') - \Delta^k, E_k(\sigma)\} - \Delta^k_{WT}$ |
| Latest feasible starting time | $L_k(\sigma^0) = b_i$ | $L_k(\sigma \oplus \sigma') = \min\{L_k(\sigma') - \Delta^k, L_k(\sigma)\} + \Delta^k_{TW}$ |
| Duration | $D_k(\sigma^0) = s^{\mathrm{D}}_{ik}$ | $D_k(\sigma \oplus \sigma') = D_k(\sigma) + D_k(\sigma') + \delta^k_{\sigma_{\lvert\sigma\rvert}\sigma'_1} + \Delta^k_{WT}$ |
| Incompatibilities | $I_k(\sigma^0) = I_{ik}$ | $I_k(\sigma \oplus \sigma') = I_k(\sigma) + I_k(\sigma')$ |
| | | $\Delta^k = D_k(\sigma) - TW_k(\sigma) + \delta^k_{\sigma_{\lvert\sigma\rvert}\sigma'_1}$ |
| | | $\Delta^k_{WT} = \max\{E_k(\sigma') - \Delta^k - L_k(\sigma), 0\}$ |
| | | $\Delta^k_{TW} = \max\{E_k(\sigma) + \Delta^k - L_k(\sigma'), 0\}$ |

either $i = 0$ (any ship initial location) or $j \in \Gamma(i)$. The set $\Gamma(i)$ has the $|\Gamma|$ most promising successors of $i$. To reasonably evaluate how good a successor is, we use a metric $\gamma(i, j)$ that considers spatial and temporal proximity between nodes. Temporal proximity is evaluated trough minimum waiting time and minimum time warp terms, with respective weight parameters $\gamma^{WT}$ and $\gamma^{TW}$. We base our metric on Vidal et al. (2013) and adapt it for our application: due to the heterogeneous fleet, values are averaged over all ships, and travel cost and time are scaled since they are in different units. The metric is defined as

$$\gamma(i,j) = (\bar{c}/\bar{\delta})\bar{c}_{ij} + \gamma^{WT}\max\{a_j - \bar{s}^{\mathrm{D}}_{\boxdot i} - \bar{\delta}_{ij} - b_i, 0\} + \gamma^{TW}\max\{a_i + \bar{s}^{\mathrm{D}}_{\boxdot i} + \bar{\delta}_{ij} - b_j, 0\}, \tag{4-9}$$

where $\bar{c} = \frac{\sum_{(i,j)^k \in A^+} c^k_{ij}}{|A^+|}$, $\bar{\delta} = \frac{\sum_{(i,j)^k \in A^+} \delta^k_{ij}}{|A^+|}$, $\bar{c}_{ij} = \frac{\sum^m_{k=1} c^k_{ij}}{m}$, $\bar{s}^{\mathrm{D}}_{\boxdot i} = \frac{\sum^m_{k=1} \bar{s}^{\mathrm{D}}_{ik}}{m}$, and $\bar{\delta}_{ij} = \frac{\sum^m_{k=1} \delta^k_{ij}}{m}$.

Some edge cases are removed during the successor list construction to avoid breaking precedence constraints or to avoid the introduction of moves that create unnecessary infeasibilities:

- $n + i$ is never a successor of 0, $\forall n + i \in D$.
- $i$ is never a successor of $n + i$, $\forall i \in P$.
- $i$ is never a successor of $j$ if $q_j + q_i > \max_{k=1,\ldots,m} Q_k, \forall (i, j) \in (P \cup D)^2, i \neq j$.
- $n + i$ is never a successor of $j$ if $q_i + q_j > \max_{k=1,\ldots,m} Q_k, \forall (i, j) \in P^2, i \neq j$.
- $i$ is never a successor of $j$ if $\nexists k \mid I_{ik} = I_{jk} = 1, \forall (i, j) \in (P \cup D)^2, i \neq j$.

### 4.1.5 Population management

We implement survivor selection, population diversification, and adaptive penalties mechanisms to ensure high population diversity along with high

solution quality during the execution of the HGS. A large SP-based neighborhood is explored such that new feasible individuals are generated based on the combination of previously found feasible routes.

**Initialization.** To initialize the population, the HGS generates $4\mu^{MIN}$ random individuals. Random individuals are generated from giant tours where a sequence of pickups is shuffled and then deliveries are placed immediately after their respective pickups. These individuals are educated, possibly repaired and inserted into their respective subpopulation.

**Survivor selection.** A survivor selection mechanism occurs whenever a subpopulation reaches the maximum size of $\mu^{MIN} + \mu^{GEN}$ individuals. The $\mu^{GEN}$ individuals with maximum biased fitness are removed, considering first all individuals that have a clone. An individual $P$ has a clone if another individual $Q$ exists such that either (a) $\phi(P) = \phi(Q)$ or (b) $d(P,Q) = 0 \vee d(Q,P) = 0$. This survivor selection procedure has the property that, after clone removal, the best $\mu^{ELITE}$ individuals with respect to penalized cost are not discarded (Vidal et al., 2012). Thus, it establishes a balance between elitism and diversity.

**Diversification.** The population is diversified if no new best-known solution (BKS) was found during the last $It_{DIV} = 0.4 \cdot It_{NI}$ iterations. First, we discard all but the $\mu^{MIN}/3$ individuals with smaller biased fitness in each subpopulation. Then, we generate $4\mu^{MIN}$ new random individuals that are educated, possibly repaired and inserted in their subpopulation.

**Set partitioning.** To improve the solution quality of the HGS, a set-partitioning-based large neighborhood is explored to find new improving solutions based on previously found routes. This approach is inspired by the work of Subramanian et al. (2013). During the execution of the HGS, all feasible routes from generated individuals are added to the Set Partitioning (SP) formulation (Eqs. (2-1) to (2-5)). The SP is solved if no new BKS was found during the last $It_{SP} = 0.2 \cdot It_{NI}$ iterations. If the best solution found improves the BKS of the HGS, then it is inserted into the population. The SP large neighborhood provides the means to generate new solutions with an entirely different approach: instead of manipulating small segments of routes during local search, the SP neighborhood finds good combinations of previously found routes. The execution time limit of the SP is defined with a parameter $T^{SP}_{\max}$.

**Penalty coefficient adjustment.** Penalty coefficients are periodically adjusted to control the proportion of partially feasible individuals with respect to

each relaxed constraint. For each relaxed constraint $X$, we keep the proportion $\xi^X$ of partially feasible individuals with respect to $X$ in the last 100 iterations. This proportion does not include individuals generated by *repair* and *SP*. These coefficients are adjusted every $It_{NI}/100$ iterations: if $\xi^X \leq \xi^{REF} - 5\%$, $\xi^X$ is multiplied by 1.2. Otherwise, if $\xi^X \geq \xi^{REF} + 5\%$, $\xi^X$ is multiplied by 0.85. Whenever penalty coefficients are updated, each individual penalized cost and biased fitness is updated accordingly.

## 4.2 Branch-and-Price

Since the work of Christofides et al. (1981), Column Generation (CG) can be considered the most successful exact approach used to solve routing problems in the last years (Fukasawa et al., 2006; Ropke & Cordeau, 2009; Contardo & Martinelli, 2014). It solves the linear relaxation of a formulation with an exponential number of variables (like our SP formulation of Chapter 2) by iteratively generating the variables solving a pricing subproblem. This approach usually results in linear relaxation bounds stronger than the ones obtained by other formulations, such as flow formulations. When the CG is combined with a branch-and-bound algorithm to obtain integer solutions, it is called Branch-and-Price (B&P). In the following, we present how to consider the different attributes of the ITSRSP for both the CG and the B&P.

### 4.2.1 Column generation

The CG algorithm is used to avoid the enumeration of all variables of the SP formulation. Therefore, at each iteration, after solving the linear relaxation of the Master Problem (2-1)-(2-5), it calls a pricing subproblem to check the existence of a variable with negative reduced cost. In routing problems with a homogeneous fleet, the same pricing subproblem can be solved for all vehicles. This is not the case for the ITSRSP, as each ship may have a different starting location, cargo compatibility, capacity, travel costs and times. For this reason, to obtain the optimal solution of the linear relaxation, we must solve one pricing subproblem for each ship.

Let $\gamma_k$ and $\beta_i$ be the dual variables associated to Constraints (2-2) and (2-3), respectively. Given $a^k_{ri}$, a binary constant representing whether route $r$ of ship $k$ transports cargo $i$, the reduced cost of a route is defined in Equation (4-10). By decomposing this equation, we obtain the reduced cost

for each arc, as shown in Equation (4-11).

$$\bar{c}_r^k = c_r^k - \gamma_k - \sum_{k=1}^{m} a_{ri}^k \beta_i \qquad \forall k \in \{1,\ldots,m\}, r \in \Omega_k. \tag{4-10}$$

$$\bar{c}_{ij}^k = \begin{cases} c_{ij}^k - \gamma_k & \forall k \in \{1,\ldots,m\}, i = 0, j \in V, \\ c_{ij}^k - \beta_i & \forall k \in \{1,\ldots,m\}, i \in P, j \in V, \\ c_{ij}^k & \forall k \in \{1,\ldots,m\}, i \in D, j \in V. \end{cases} \tag{4-11}$$

**Pricing.** The pricing subproblem is an Elementary Shortest Path Problem with Resource Constraints (ESPPRC). As being an $\mathcal{NP}$-Hard problem, it is often prohibitively difficult to solve it for large instances. Several works in the literature present ways to improve its resolution mainly using route relaxation techniques (Irnich & Villeneuve, 2006; Baldacci et al., 2011). As we further discuss, we do not relax the definition of routes used in the SP formulation, but we use the Decremental State-Space Relaxation (DSSR) of Righini & Salani (2008) in the pricing subproblem.

The ESPPRC is solved using a forward dynamic programming algorithm which starts at the depot and at each iteration extends a partial path to a vertex until no further extensions are possible. For each partial path $\mathcal{P}$, we define a label $\mathcal{L}(\mathcal{P}) = (v(\mathcal{P}), \bar{c}(\mathcal{P}), q(\mathcal{P}), t(\mathcal{P}), \mathcal{O}(\mathcal{P}), \mathcal{U}(\mathcal{P}))$ containing the last vertex of the path, the accumulated reduced cost, the total load, the total time, the set of opened pairs and the set of unreachable pairs, respectively. This definition follows the one used by Ropke & Cordeau (2009) for the Pickup and Delivery Problem with Time Windows (PDPTW). Extending a path $\mathcal{P}$ to a vertex $j \in V$ is allowed only if $q(\mathcal{P}) + q_j \leq Q_k$, $t(\mathcal{P}) + \delta_{ij}^k \leq b_j$ and:

$$\begin{cases} j \notin \mathcal{U}(\mathcal{P}) & \text{if } j \in P, \\ j - n \in \mathcal{O}(\mathcal{P}) & \text{if } j \in D. \end{cases} \tag{4-12}$$

The extension being allowed, it generates the new label presented in Equation (4-13).

$$\mathcal{L}(\mathcal{P}') = \begin{cases} (j, \bar{c}(\mathcal{P}) + \bar{c}_{ij}^k, q(\mathcal{P}) + q_j, t(\mathcal{P}) + \delta_{ij}^k, \mathcal{O}(\mathcal{P}) \cup \{j\}, \mathcal{U}(\mathcal{P}) \cup \{j\}) & \text{if } j \in P, \\ (j, \bar{c}(\mathcal{P}) + \bar{c}_{ij}^k, q(\mathcal{P}) + q_j, t(\mathcal{P}) + \delta_{ij}^k, \mathcal{O}(\mathcal{P}) \backslash \{j-n\}, \mathcal{U}(\mathcal{P})) & \text{if } j \in D. \end{cases} \tag{4-13}$$

To reduce the number of labels during the dynamic programming algorithm, we use the following dominance rule: a path $\mathcal{P}_1$ dominates a path $\mathcal{P}_2$

if Eqs. (4-14) to (4-18) hold.

$$v(\mathcal{P}_1) = v(\mathcal{P}_2), \tag{4-14}$$

$$\bar{c}(\mathcal{P}_1) \leq \bar{c}(\mathcal{P}_2) \tag{4-15}$$

$$t(\mathcal{P}_1) \leq t(\mathcal{P}_2), \tag{4-16}$$

$$\mathcal{O}(\mathcal{P}_1) \subseteq \mathcal{O}(\mathcal{P}_2), \tag{4-17}$$

$$\mathcal{U}(\mathcal{P}_1) \subseteq \mathcal{U}(\mathcal{P}_2). \tag{4-18}$$

There are two important aspects of the dominance rule to discuss. First, there is no need to consider the load, since Equation (4-17) will always guarantee that $q(\mathcal{P}_1) \leq q(\mathcal{P}_2)$. Second, as discussed in Ropke & Cordeau (2009), in order to Equation (4-18) be valid, the reduced costs must satisfy the delivery triangle inequality, i.e. $\bar{c}^k_{ij} \leq \bar{c}^k_{i\ell} + \bar{c}^k_{\ell j}, \forall i \in V, j \in V, \ell \in D, k \in \{1, \ldots, m\}$. Given the definition of $\bar{c}^k_{ij}$ presented in Equation (4-11), the delivery triangle inequality holds for the reduced costs whenever it holds for the original costs $c^k_{ij}$. When it is not the case, a way to ensure the property is presented in Ropke & Cordeau (2009). We will discuss it further in Section 4.2.2, when we will need to apply this correction.

**Decremental state-space relaxation.** The DSSR is an iterative technique that relaxes a set of constraints and at each iteration restores some of them based on any infeasibility found in the current solution. The goal is to obtain the optimal solution in few iterations, restoring only a small portion of the relaxed constraints. In the case of the pricing subproblem, we relax the constraint that forbids a pair $(i, n+i)$ to be visited again by considering a set $\Gamma \subseteq P$ of pickups that are allowed to be opened again. This relaxation is done by replacing Condition (4-12) with:

$$\begin{cases} j \notin \mathcal{O}(\mathcal{P}) & \text{if } j \in \Gamma, \\ j \notin \mathcal{U}(\mathcal{P}) & \text{if } j \in P \backslash \Gamma, \\ j - n \in \mathcal{O}(\mathcal{P}) & \text{if } j \in D. \end{cases} \tag{4-19}$$

This change allows a pair to repeat, forming a cycle of pairs, but the precedence and pairing constraints for each pair occurrence are still valid. The benefit of this relaxation is to enforce the dominance rule, however, this can only be obtained changing the extension of a label from Eqs. (4-13) to (4-20).

$$\mathcal{L}(\mathcal{P}') = \begin{cases} (j, \bar{c}(\mathcal{P}) + \bar{c}^k_{ij}, q(\mathcal{P}) + q_j, t(\mathcal{P}) + \delta^k_{ij}, \mathcal{O}(\mathcal{P}) \cup \{j\}, \mathcal{U}(\mathcal{P})) & \text{if } j \in \Gamma, \\ \text{(4-13)} & \text{otherwise.} \end{cases} \tag{4-20}$$

To the best of our knowledge, this approach was never tested on the

PDPTW pricing subproblem, but it is suggested by Ropke & Cordeau (2009) almost in the same manner we propose in this work, i.e. a relaxation of $\mathcal{U}(\mathcal{P})$ sets. The authors also suggest applying the DSSR to relax $\mathcal{O}(\mathcal{P})$ sets. However, we tested this approach and it resulted in a slow convergence.

**Ship ordering.** As mentioned before, the ITSRSP has a heterogeneous fleet of ships. The drawback of having different ship types is to run one pricing subproblem for each ship. Since most of the time is spent on solving the subproblems, it is important to obtain a way to reduce the number of calls to them. We tested different approaches, like ship grouping and different orderings, but none of them performed well. Therefore, the CG put the ships on a list using their original ordering, and at each iteration it calls the pricing subproblem of the last ship which succeeded to obtain a new route. If the current pricing is not able to generate a new route, the procedure selects the next in the list in a circular manner. When a full round of the list is performed without generating any new route, the CG stops and returns the current solution as the linear relaxation optimal.

**Heuristic pricing.** As a further improvement on the resolution of the CG, the algorithm starts by solving a simple and fast heuristic pricing. During the dynamic programming, it keeps only the label with the minimum reduced cost for each vertex and each time, reducing drastically the number of labels. The ship ordering is kept the same and as soon as a full round on the list fails to obtain a new route with the heuristic pricing, the CG starts to use the exact pricing and it never uses the heuristic pricing again.

**Initial solution.** Considering the existence of the charters variables in the SP formulation, the CG may start with empty $\Omega_k$ sets, resulting in a solution with a high objective value, using charters for all cargoes. If there were no charters in the problem, one could use two approaches. The first is to start with a feasible solution generated by a heuristic like the one presented in Section 4.1. The second one is to introduce artificial variables in the infeasible constraints and to solve a two-phase CG, which resembles the two-phase Simplex method, minimizing the infeasibility in the first phase. The second approach is used in the Branch-and-Bound of Section 4.2.2 when new constraints are introduced in the problem.

**Preprocessing.** Our CG performs some preprocessing procedures based on the work of Dumas et al. (1991) to remove some arcs in the pricing subproblem. These procedures are further extended to consider the different attributes of the ITSRSP.

### 4.2.2 Branch-and-Bound

The CG presented in the previous section is able to produce strong lower bounds for the ITSRSP. Nevertheless, it solves only the linear relaxation of the problem, not reaching the optimal solution in most cases. In the effort to obtain the integer optimal solution, one can use several known approaches, being the Branch-and-Bound (B&B) (Land & Doig, 1960) the most successful in the known literature. The approach works by solving a relaxation of the problem and recursively splitting (branching) it into smaller subproblems, adding new constraints which will gradually enforce integrality. The full enumeration is avoided by pruning some subproblems based on their bounds. As mentioned before, when the relaxation used on each node of the B&B tree (recursion tree) is a CG algorithm, the approach is called B&P.

**Branching rules.** Any branching rule may be created for the B&B, as long as the resulting subproblems include all integer points from the original problem. We use three branching rules, in the order given below. Moreover, for all branching rules, the priority is given to the most fractional element.

1. Branching on charters: if any $y_i$ variable is fractional, the B&B creates two branches, $y_i = 0$ and $y_i = 1$.

2. Branching on ships: if $\sum_{r \in \Omega_k} \lambda_r^k$ is fractional for any ship $k$, the B&B creates two branches, $\sum_{r \in \Omega_k} \lambda_r^k = 0$ and $\sum_{r \in \Omega_k} \lambda_r^k = 1$.

3. Branching on edges for all ships: given $b_{ra}^k$, a binary constant representing if route $r$ of ship $k$ traverses arc $a = (i,j)^k$, let us define the number of times any ship traverses $a_1 = (i,j)$ or $a_2 = (j,i)$ as $x_e = \sum_{k=1}^{m} \sum_{r \in \Omega_k} (b_{ra_1}^k + b_{ra_2}^k) \lambda_r^k$. If $x_e$ is fractional, the B&B creates two branches, $x_e = 0$ and $x_e = 1$.

Note that we also use another branching rule based on arcs for each ship. However, in our tests, the B&B never used this last branching rule, even for the instances it was able to obtain the optimal integer solution.

The first branching rule has no impact on the pricing subproblems. On the other hand, each new constraint generated by the second and third branching rules introduces a new dual variable that must be considered by the pricing subproblems, described next.

**Reduced cost.** Each constraint generated by the branching on ships introduces a new dual variable $\tau_k$, which can be considered in the reduced cost of a route like $\gamma_k$ variables. These dual variables do not violate the delivery triangle

inequality since the first visited node must be a pickup node. In the case of the branching on edges for all ships, each constraint introduces a dual variable $\rho_e$, which will subtract the right-hand side of (4-11) in the respective case. When the third case happens, i.e. $i \in D, j \in V$, this change violates the delivery triangle inequality. To circumvent this issue, we apply the method of Ropke & Cordeau (2009) to fix the delivery triangle inequality.

**Artificial variables.** The branching rules presented in this section may turn the solution of a child node infeasible. However, at first, it is not possible to be sure about the feasibility of the solution because it may just be missing some columns to become feasible again. For this reason, in every node of the B&B that results in an infeasible solution, the algorithm solves the CG like a two-phase Simplex method, briefly described in Section 4.2.1. It introduces an artificial variable on each branching constraint and changes the objective function to minimize the sum of all of them, thus minimizing infeasibility. As soon as the solution becomes feasible again, the artificial variables are removed and the original objective function is restored. If the CG terminates before reaching this state, the solution is then confirmed to be infeasible.

**Strong branching.** Usually, we define the choice of the element to branch using a simple strategy, like selecting the most fractional variable among the branching candidates. Strong branching is a technique devised to reduce the size of the B&B tree by predicting which element will result in child nodes with better solutions. Thus, after solving the CG of each B&B node, strong branching builds a set of branching candidates for one of the branching rules explained above and simulates the branching for each element by solving both child nodes. The method then keeps the best one, i.e. the branching having the best worst child node. Furthermore, a branching with one infeasible child node is always better than one with no infeasible child node, and a branching with both child nodes infeasible is immediately chosen. Strong branching may be applied to the complete set of candidates or only to some of the most fractional candidates.

**Heuristic strong branching.** When the relaxation used by the B&B algorithm is the regular linear relaxation solved with the Simplex method, it is often possible to perform a complete and exact strong branching. However, this is not the case when using CG, as it is prohibitively expensive to solve it several times to obtain only two child nodes. To deal with this issue, there are some alternatives, where one is to perform strong branching only to a small subset of candidates, reducing the improvements of the method. We use another alternative that performs a heuristic strong branching, executing the

CG only with the heuristic pricing. Even with the non-optimal linear solution, it gives a good prediction for the quality of each child node and can be used to compare the result of the branching candidates. When the branching candidate is chosen, the exact pricing is executed on both child nodes.

## 4.3 Computational Experiments

In this section, we evaluate how efficient the HGS and the B&P are on the ITSRSP instances. Additionally, we analyze the solution quality impact of the SP component on the HGS. Finally, we evaluate how the HGS performs on ITSRSP subproblems.

**Computational environment.** We implemented both the HGS and the B&P in C++ using double precision floating point number representation. We compiled our code with GCC 6.3.0 using the optimization flags -O3 and -march=native. We used CPLEX 12.7 to solve the integer SP inside the HGS and the B&P master problem. We conducted our experiments on a computer with an i7-3960X CPU, 64GB of RAM, and a 64 bits Ubuntu 14.04 LTS operating system.



### 4.3.1 Benchmark instances for the ITSRSP

We evaluated the HGS and the B&P on a benchmark suite for the ITSRSP based on real-life scenarios, presented in Hemmati et al. (2014) and currently available at `http://home.himolde.no/~hvattum/benchmarks/`. The instances are divided in four groups of size 60, according to problem topology and cargo type: *short sea mixed load (SS_MUN)*, *short sea full load (SS_FUN)*, *deep sea mixed load (DS_MUN)*, and *deep sea full load (DS_FUN)*. For each group, there are subgroups of size 5 for each problem size. The mixed load instances have up to 130 cargoes and 40 ships, while the full load instances have up to 100 cargoes and 50 ships. To this date, 123 out of 240 instances remain open, and the lower bound of eight instances are still not known.

**Adaptations for full load instances.** The full load instances are a special case of the ITSRSP, similar to an asymmetric vehicle routing problem, where deliveries are performed immediately after their respective pickups. To improve the HGS execution time, we disabled some components that are not necessary to solve these instances: neighborhoods $\mathcal{N}_1$ and $\mathcal{N}_2$ are not used, and neighborhood $\mathcal{N}_3^{\Delta}$ is restricted to $\Delta = 0$. The granular search is also modified to consider a more relevant search space: $i \in D$ is the only possible successor

of $i - n$, and only pickup nodes may be successors of any delivery $i \in D$.

### 4.3.2 Parameters for the hybrid genetic search

We based our HGS parameters on previous values found by extensive calibration experiments on similar heuristics for related vehicle routing problems (Vidal et al., 2012, 2013). This way, we mitigated the risks of overfitting our parameters on the benchmark instances. Thus, $(\mu^{MIN}, \mu^{GEN}) = (25, 40)$, $\mu^{ELITE} = 10$, $\mu^{CLOSE} = 5$, $p_{rep} = 0.5$, $\xi^{REF} = 0.2$, $|\Gamma| = 30$, and $(\gamma^{TW}, \gamma^{WT}) = (1.0, 0.2)$. Penalty coefficients were initialized as $(\omega^{Q^{\max}}, \omega^{TW}, \omega^{I}) = (\bar{c}/\bar{q}, 100, \bar{c})$, where $\bar{q} = \frac{\sum_{i \in V} |q_i|}{|V|}$. To achieve a similar execution time with previous literature, we set $(It_{NI}, T_{\max}) = (2.5 \cdot 10^3, 15min)$, and $T^{SP}_{\max} = 30s$.

### 4.3.3 Performance on the ITSRSP

**Hybrid genetic search.** We compared our HGS results with the state-of-the-art ITSRSP heuristics from Hemmati et al. (2014) (ALNS) and Hemmati & Hvattum (2016) (ALNS-1 to ALNS-6). To measure the effectiveness of the specialized SP component, we reported results for two different versions of the HGS: one without SP (HGS-NO), and one with SP (HGS-SP). The comparison with Hemmati et al. (2014) is shown in Tables 4.2 to 4.5, while the comparison with Hemmati & Hvattum (2016) is shown in Table 4.6. Results are aggregated in groups based on instance type and size, and the reported numbers represent the average of all results for each group. As Hemmati & Hvattum (2016) used the first instance of each group (HE_1) to calibrate their heuristic, these instances are not included in the comparison presented in Table 4.6. Columns "Best" and "Avg" give, respectively, the best and the average gap (in percentage) to the previously BKS (over 10 runs). Column "T" gives the average CPU time (in minutes). Detailed results for HGS-NO and HGS-SP are shown in Tables A.1 to A.4. Full results for both Hemmati et al. (2014) and Hemmati & Hvattum (2016) were privately provided by the authors.

Both the HGS-NO and the HGS-SP largely outperform all previous heuristics, both in solution quality and execution time, becoming the new state-of-the-art heuristic for the ITSRSP. Full load instances are considerably easier to solve than mixed load instances, since the problem simplifies. The SP component of HGS-SP had a huge impact on solution quality: the average gap dropped from $-0.03\%$ to $-0.36\%$. An interesting observation is that the

average execution time of the HGS-SP (1.22 min) is smaller than the average execution time of the HGS-NO (1.60 min). A possible explanation for this is that the SP component may contribute to bigger improvements earlier, whereas the HGS-NO may spend more time to optimize the complex decisions necessary to find these solutions.

Table 4.2: Comparison with Hemmati et al. (2014) on SS_MUN instances.

| | **ALNS** | | | **HGS-NO** | | | **HGS-SP** | | |
|---|---|---|---|---|---|---|---|---|---|
| Group | Best | Avg | T | Best | Avg | T | Best | Avg | T |
| SS_MUN_C7_V3 | 0.00 | 0.00 | 0.03 | 0.00 | 0.00 | 0.02 | 0.00 | 0.00 | 0.02 |
| SS_MUN_C10_V3 | 0.00 | 0.00 | 0.04 | 0.00 | 0.00 | 0.03 | 0.00 | 0.00 | 0.03 |
| SS_MUN_C15_V4 | 0.00 | 0.58 | 0.09 | 0.00 | 0.00 | 0.07 | 0.00 | 0.00 | 0.07 |
| SS_MUN_C18_V5 | 0.00 | 0.51 | 0.13 | 0.00 | 0.09 | 0.11 | 0.00 | 0.01 | 0.11 |
| SS_MUN_C22_V6 | 0.00 | 1.82 | 0.19 | 0.00 | 0.00 | 0.13 | 0.00 | 0.00 | 0.14 |
| SS_MUN_C23_V13 | 0.00 | 0.57 | 0.25 | 0.00 | 0.06 | 0.18 | 0.00 | 0.00 | 0.17 |
| SS_MUN_C30_V6 | 0.12 | 1.60 | 0.38 | 0.00 | 0.00 | 0.29 | 0.00 | 0.00 | 0.26 |
| SS_MUN_C35_V7 | 0.05 | 1.71 | 0.54 | -0.08 | 0.21 | 0.44 | -0.20 | -0.19 | 0.41 |
| SS_MUN_C60_V13 | 0.13 | 1.05 | 2.01 | -0.51 | -0.15 | 1.68 | -0.64 | -0.59 | 1.51 |
| SS_MUN_C80_V20 | 0.00 | 0.91 | 4.13 | -0.98 | -0.32 | 4.39 | -1.50 | -1.49 | 2.99 |
| SS_MUN_C100_V30 | 0.00 | 0.95 | 7.77 | -1.16 | -0.50 | 7.95 | -1.69 | -1.68 | 3.93 |
| SS_MUN_C130_V40 | 0.00 | 0.70 | 16.95 | -0.70 | -0.30 | 13.31 | -1.82 | -1.82 | 10.12 |
| Avg | 0.03 | 0.87 | 2.71 | -0.29 | -0.08 | 2.38 | -0.49 | -0.48 | 1.65 |

Table 4.3: Comparison with Hemmati et al. (2014) on SS_FUN instances.

| | **ALNS** | | | **HGS-NO** | | | **HGS-SP** | | |
|---|---|---|---|---|---|---|---|---|---|
| Group | Best | Avg | T | Best | Avg | T | Best | Avg | T |
| SS_FUN_C8_V3 | 0.00 | 0.00 | 0.03 | 0.00 | 0.00 | 0.01 | 0.00 | 0.00 | 0.01 |
| SS_FUN_C11_V4 | 0.00 | 0.13 | 0.05 | 0.00 | 0.00 | 0.02 | 0.00 | 0.00 | 0.02 |
| SS_FUN_C13_V5 | 0.00 | 0.07 | 0.07 | 0.00 | 0.00 | 0.02 | 0.00 | 0.00 | 0.02 |
| SS_FUN_C16_V6 | 0.00 | 0.05 | 0.10 | 0.00 | 0.00 | 0.03 | 0.00 | 0.00 | 0.03 |
| SS_FUN_C17_V13 | 0.01 | 0.01 | 0.14 | 0.00 | 0.00 | 0.04 | 0.00 | 0.00 | 0.04 |
| SS_FUN_C20_V6 | 0.00 | 0.14 | 0.18 | 0.00 | 0.00 | 0.04 | 0.00 | 0.00 | 0.04 |
| SS_FUN_C25_V7 | 0.00 | 0.22 | 0.27 | 0.00 | 0.00 | 0.06 | 0.00 | 0.00 | 0.07 |
| SS_FUN_C35_V13 | 0.00 | 0.29 | 0.60 | 0.00 | 0.00 | 0.16 | 0.00 | 0.00 | 0.16 |
| SS_FUN_C50_V20 | 0.00 | 0.35 | 1.38 | -0.13 | -0.01 | 0.51 | -0.17 | -0.17 | 0.38 |
| SS_FUN_C70_V30 | 0.00 | 0.70 | 3.51 | -0.30 | -0.07 | 1.43 | -0.58 | -0.58 | 0.94 |
| SS_FUN_C90_V40 | 0.00 | 0.47 | 6.98 | -0.67 | -0.42 | 3.37 | -0.97 | -0.97 | 1.68 |
| SS_FUN_C100_V50 | 0.00 | 0.35 | 9.79 | -0.40 | -0.27 | 4.57 | -0.60 | -0.60 | 2.25 |
| Avg | 0.00 | 0.23 | 1.93 | -0.12 | -0.06 | 0.86 | -0.19 | -0.19 | 0.47 |

Table 4.4: Comparison with Hemmati et al. (2014) on DS_MUN instances.

| | **ALNS** | | | **HGS-NO** | | | **HGS-SP** | | |
|---|---|---|---|---|---|---|---|---|---|
| Group | Best | Avg | T | Best | Avg | T | Best | Avg | T |
| DS_MUN_C7_V3 | 0.00 | 0.00 | 0.03 | 0.00 | 0.00 | 0.02 | 0.00 | 0.00 | 0.02 |
| DS_MUN_C10_V3 | 0.00 | 0.01 | 0.04 | 0.00 | 0.00 | 0.03 | 0.00 | 0.00 | 0.03 |
| DS_MUN_C15_V4 | 0.00 | 1.26 | 0.08 | 0.00 | 0.00 | 0.07 | 0.00 | 0.00 | 0.06 |
| DS_MUN_C18_V5 | 0.00 | 0.47 | 0.13 | 0.00 | 0.00 | 0.10 | 0.00 | 0.00 | 0.10 |
| DS_MUN_C22_V6 | 0.00 | 2.18 | 0.19 | 0.00 | 0.00 | 0.14 | 0.00 | 0.00 | 0.14 |
| DS_MUN_C23_V13 | 0.00 | 0.12 | 0.24 | 0.00 | 0.00 | 0.15 | 0.00 | 0.00 | 0.15 |
| DS_MUN_C30_V6 | 0.24 | 1.04 | 0.37 | 0.11 | 0.15 | 0.27 | 0.00 | 0.01 | 0.25 |
| DS_MUN_C35_V7 | 0.09 | 1.07 | 0.51 | 0.08 | 0.13 | 0.38 | -0.01 | -0.01 | 0.33 |
| DS_MUN_C60_V13 | 0.24 | 2.66 | 1.92 | -0.60 | -0.12 | 2.01 | -1.04 | -1.03 | 1.36 |
| DS_MUN_C80_V20 | 0.00 | 1.83 | 4.26 | -0.77 | -0.02 | 3.96 | -1.23 | -1.21 | 2.87 |
| DS_MUN_C100_V30 | 0.00 | 1.50 | 8.00 | -0.52 | 0.55 | 7.26 | -2.10 | -2.10 | 7.38 |
| DS_MUN_C130_V40 | 0.00 | 1.44 | 17.47 | -0.77 | 0.22 | 12.90 | -3.55 | -3.51 | 14.26 |
| Avg | 0.05 | 1.13 | 2.77 | -0.21 | 0.08 | 2.27 | -0.66 | -0.65 | 2.25 |



Table 4.5: Comparison with Hemmati et al. (2014) on DS_FUN instances.

| | **ALNS** | | | **HGS-NO** | | | **HGS-SP** | | |
|---|---|---|---|---|---|---|---|---|---|
| Group | Best | Avg | T | Best | Avg | T | Best | Avg | T |
| DS_FUN_C8_V3 | 0.00 | 0.00 | 0.03 | 0.00 | 0.00 | 0.01 | 0.00 | 0.00 | 0.01 |
| DS_FUN_C11_V4 | 0.00 | 0.00 | 0.05 | 0.00 | 0.00 | 0.02 | 0.00 | 0.00 | 0.02 |
| DS_FUN_C13_V5 | 0.00 | 0.00 | 0.06 | 0.00 | 0.00 | 0.02 | 0.00 | 0.00 | 0.02 |
| DS_FUN_C16_V6 | 0.00 | 0.03 | 0.10 | 0.00 | 0.00 | 0.03 | 0.00 | 0.00 | 0.03 |
| DS_FUN_C17_V13 | 0.00 | 0.00 | 0.13 | 0.00 | 0.00 | 0.04 | 0.00 | 0.00 | 0.04 |
| DS_FUN_C20_V6 | 0.00 | 0.01 | 0.16 | 0.00 | 0.00 | 0.04 | 0.00 | 0.00 | 0.04 |
| DS_FUN_C25_V7 | 0.00 | 0.41 | 0.26 | 0.00 | 0.00 | 0.06 | 0.00 | 0.00 | 0.07 |
| DS_FUN_C35_V13 | 0.00 | 1.03 | 0.59 | 0.00 | 0.01 | 0.21 | 0.00 | 0.00 | 0.19 |
| DS_FUN_C50_V20 | 0.04 | 0.48 | 1.41 | -0.11 | -0.01 | 0.58 | -0.14 | -0.14 | 0.39 |
| DS_FUN_C70_V30 | 0.00 | 0.28 | 3.55 | -0.23 | -0.11 | 1.38 | -0.31 | -0.31 | 0.90 |
| DS_FUN_C90_V40 | 0.00 | 0.60 | 7.01 | -0.37 | -0.27 | 3.27 | -0.50 | -0.50 | 1.95 |
| DS_FUN_C100_V50 | 0.00 | 0.60 | 9.85 | -0.34 | -0.20 | 4.77 | -0.46 | -0.46 | 2.63 |
| Avg | 0.00 | 0.29 | 1.93 | -0.09 | -0.05 | 0.87 | -0.12 | -0.12 | 0.52 |

Table 4.6: Comparison with Hemmati & Hvattum (2016).

| | **ALNS-1** | | | **ALNS-2** | | | **ALNS-3** | | | **ALNS-4** | | | **ALNS-5** | | | **ALNS-6** | | | **HGS-NO** | | | **HGS-SP** | | |
|---|---|---|---|---|---|---|---|---|---|---|---|---|---|---|---|---|---|---|---|---|---|---|---|---|
| Group | Best | Avg | T | Best | Avg | T | Best | Avg | T | Best | Avg | T | Best | Avg | T | Best | Avg | T | Best | Avg | T | Best | Avg | T |
| SS_MUN_C22_V6 | 0.00 | 0.29 | 0.18 | 0.00 | 0.29 | 0.20 | 0.00 | 0.23 | 0.19 | 0.00 | 0.17 | 0.19 | 0.00 | 0.35 | 0.20 | 0.00 | 0.53 | 0.18 | 0.00 | 0.00 | 0.14 | 0.00 | 0.00 | 0.14 |
| SS_MUN_C23_V13 | 0.51 | 0.81 | 0.25 | 0.00 | 0.34 | 0.25 | 0.00 | 0.35 | 0.26 | 0.00 | 0.28 | 0.26 | 0.02 | 0.23 | 0.25 | 0.00 | 0.46 | 0.25 | 0.00 | 0.07 | 0.20 | 0.00 | 0.00 | 0.18 |
| SS_MUN_C30_V6 | 0.17 | 1.32 | 0.35 | 0.00 | 0.66 | 0.40 | 0.10 | 1.14 | 0.41 | 0.00 | 0.90 | 0.42 | 0.00 | 1.04 | 0.39 | 0.00 | 1.94 | 0.38 | 0.00 | 0.00 | 0.28 | 0.00 | 0.00 | 0.26 |
| SS_MUN_C35_V7 | 0.65 | 1.40 | 0.51 | 0.13 | 1.51 | 0.58 | 0.36 | 1.69 | 0.58 | 0.17 | 1.21 | 0.58 | 0.02 | 1.03 | 0.55 | 0.29 | 1.97 | 0.53 | 0.14 | 0.37 | 0.44 | 0.00 | 0.01 | 0.38 |
| SS_MUN_C60_V13 | 1.02 | 2.28 | 2.05 | 0.58 | 1.69 | 2.18 | 1.22 | 2.23 | 2.29 | 0.66 | 1.70 | 2.42 | 0.69 | 2.02 | 2.06 | 0.28 | 1.21 | 1.95 | -0.48 | -0.08 | 1.64 | -0.59 | -0.53 | 1.35 |
| DS_MUN_C22_V6 | 0.09 | 0.35 | 0.18 | 0.00 | 0.31 | 0.19 | 0.00 | 0.15 | 0.20 | 0.00 | 0.15 | 0.20 | 0.00 | 0.19 | 0.19 | 0.00 | 1.66 | 0.18 | 0.00 | 0.00 | 0.14 | 0.00 | 0.00 | 0.14 |
| DS_MUN_C23_V13 | 0.00 | 0.00 | 0.26 | 0.00 | 0.00 | 0.26 | 0.00 | 0.02 | 0.28 | 0.00 | 0.01 | 0.28 | 0.00 | 0.00 | 0.25 | 0.00 | 0.00 | 0.24 | 0.00 | 0.00 | 0.15 | 0.00 | 0.00 | 0.15 |
| DS_MUN_C30_V6 | 0.38 | 0.67 | 0.36 | 0.06 | 0.34 | 0.42 | 0.13 | 0.36 | 0.42 | 0.00 | 0.34 | 0.42 | 0.30 | 0.42 | 0.39 | 0.16 | 0.58 | 0.37 | 0.13 | 0.18 | 0.28 | 0.00 | 0.01 | 0.26 |
| DS_MUN_C35_V7 | 0.30 | 0.60 | 0.52 | 0.13 | 0.50 | 0.60 | 0.10 | 0.49 | 0.60 | 0.13 | 0.57 | 0.63 | 0.01 | 0.37 | 0.54 | 0.20 | 0.68 | 0.51 | -0.01 | 0.02 | 0.39 | -0.01 | -0.01 | 0.32 |
| DS_MUN_C60_V13 | 2.22 | 3.36 | 2.18 | 0.78 | 2.50 | 2.41 | 0.77 | 3.10 | 2.39 | 0.58 | 3.10 | 2.39 | 0.47 | 2.23 | 1.99 | 0.09 | 2.41 | 1.85 | -0.47 | 0.02 | 2.03 | -0.97 | -0.97 | 1.22 |
| Avg | 0.53 | 1.11 | 0.68 | 0.17 | 0.81 | 0.75 | 0.27 | 0.98 | 0.76 | 0.15 | 0.84 | 0.78 | 0.15 | 0.79 | 0.68 | 0.10 | 1.14 | 0.64 | -0.07 | 0.06 | 0.57 | -0.16 | -0.15 | 0.44 |

**Branch-and-price.** We compared our B&P results against the results obtained from the ITSRSP mathematical formulation evaluated in Hemmati et al. (2014) with a commercial solver (MIP). The CPU time of both methods was bounded to one hour. Aggregated results are shown in Tables 4.7 to 4.10. Columns "LB Imp" and "UB Imp" represent the average relative improvement of the lower and upper bound of each instance group (in percentage), column "Opt" represents the number of optimal solutions found for each instance group, and column "T" represents the average execution time (in minutes). The results found by the B&P are largely better than the ones found by previous work: huge lower and upper bound improvements are achieved, all full cargo instances are closed, and the number of open instances went from 123 to 17. Detailed results for the B&P are shown in Tables A.5 to A.8.

Table 4.7: Comparison with Hemmati et al. (2014) on SS_MUN instances.

| | | | **MIP** | | **B&P** | |
|---|---|---|---|---|---|---|
| | LB Imp | UB Imp | Opt | T | Opt | T |
| SS_MUN_C7_V3 | 0.00 | 0.00 | 5 | 0.00 | 5 | 0.00 |
| SS_MUN_C10_V3 | 0.00 | 0.00 | 5 | 0.01 | 5 | 0.00 |
| SS_MUN_C15_V4 | 0.00 | 0.00 | 5 | 1.42 | 5 | 0.00 |
| SS_MUN_C18_V5 | 2.12 | 0.93 | 4 | 42.50 | 5 | 0.00 |
| SS_MUN_C22_V6 | 12.70 | 2.84 | 1 | 50.63 | 5 | 0.01 |
| SS_MUN_C23_V13 | 16.60 | 14.88 | 0 | 59.99 | 5 | 0.14 |
| SS_MUN_C30_V6 | 29.56 | 71.08 | 0 | 59.99 | 5 | 0.10 |
| SS_MUN_C35_V7 | 34.95 | 73.34 | 0 | 59.99 | 5 | 0.42 |
| SS_MUN_C60_V13 | 37.92 | 76.68 | 0 | 60.01 | 5 | 14.83 |
| SS_MUN_C80_V20 | 43.64 | 76.35 | 0 | 60.05 | 5 | 10.16 |
| SS_MUN_C100_V30 | 89.43 | 77.89 | 0 | 60.25 | 2 | 44.03 |
| SS_MUN_C130_V40 | 99.76 | 77.90 | 0 | 61.52 | 0 | 60.00 |
| Average / Total | 30.56 | 39.33 | 20 | 43.03 | 52 | 10.81 |



### 4.3.4 Hybrid genetic search adaptations and performance on related problems

We validated the HGS on the PDPTW, the Vehicle Routing Problem with Time Windows (VRPTW) and the CVRP against Ropke & Pisinger (2006), Vidal et al. (2013), and Vidal et al. (2012), respectively.

We used some specialized components to solve each problem variant. In the VRPTW and the CVRP, (a) our neighborhoods are the same as Prins (2004), (b) Split is constrained to arcs with at most twice the maximum vehicle capacity. Whenever no shortest path is found, the value is permanently scaled by 1.1, and (c) we use the classical OX crossover (Prins, 2004). Some CVRP instances have a maximum route duration constraint. We penalized the excess of route duration in the same way as the capacity violation. To achieve

Table 4.8: Comparison with Hemmati et al. (2014) on SS_FUN instances.

| | | | **MIP** | | **B&P** | |
|---|---|---|---|---|---|---|
| | LB Imp | UB Imp | Opt | T | Opt | T |
| SS_FUN_C8_V3 | 0.00 | 0.00 | 5 | 0.00 | 5 | 0.00 |
| SS_FUN_C11_V4 | 0.00 | 0.00 | 5 | 0.01 | 5 | 0.00 |
| SS_FUN_C13_V5 | 0.00 | 0.00 | 5 | 0.00 | 5 | 0.00 |
| SS_FUN_C16_V6 | 0.00 | 0.00 | 5 | 0.01 | 5 | 0.00 |
| SS_FUN_C17_V13 | 0.00 | 0.00 | 5 | 0.02 | 5 | 0.00 |
| SS_FUN_C20_V6 | 0.00 | 0.00 | 5 | 0.80 | 5 | 0.00 |
| SS_FUN_C25_V7 | 0.87 | 0.00 | 3 | 40.47 | 5 | 0.00 |
| SS_FUN_C35_V13 | 8.02 | 0.56 | 0 | 60.00 | 5 | 0.00 |
| SS_FUN_C50_V20 | 12.05 | 2.01 | 0 | 60.01 | 5 | 0.01 |
| SS_FUN_C70_V30 | 14.24 | 61.02 | 0 | 60.06 | 5 | 0.03 |
| SS_FUN_C90_V40 | 17.84 | 73.65 | 0 | 60.29 | 5 | 0.22 |
| SS_FUN_C100_V50 | 22.35 | 73.15 | 0 | 60.85 | 5 | 1.02 |
| Average / Total | 6.28 | 17.53 | 33 | 28.54 | 60 | 0.11 |

Table 4.9: Comparison with Hemmati et al. (2014) on DS_MUN instances.

| | | | **MIP** | | **B&P** | |
|---|---|---|---|---|---|---|
| | LB Imp | UB Imp | Opt | T | Opt | T |
| DS_MUN_C7_V3 | 0.00 | 0.00 | 5 | 0.01 | 5 | 000 |
| DS_MUN_C10_V3 | 0.00 | 0.00 | 5 | 0.01 | 5 | 0.00 |
| DS_MUN_C15_V4 | 0.00 | 0.00 | 5 | 0.35 | 5 | 0.00 |
| DS_MUN_C18_V5 | 1.61 | 0.00 | 4 | 16.32 | 5 | 0.00 |
| DS_MUN_C22_V6 | 2.77 | 0.09 | 4 | 26.16 | 5 | 0.00 |
| DS_MUN_C23_V13 | 3.76 | 0.09 | 3 | 26.38 | 5 | 0.00 |
| DS_MUN_C30_V6 | 31.55 | 49.87 | 0 | 60.00 | 5 | 0.03 |
| DS_MUN_C35_V7 | 31.70 | 52.55 | 0 | 60.01 | 5 | 0.04 |
| DS_MUN_C60_V13 | 53.58 | 76.90 | 0 | 60.03 | 5 | 3.84 |
| DS_MUN_C80_V20 | 61.56 | 78.17 | 0 | 60.06 | 4 | 15.10 |
| DS_MUN_C100_V30 | 95.88 | 76.91 | 0 | 60.27 | 2 | 42.97 |
| DS_MUN_C130_V40 | 99.99 | 79.00 | 0 | 61.29 | 0 | 60.00 |
| Average / Total | 31.87 | 34.46 | 26 | 35.91 | 51 | 10.16 |



Table 4.10: Comparison with Hemmati et al. (2014) on DS_FUN instances.

| | | | **MIP** | | **B&P** | |
|---|---|---|---|---|---|---|
| | LB Imp | UB Imp | Opt | T | Opt | T |
| DS_FUN_C8_V3 | 0.00 | 0.00 | 5 | 0.01 | 5 | 0.00 |
| DS_FUN_C11_V4 | 0.00 | 0.00 | 5 | 0.01 | 5 | 0.00 |
| DS_FUN_C13_V5 | 0.00 | 0.00 | 5 | 0.01 | 5 | 0.00 |
| DS_FUN_C16_V6 | 0.00 | 0.00 | 5 | 0.01 | 5 | 0.00 |
| DS_FUN_C17_V13 | 0.00 | 0.00 | 5 | 0.02 | 5 | 0.00 |
| DS_FUN_C20_V6 | 0.00 | 0.00 | 5 | 0.02 | 5 | 0.00 |
| DS_FUN_C25_V7 | 0.00 | 0.00 | 5 | 0.13 | 5 | 0.00 |
| DS_FUN_C35_V13 | 4.18 | 0.27 | 2 | 45.55 | 5 | 0.00 |
| DS_FUN_C50_V20 | 7.87 | 0.91 | 1 | 56.25 | 5 | 0.00 |
| DS_FUN_C70_V30 | 10.07 | 1.50 | 0 | 60.07 | 5 | 0.01 |
| DS_FUN_C90_V40 | 11.74 | 47.49 | 0 | 60.25 | 5 | 0.10 |
| DS_FUN_C100_V50 | 14.99 | 54.60 | 0 | 60.51 | 5 | 0.03 |
| Average / Total | 4.07 | 8.73 | 38 | 23.57 | 60 | 0.01 |

similar execution time to results on previous subproblems, we set $(It_{NI}, T_{\max})$ as $(2.5 \cdot 10^3, \infty)$ for the PDPTW, $(5 \cdot 10^3, \infty)$ for the VRPTW, and $(10^4, \infty)$ for the CVRP.

**Giant tour ordering.** For problems with a homogeneous fleet (PDPTW, VRPTW, and CVRP), after local search, the giant tour of a solution is obtained from the ordered concatenation of routes, according to the polar angle of their centroids.

**Multistage optimization for the PDPTW and the VRPTW.** Traditionally, the PDPTW and VRPTW have a hierarchical objective of minimizing fleet size first and travel cost second. We used a two-stage optimization approach to address this objective, as in Vidal et al. (2013). To minimize the fleet size, we iteratively run the HGS constraining solutions to at most $m$ routes (initially set to a big value). As soon as a feasible solution is found, $m$ is decremented and the search starts again, until no feasible solution is found. During the fleet minimization phase, all routes are inserted into the SP formulation, regardless of feasibility, and their cost corresponds to the sum of all infeasibilities. Then, we run the second optimization stage constraining the number of routes with the best feasible value of $m$ found. We always reuse the population from the previous HGS call. We use the same parameters for all HGS calls.

**Results for the PDPTW.** We compared our results against the Adaptive Large Neighborhood Search (ALNS) of Ropke & Pisinger (2006) (RP) on the Li & Lim (2003) benchmark instances. Average results over 10 runs are shown in Table 4.11, and are grouped according to instance size. Columns "CNV" and "CTD" give the cumulative number of vehicles and the cumulative travel distance, while column "T" gives the average CPU time (in minutes). On average, for instances with size 100 and 200, the HGS-SP outperformed the ALNS. For instances with size 400, the HGS-SP performed almost as well as the ALNS.

Table 4.11: Results on Li & Lim (2003) PDPTW instances.

| | **RP** | | | **HGS-SP** | | |
|---|---|---|---|---|---|---|
| n | CNV | CTD | T | CNV | CTD | T |
| 100 | 403.00 | 58249.42 | 1.10 | 402.00 | 58060.15 | 0.49 |
| 200 | 608.10 | 181707.35 | 4.40 | 606.00 | 182177.89 | 3.08 |
| 400 | 1167.80 | 425816.87 | 14.68 | 1168.00 | 428989.38 | 19.29 |
| | Pentium IV 1.5GHz | | | i7-3960X 3.3GHz | | |

**Results for the VRPTW.** We evaluated our method with the Solomon

& Desrosiers (1988) and Gehring & Homberger (1999) VRPTW benchmark instances. We compared our results against the HGSADC of Vidal et al. (2013). Average results over five runs are shown in Table 4.12, and are grouped according to instance size. Columns "CNV" and "CTD" give the cumulative number of vehicles and the cumulative travel distance, while column "T" gives the CPU time (in minutes). On average, for instances with size 100, the HGS-SP outperformed HGSADC. For instances with size 200 and 400, the HGS-SP performed almost as well as the HGSADC.

Table 4.12: Results on Solomon & Desrosiers (1988) and Gehring & Homberger (1999) VRPTW instances.

| | **HGSADC** | | | **HGS-SP** | | |
|---|---|---|---|---|---|---|
| n | CNV | CTD | T | CNV | CTD | T |
| 100 | 405.00 | 57218.00 | 2.68 | 405.00 | 57209.70 | 1.81 |
| 200 | 694.00 | 168407.00 | 8.40 | 694.00 | 168585.64 | 7.40 |
| 400 | 1382.00 | 388697.00 | 34.10 | 1382.20 | 391079.52 | 41.30 |
| | Xe-2.93G | | | i7-3960X 3.3GHz | | |



**Results for the CVRP.** We evaluated our method on Christofides et al. (1979) (*CMT*) and Golden et al. (1998) (*Golden*) CVRP benchmark instances and compared our results against the HGSADC of Vidal et al. (2012). Results over 10 runs are shown in Table 4.13. Column "Gap" gives the gap of the average solution (in percentage) to the BKS, and column "T" gives the average execution time (in minutes). The HGS-SP results are nearly as good as the HGSADC results.

Table 4.13: Results on Christofides et al. (1979) and Golden et al. (1998) CVRP instances.

| | **HGSADC** | | **HGS-SP** | |
|---|---|---|---|---|
| Group | Gap | T | Gap | T |
| CMT | 0.05 | 2.21 | 0.06 | 3.43 |
| Golden | 0.28 | 28.53 | 0.38 | 22.83 |
| Avg | 0.16 | 15.37 | 0.22 | 13.13 |
| | Pentium IV 3.0GHz | | i7-3960X 3.3GHz | |

# 5
# Joint Ship Speed Optimization and Heuristics

Fuel consumption is a significant component of the operating costs of ships (Psaraftis & Kontovas, 2013). The fuel consumption per time unit of ships can be approximated by a cubic function of speed (Ronen, 1982), meaning that different speeds can considerably change the costs associated with fuel consumption. Speed optimization is notably relevant for the shipping industry: operators often sail at slow speeds (*slow steaming*) to minimize fuel costs when there is an oversupply of shipping capacity in the market (Ronen, 1982). However, most routing models assume a constant speed, making it impossible to efficiently explore the trade-off between routing decisions and fuel consumption. Other factors may also contribute to fuel consumption, such as the ship payload, weather conditions, and the ship machinery type (Psaraftis & Kontovas, 2013). Overall, the integration of speed decisions into the routing process and the evaluation of fuel costs based on speed (and other factors) may lead to a better fleet utilization and increased profits.

In this work, we study heuristic methods for a ship routing problem where the speed on each sailing leg (route segment) is a decision variable, and fuel consumption is a convex function of speed and payload. The studied problem is referred to as the Industrial and Tramp Ship Routing and Scheduling Problem with Speed Optimization (ITSRSPSO), and it extends the Industrial and Tramp Ship Routing and Scheduling Problem (ITSRSP) with speed decisions. The influence of payload on fuel consumption extends previous work (Norstad et al., 2011), and results in leg-dependent fuel consumption functions, as the load on board of the ship changes at every port visit.

The problem of finding the optimal speed for each segment of a route is referred to as the Speed Optimization Problem (SOP). The SOP with fuel consumption functions and time-window constraints can be viewed as a Resource Allocation Problem with Nested Constraints (RAP-NC), where a time budget is allocated on sailing legs. If the fuel consumption functions are convex, the RAP-NC can be solved in $\mathcal{O}(n \log m \log \frac{nB}{\epsilon})$ with the Monotonic Decomposition Algorithm (MDA) of Vidal et al. (2017). We propose an extension of the Hybrid Genetic Search (HGS) described in Section 4.1 for the ITSRSPSO. This extension uses the MDA to solve the SOP on every local

search move evaluation.

## 5.1 Hybrid Genetic Search with Optimal Speed Decisions

We propose a local search framework inside the HGS where all time-window feasible routes have optimal speed decisions. As our moves always involve one or two routes, we must solve at most two SOPs every time a move is evaluated. We discuss how to find optimal speed decisions on fixed routes, then propose lower bounds for move evaluations, and finally describe how to extend the HGS.

### 5.1.1 Optimization of speed decisions on a fixed route

We now consider the SOP on a fixed route $r = (r_1, \ldots, r_n)$, serviced by ship $k$. Let $w_i$ be a constant that represents the proportion of maximum load on board the ship before arriving node $r_i$ (with $w_1 = 0$). The RAP-NC formulation of the SOP is shown in Eqs. (5-1) to (5-4), where: (a) $F_c$ is the fuel cost per tonne, (b) $v_i$ is the speed (in knots) used to sail from node $r_{i-1}$ to $r_i$, (c) $\ell^k_{ij}$ is the travel distance between the two nodes (in nautical miles), and (d) $B$ is the total time budget that can be allocated, and is equal to the latest feasible arrival time at the last node of $r$. Next, we describe two algorithms for solving the SOP.

$$\min\ f(\mathbf{x}) = F_c \sum_{i=1}^{n} f^k_{r_{i-1},r_i}(v_i, w_i) \tag{5-1}$$

$$\text{s.t.}\quad a_i \leq \sum_{j=1}^{i} \frac{\ell^k_{r_{j-1},r_j}}{v_j} \leq b_i \qquad i \in \{1, \ldots, m-1\} \tag{5-2}$$

$$\sum_{i=1}^{n} \frac{\ell^k_{r_{i-1},r_i}}{v_i} = B \tag{5-3}$$

$$v^k_{\min} \leq v_i \leq v^k_{\max} \qquad i \in \{1, \ldots, n\}. \tag{5-4}$$

**A discretized arrival times algorithm.** A Discretized Arrival Times (DAT) algorithm can be used to solve the SOP on a route $r$ (Fagerholt et al., 2010). We build a directed acyclic graph $G_r = (V_r, A_r)$ where route visits are replicated with discretized arrival times over their respective time windows. A node $(r_i, t) \in V_r$ represents an arrival at $r_i$ at time $t \in [a_{r_i}, b_{r_i}]$. An edge $((r_{i-1}, t), (r_i, t')) \in A_r$ represents a trip from node $r_{i-1}$ to $r_i$ in $t' - t$ hours, at speed $v_i = \frac{\ell^k_{r_{i-1},r_i}}{t'-t}$, with a cost $F_c f^k_{r_{i-1},r_i}(v_i, w_i)$. We connect a source node to all nodes $(r_1, t), \forall t$, and all nodes $(r_{|r|}, t), \forall$ to a sink node, and obtain the shortest

path from source to sink to solve the SOP. The complexity of this algorithm is $\mathcal{O}(|V_r|^2)$, where the size of $V_r$ depends on the number of replicated nodes.

**A monotonic decomposition algorithm.** The MDA is a divide-and-conquer algorithm that solves four Resource Allocation Problem (RAP) subproblems on each node of the recursion tree. The RAP formulations are equivalent to a RAP-NC due to variable bounds obtained from optimal solutions deeper into the recursion tree. To solve a RAP subproblem, we adopt a simple strategy that performs a binary search over its single dual variable (Patriksson, 2008). The MDA has a complexity of $\mathcal{O}(n \log m \log \frac{nB}{\epsilon})$, where $n$ is the route size, $m$ is the number of nested time-window constraints (in our case, $n = m$), $B$ is the total time budget, and $\epsilon$ is a tolerance parameter.

**Service cost and time.** For a fixed route, service costs $s^{\mathrm{C}}_{ik}$ are always constant. Thus, they are not taken into consideration during the speed optimization. Service times can be represented by manipulating the RAP-NC formulation: for every node $r_i, i = 1, \ldots, n$, we calculate the sum of previous service times $S_{i-1} = \sum_{j=1}^{i-1} s^{\mathrm{D}}_{r_j k}$ and set $a_i \leftarrow a_i - S_{i-1}$ and $b_i \leftarrow b_i - S_{i-1}$.

**Waiting times.** Ships have a minimum and maximum sailing speed. Therefore, they may wait on an early arrival due to a combination of speed bounds and time windows. This leads to fuel consumption functions that are not strictly-convex ($if\ v < v^k_{\min}, f^k_{ij}(v, w) = f^k_{ij}(v^k_{\min}, w)$) in the RAP-NC formulation. Fortunately, both algorithms do not require strict convexity, and are therefore able to account for waiting times.

### 5.1.2 Local search

The speed of each leg is jointly optimized *on every local search move evaluation*. If a neighbor solution is time-window infeasible, the move is evaluated in $\mathcal{O}(1)$ using preprocessed information and route concatenation techniques. For this scenario, travel cost is obtained from the fuel consumption functions assuming maximum ship speed and full load. Otherwise, if a neighbor solution is time-window feasible, the optimal speed for each leg is found with the MDA.

**Lower bounds on move evaluations.** A significant amount of computational effort is necessary to solve the SOP on every move evaluation. To reduce this effort, we introduce a two-phase neighbor evaluation scheme. First, the move evaluation compares the cost of the current solution with a lower bound on the neighbor cost. If the lower bound is worse than the current solu-

tion, then the SOP is not solved. Otherwise, we run the MDA. We use the following lower bound: $v_i = v^k_{\min}, i = 1, \ldots, n$.

### 5.1.3 A hybrid genetic search extension

To solve the ITSRSPSO, we introduce an extension of the HGS described in Section 4.1. There are two components of the HGS that must be adapted: the local search used during education and repair, and the Split algorithm. We adapt the local search component with the methodology covered in Section 5.1. In the ITSRSP, the Split routes can be evaluated incrementally, thus, allowing a constant-time evaluation of route information. This is not the case for the ITSRSPSO, since the optimal speed decisions must be re-evaluated as the routes are incremented. Hence, every route evaluated by Split solves a SOP with the MDA.

## 5.2 Computational Experiments

We introduced a new set of ITSRSPSO instances based on the Hemmati et al. (2014) benchmark suite for the ITSRSP. Then, we compared the performance of the MDA and the DAT on fixed routes. Finally, we evaluated the HGS with joint speed optimization against a strategy that only optimizes the speed once at the end.

**Computational environment.** We used the same computational environment and parameters described in Section 4.3, and set a tolerance of $\epsilon = 1\text{e}{-5}$ for the MDA.

### 5.2.1 Benchmark instances

We generated ITSRSPSO instances based on the ITSRSP instances of Hemmati et al. (2014). As the ITSRSPSO is a heterogeneous ship routing problem, different ships may have different speed bounds and fuel consumption profiles. The type of any ship $k \in \{1, \ldots, m\}$ is specified by the instance files. This type defines the ship design speed $v^k_{\text{D}}$ and a ship-specific coefficient $\mu_k$, related to fuel consumption. These values are detailed in Table 5.1. Next, we describe how we adapted data from the original instances, and detail information related to speed bounds and fuel consumption.

**Arc lengths.** We assumed that the original ITSRSP travel time values $\delta^k_{ij}$ correspond to the time needed to sail an arc at design speed. Hence, we calculated the length of an arc $(i, j)^k \in A$ as follows: $\ell^k_{ij} = v^k_{\text{D}} \delta^k_{ij}$.

**Speed bounds.** We defined the minimum and maximum ship sailing speed as a proportion of its design speed. Thus, $v^k_{\min} = 0.6v^k_{\text{D}}$ and $v^k_{\max} = 1.2v^k_{\text{D}}$.

**Fuel consumption functions and fuel cost.** For any arc $(i,j)^k \in A$, we used fuel consumption functions in the form $f^k_{ij}(v,w) = \frac{1}{24}\mu_k v^2 \ell^k_{ij}(0.8 + 0.2w)$. We assumed a fuel cost per tonne of 590.

Table 5.1: Information for each ship type.

| | **Short sea** | | **Deep sea** | |
|---|---|---|---|---|
| Ship type | Design speed | Coefficient | Design speed | Coefficient |
| 1 | 13.5 | 0.0106 | 14.5 | 0.0148 |
| 2 | 14.5 | 0.0079 | 13.5 | 0.0126 |
| 3 | 12.0 | 0.0139 | 24.6 | 0.0134 |
| 4 | 13.2 | 0.0137 | 14.5 | 0.0164 |
| 5 | 13.5 | 0.0057 | 25.0 | 0.0160 |
| 6 | 13.0 | 0.0046 | 14.5 | 0.0197 |
| 7 | 12.5 | 0.0072 | 15.5 | 0.0250 |
| 8 | - | - | 15.5 | 0.0234 |



### 5.2.2 Evaluation of fixed routes

We evaluated both the MDA and the DAT algorithms on a set of 90 routes obtained from the ITSRSPSO instances. Route sizes vary between three and 19 nodes. There are 10 routes per instance size. We evaluated the DAT algorithm with three different discretization levels: 10, 50, and 100 (respectively, DAT-10, DAT-50, and DAT-100). Results over 5.000 runs are illustrated in Fig. 5.1 and detailed in Table 5.2. The reported numbers represent the average of all results for each instance group. Column "Gap" gives the gap to the best known solution (BKS), while column "T" gives the CPU time (in seconds). Our results show that the MDA has the best trade-off between solution quality and execution time. The solution quality of the MDA is always the best one, and its execution time is only dominated by the DAT-10. However, the DAT-10 has the worst gap to the BKS. Furthermore, as the DAT discretization level increases, the CPU time grows excessively. Therefore, the DAT is unfit for usage during local search.

### 5.2.3 Routing with joint speed optimization

We compared our HGS with joint speed optimization (HGS-J) against a version of the HGS that assumes a fixed speed and optimizes speed once at the

Figure 5.1: Comparison of MDA against DAT on fixed routes.

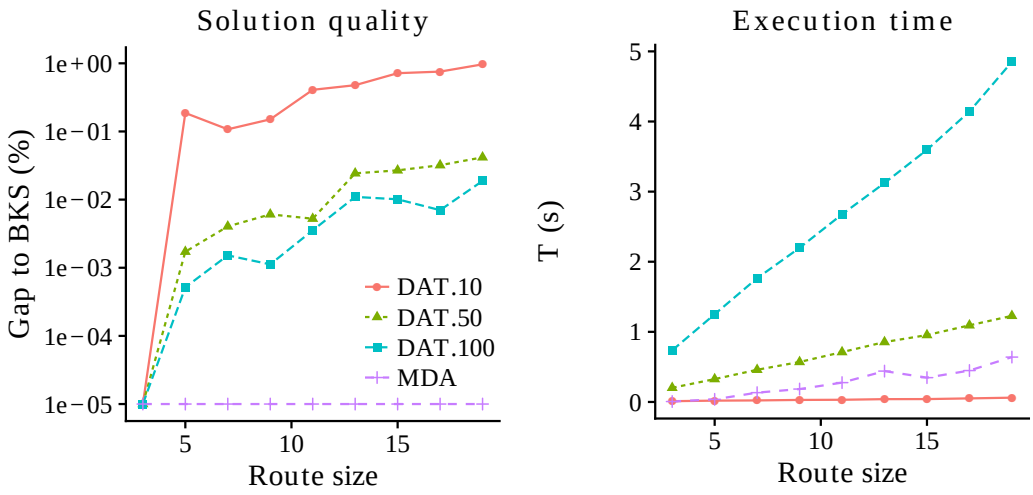


end (HGS-O). Both versions use the MDA as a SOP solver. Results are shown in Tables 5.3 to 5.6, and are grouped according to problem topology (short sea, deep sea) and cargo type (mixed load, full load). The reported numbers represent the average of all results for each instance group. Average values for the gap to the previously BKS (in percentage) and CPU time (in minutes) are respectively given by "Gap" and "T".

The average solution quality of the HGS-J is largely better than the one of HGS-O, with only a moderate increase (7.1×) of computational effort. Given the complexity of a tight integration of speed optimization and routing decisions in a metaheuristic, the observed CPU time is very satisfying. However, for instances with 30 cargoes or more, the HGS-J easily reaches the CPU time limit. Nevertheless, for most instance groups, the HGS-J results still outperform the HGS-O. But this is not the case for DS_MUN_C130_V40: the solutions found by the HGS-J have a gap of 8.78% to the BKS (found by the HGS-O). This happens because most of the CPU time is spent during the HGS-J population initialization, leaving little CPU time left to improve the solutions found. This scenario can be circumvented either by increasing the CPU time limit of the HGS-J, or by introducing further improvements into the SOP solver.

Table 5.2: Comparison of the MDA and DAT on fixed routes.

| | **DAT-10** | | **DAT-50** | | **DAT-100** | | **MDA** | |
|---|---|---|---|---|---|---|---|---|
| n | Gap | T | Gap | T | Gap | T | Gap | T |
| 3 | 0.00 | 0.01 | 0.00 | 0.20 | 0.00 | 0.74 | 0.00 | 0.01 |
| 5 | 0.19 | 0.02 | 0.00 | 0.33 | 0.00 | 1.25 | 0.00 | 0.04 |
| 7 | 0.11 | 0.02 | 0.00 | 0.46 | 0.00 | 1.76 | 0.00 | 0.13 |
| 9 | 0.15 | 0.03 | 0.01 | 0.57 | 0.00 | 2.20 | 0.00 | 0.18 |
| 11 | 0.41 | 0.03 | 0.01 | 0.71 | 0.00 | 2.68 | 0.00 | 0.28 |
| 13 | 0.48 | 0.04 | 0.02 | 0.85 | 0.01 | 3.12 | 0.00 | 0.44 |
| 15 | 0.72 | 0.04 | 0.03 | 0.95 | 0.01 | 3.60 | 0.00 | 0.35 |
| 17 | 0.76 | 0.05 | 0.03 | 1.09 | 0.01 | 4.14 | 0.00 | 0.45 |
| 19 | 0.97 | 0.06 | 0.04 | 1.23 | 0.02 | 4.85 | 0.00 | 0.64 |
| Avg | 0.42 | 0.03 | 0.02 | 0.71 | 0.01 | 2.70 | 0.00 | 0.28 |



Table 5.3: Evaluation of the impact of joint speed optimization on ITSRSPSO SS_MUN instances.

| | **HGS-O** | | | **HGS-J** | | |
|---|---|---|---|---|---|---|
| Group | Best | Avg | T | Best | Avg | T |
| SS_MUN_C7_V3 | 1.75 | 1.90 | 0.02 | 0.00 | 0.00 | 0.31 |
| SS_MUN_C10_V3 | 3.21 | 3.25 | 0.04 | 0.00 | 0.00 | 0.94 |
| SS_MUN_C15_V4 | 7.63 | 8.21 | 0.08 | 0.00 | 0.00 | 3.64 |
| SS_MUN_C18_V5 | 8.94 | 9.14 | 0.12 | 0.00 | 0.00 | 5.49 |
| SS_MUN_C22_V6 | 8.14 | 8.25 | 0.17 | 0.00 | 0.00 | 8.23 |
| SS_MUN_C23_V13 | 5.09 | 5.30 | 0.19 | 0.00 | 0.00 | 5.79 |
| SS_MUN_C30_V6 | 10.07 | 10.24 | 0.30 | 0.00 | 0.15 | 15.00 |
| SS_MUN_C35_V7 | 7.65 | 7.95 | 0.46 | 0.00 | 0.32 | 15.00 |
| SS_MUN_C60_V13 | 9.52 | 10.23 | 1.53 | 0.00 | 1.00 | 15.01 |
| SS_MUN_C80_V20 | 5.95 | 6.45 | 3.61 | 0.00 | 0.88 | 15.02 |
| SS_MUN_C100_V30 | 5.38 | 5.75 | 5.76 | 0.00 | 0.28 | 15.02 |
| SS_MUN_C130_V40 | 4.61 | 5.29 | 12.48 | 0.00 | 0.49 | 15.03 |
| Avg | 6.49 | 6.83 | 2.06 | 0.00 | 0.26 | 9.54 |

Table 5.4: Evaluation of the impact of joint speed optimization on ITSRSPSO SS_FUN instances.

| | **HGS-O** | | | **HGS-J** | | |
|---|---|---|---|---|---|---|
| Group | Best | Avg | T | Best | Avg | T |
| SS_FUN_C8_V3 | 3.83 | 3.83 | 0.01 | 0.00 | 0.00 | 0.45 |
| SS_FUN_C11_V4 | 9.31 | 9.31 | 0.02 | 0.00 | 0.00 | 1.20 |
| SS_FUN_C13_V5 | 6.28 | 6.65 | 0.03 | 0.00 | 0.00 | 1.41 |
| SS_FUN_C16_V6 | 4.56 | 4.83 | 0.04 | 0.00 | 0.00 | 2.14 |
| SS_FUN_C17_V13 | 6.06 | 6.84 | 0.06 | 0.00 | 0.00 | 1.65 |
| SS_FUN_C20_V6 | 10.03 | 11.10 | 0.05 | 0.00 | 0.00 | 4.55 |
| SS_FUN_C25_V7 | 8.61 | 9.08 | 0.08 | 0.00 | 0.00 | 8.17 |
| SS_FUN_C35_V13 | 8.55 | 9.16 | 0.21 | 0.00 | 0.00 | 14.59 |
| SS_FUN_C50_V20 | 10.19 | 10.99 | 0.55 | 0.00 | 0.00 | 15.04 |
| SS_FUN_C70_V30 | 12.40 | 12.82 | 1.43 | 0.00 | 0.72 | 15.01 |
| SS_FUN_C90_V40 | 12.26 | 12.92 | 2.78 | 0.00 | 0.28 | 15.01 |
| SS_FUN_C100_V50 | 16.68 | 17.30 | 3.73 | 0.00 | 0.12 | 15.01 |
| Avg | 9.06 | 9.57 | 0.75 | 0.00 | 0.09 | 7.85 |



Table 5.5: Evaluation of the impact of joint speed optimization on ITSRSPSO DS_MUN instances.

| | **HGS-O** | | | **HGS-J** | | |
|---|---|---|---|---|---|---|
| Group | Best | Avg | T | Best | Avg | T |
| DS_MUN_C7_V3 | 4.02 | 4.11 | 0.02 | 0.00 | 0.00 | 0.39 |
| DS_MUN_C10_V3 | 5.26 | 5.34 | 0.03 | 0.00 | 0.00 | 0.90 |
| DS_MUN_C15_V4 | 7.79 | 7.84 | 0.07 | 0.00 | 0.00 | 3.86 |
| DS_MUN_C18_V5 | 10.06 | 10.08 | 0.11 | 0.00 | 0.00 | 5.90 |
| DS_MUN_C22_V6 | 17.32 | 17.52 | 0.16 | 0.00 | 0.00 | 9.08 |
| DS_MUN_C23_V13 | 11.33 | 11.80 | 0.19 | 0.00 | 0.00 | 5.37 |
| DS_MUN_C30_V6 | 11.86 | 12.81 | 0.27 | 0.00 | 0.07 | 15.06 |
| DS_MUN_C35_V7 | 8.92 | 9.39 | 0.37 | 0.00 | 0.69 | 15.01 |
| DS_MUN_C60_V13 | 8.58 | 9.15 | 1.62 | 0.00 | 1.99 | 15.03 |
| DS_MUN_C80_V20 | 16.45 | 18.65 | 3.54 | 0.00 | 1.47 | 15.02 |
| DS_MUN_C100_V30 | 12.45 | 13.38 | 8.36 | 0.00 | 1.04 | 15.03 |
| DS_MUN_C130_V40 | 0.00 | 0.97 | 15.08 | 8.78 | 12.60 | 15.06 |
| Avg | 9.50 | 10.09 | 2.48 | 0.73 | 1.49 | 9.64 |

Table 5.6: Evaluation of the impact of joint speed optimization on ITSRSPSO DS_FUN instances.

| | **HGS-O** | | | **HGS-J** | | |
|---|---|---|---|---|---|---|
| Group | Best | Avg | T | Best | Avg | T |
| DS_FUN_C8_V3 | 8.72 | 8.72 | 0.01 | 0.00 | 0.00 | 0.56 |
| DS_FUN_C11_V4 | 15.41 | 15.41 | 0.02 | 0.00 | 0.00 | 1.16 |
| DS_FUN_C13_V5 | 2.82 | 2.92 | 0.03 | 0.00 | 0.00 | 1.62 |
| DS_FUN_C16_V6 | 12.59 | 12.76 | 0.04 | 0.00 | 0.00 | 2.58 |
| DS_FUN_C17_V13 | 10.79 | 11.16 | 0.06 | 0.00 | 0.00 | 2.07 |
| DS_FUN_C20_V6 | 9.96 | 10.40 | 0.05 | 0.00 | 0.00 | 5.03 |
| DS_FUN_C25_V7 | 8.73 | 9.60 | 0.08 | 0.00 | 0.00 | 9.86 |
| DS_FUN_C35_V13 | 9.70 | 9.81 | 0.26 | 0.00 | 0.00 | 15.05 |
| DS_FUN_C50_V20 | 18.12 | 18.48 | 0.63 | 0.00 | 0.03 | 15.04 |
| DS_FUN_C70_V30 | 20.92 | 21.20 | 1.48 | 0.00 | 0.48 | 15.01 |
| DS_FUN_C90_V40 | 17.15 | 17.56 | 3.23 | 0.00 | 0.64 | 15.02 |
| DS_FUN_C100_V50 | 19.82 | 20.05 | 4.43 | 0.00 | 0.51 | 15.03 |
| Avg | 12.89 | 13.17 | 0.86 | 0.00 | 0.14 | 8.17 |

# 6
# Concluding Remarks

In this work, we explored heuristic and exact solution methodologies for a routing problem with important applications in the shipping industry. We showed how successful methodologies for related routing problems can be adapted to efficiently solve ship routing problems. We conducted extensive computational experiments on a set of benchmark instances based on real shipping segments. The results found demonstrate that our methodologies largely outperform the state-of-the-art heuristic and exact methods for the ITSRSP.

Then, we extended our heuristic method to solve a ship routing problem extension where speed is a decision variable. Our results demonstrated that a joint speed and routing optimization methodology is highly profitable from an operational cost perspective. As the model becomes richer with details, it better represents reality, with the drawback of increasing the complexity to solve it. Thus, the need for efficient algorithms becomes clear, and solving such model is only made possible with the use of an efficient linearithmic algorithm such as the MDA.

A promising research venue remains open: being a divide-and-conquer algorithm, the MDA can be adapted to work on preprocessed subsequence information, similar to the concatenation-based move evaluations presented in Section 4.1.4. This may allow the pruning of the MDA recursion tree, and contribute to significant CPU time improvements.

# Bibliography


Andersson, H., Christiansen, M. & Fagerholt, K. (2011), 'The maritime pickup and delivery problem with time windows and split loads', *INFOR: Information Systems and Operational Research* **49**(2), 79–91.

Baldacci, R., Mingozzi, A. & Roberti, R. (2011), 'New route relaxation and pricing strategies for the vehicle routing problem', *Operations Research* **59**(5), 1269–1283.

Borthen, T., Loennechen, H., Wang, X., Fagerholt, K. & Vidal, T. (2017), 'A genetic search-based heuristic for a fleet size and periodic routing problem with application to offshore supply planning', *EURO Journal on Transportation and Logistics*.

Brønmo, G., Christiansen, M., Fagerholt, K. & Nygreen, B. (2007), 'A multi-start local search heuristic for ship scheduling—a computational study', *Computers & Operations Research* **34**(3), 900–917.

Brown, G. G., Graves, G. W. & Ronen, D. (1987), 'Scheduling ocean transportation of crude oil', *Management Science* **33**(3), 335–346.

Bulhões, T., Hà, M., Martinelli, R. & Vidal, T. (2018), 'The vehicle routing problem with service level constraints', *European Journal of Operational Research* **265**(2), 544–558.

Campos, V., Laguna, M. & Martí, R. (2005), 'Context-independent scatter and tabu search for permutation problems', *INFORMS Journal on Computing* **17**(1), 111–122.

Christiansen, M. & Fagerholt, K. (2014), Chapter 13: Ship routing and scheduling in industrial and tramp shipping, *in* P. Toth & D. Vigo, eds, 'Vehicle Routing', Society for Industrial and Applied Mathematics, pp. 381–408.

Christiansen, M., Fagerholt, K., Nygreen, B. & Ronen, D. (2007), Chapter 4 maritime transportation, *in* C. Barnhart & G. Laporte, eds, 'Transportation', Elsevier, pp. 189–284.

Christiansen, M., Fagerholt, K., Nygreen, B. & Ronen, D. (2013), 'Ship routing and scheduling in the new millennium', *European Journal of Operational Research* **228**(3), 467–483.

Christofides, N., Mingozzi, A. & Toth, P. (1979), The vehicle routing problem, *in* N. Christofides, A. Mingozzi, P. Toth & C. Sandi, eds, 'Combinatorial Optimization', Wiley, Chichester, pp. 315–338.

Christofides, N., Mingozzi, A. & Toth, P. (1981), 'Exact algorithms for the vehicle routing problem, based on spanning tree and shortest path relaxations', *Mathematical Programming* **20**, 255–282.

Contardo, C. & Martinelli, R. (2014), 'A new exact algorithm for the multi-depot vehicle routing problem under capacity and route length constraints', *Discrete Optimization* **12**, 129–146.

Duhamel, C., Gouinaud, C., Lacomme, P. & Prodhon, C. (2013), A multi-thread GRASPxELS for the heterogeneous capacitated vehicle routing problem, *in* E.-G. Talbi, ed., 'Hybrid Metaheuristics', Studies in Computational Intelligence, Springer Berlin Heidelberg, pp. 237–269.

Duhamel, C., Lacomme, P. & Prodhon, C. (2011), 'Efficient frameworks for greedy split and new depth first search split procedures for routing problems', *Computers & Operations Research* **38**(4), 723–739.

Dumas, Y., Desrosiers, J. & Soumis, F. (1991), 'The pickup and delivery problem with time windows', *European Journal of Operational Research* **54**(1), 7 – 22.

Fagerholt, K. & Christiansen, M. (2000*a*), 'A combined ship scheduling and allocation problem', *The Journal of the Operational Research Society* **51**(7), 834–842.

Fagerholt, K. & Christiansen, M. (2000*b*), 'A travelling salesman problem with allocation, time window and precedence constraints — an application to ship scheduling', *International Transactions in Operational Research* **7**(3), 231–244.

Fagerholt, K., Laporte, G. & Norstad, I. (2010), 'Reducing fuel emissions by optimizing speed on shipping routes', *Journal of the Operational Research Society* **61**(3), 523–529.

Fukasawa, R., He, Q., Santos, F. & Song, Y. (2016), 'A joint routing and speed optimization problem', *ArXiv e-prints*.

Fukasawa, R., Longo, H., Lysgaard, J., Poggi de Aragão, M., Reis, M., Uchoa, E. & Werneck, R. (2006), 'Robust branch-and-cut-and-price for the capacitated vehicle routing problem', *Mathematical Programming* **106**(3), 491–511.

Gehring, H. & Homberger, J. (1999), A parallel hybrid evolutionary metaheuristic for the vehicle routing problem with time windows, *in* 'Proceedings of EUROGEN99', Vol. 2, Springer Berlin, pp. 57–64.

Glover, F. & Hao, J.-K. (2009), 'The case for strategic oscillation', *Annals of Operations Research* **183**(1), 163–173.

Golden, B. L., Wasil, E. A., Kelly, J. P. & Chao, I.-M. (1998), The impact of metaheuristics on solving the vehicle routing problem: algorithms, problem sets, and computational results, *in* T. G. Crainic & G. Laporte, eds, 'Fleet Management and Logistics', Springer US, pp. 33–56.

Hemmati, A. & Hvattum, L. M. (2016), 'Evaluating the importance of randomization in adaptive large neighborhood search', *International Transactions in Operational Research* **24**(5), 929–942.

Hemmati, A., Hvattum, L. M., Fagerholt, K. & Norstad, I. (2014), 'Benchmark suite for industrial and tramp ship routing and scheduling problems', *INFOR: Information Systems and Operational Research* **52**(1), 28–38.

Irnich, S. (2008), 'A unified modeling and solution framework for vehicle routing and local search-based metaheuristics', *INFORMS Journal on Computing* **20**(2), 270–287.

Irnich, S. & Villeneuve, D. (2006), 'The shortest-path problem with resource constraints and k-cycle elimination for k $\geq$ 3', *INFORMS Journal on Computing* **18**(3), 391–406. ISSN 1526-5528.

Kindervater, G. A. & Savelsbergh, M. W. (1997), 'Vehicle routing: handling edge exchanges', *Local search in combinatorial optimization* pp. 337–360.

Korsvik, J. E., Fagerholt, K. & Laporte, G. (2009), 'A tabu search heuristic for ship routing and scheduling', *Journal of the Operational Research Society* **61**(4), 594–603.

Korsvik, J. E., Fagerholt, K. & Laporte, G. (2011), 'A large neighbourhood search heuristic for ship routing and scheduling with split loads', *Computers & Operations Research* **38**(2), 474–483.

Land, A. H. & Doig, A. G. (1960), 'An automatic method of solving discrete programming problems', *Econometrica* **28**(3), 497–520.

Li, H. & Lim, A. (2003), 'A metaheuristic for the pickup and delivery problem with time windows', *International Journal on Artificial Intelligence Tools* **12**(02), 173–186.

Nagata, Y., Bräysy, O. & Dullaert, W. (2010), 'A penalty-based edge assembly memetic algorithm for the vehicle routing problem with time windows', *Computers & Operations Research* **37**(4), 724–737.

Norstad, I., Fagerholt, K. & Laporte, G. (2011), 'Tramp ship routing and scheduling with speed optimization', *Transportation Research Part C: Emerging Technologies* **19**(5), 853–865.

Patriksson, M. (2008), 'A survey on the continuous nonlinear resource allocation problem', *European Journal of Operational Research* **185**(1), 1–46.

Prins, C. (2004), 'A simple and effective evolutionary algorithm for the vehicle routing problem', *Computers & Operations Research* **31**(12), 1985 – 2002.

Prins, C. (2009), 'Two memetic algorithms for heterogeneous fleet vehicle routing problems', *Engineering Applications of Artificial Intelligence* **22**(6), 916 – 928. Artificial Intelligence Techniques for Supply Chain Management.

Psaraftis, H. N. & Kontovas, C. A. (2013), 'Speed models for energy-efficient maritime transportation: a taxonomy and survey', *Transportation Research Part C: Emerging Technologies* **26**, 331–351.

Righini, G. & Salani, M. (2008), 'New dynamic programming algorithms for the resource constrained elementary shortest path problem', *Networks* **51**(3), 155–170.

Ronen, D. (1982), 'The effect of oil price on the optimal speed of ships', *Journal of the Operational Research Society* **33**(11), 1035–1040.

Ronen, D. (1983), 'Cargo ships routing and scheduling: survey of models and problems', *European Journal of Operational Research* **12**(2), 119–126.

Ropke, S. & Cordeau, J.-F. (2009), 'Branch and cut and price for the pickup and delivery problem with time windows', *Transportation Science* **43**(3), 267–286.

Ropke, S. & Pisinger, D. (2006), 'An adaptive large neighborhood search heuristic for the pickup and delivery problem with time windows', *Transportation Science* **40**(4), 455–472.

Solomon, M. M. & Desrosiers, J. (1988), 'Survey paper—time window constrained routing and scheduling problems', *Transportation Science* **22**(1), 1–13.

Subramanian, A., Uchoa, E. & Ochi, L. S. (2013), 'A hybrid algorithm for a class of vehicle routing problems', *Computers & Operations Research* **40**(10), 2519–2531.

Toth, P. & Vigo, D. (2003), 'The granular tabu search and its application to the vehicle-routing problem', *INFORMS Journal on Computing* **15**(4), 333–346.

UNCTAD (2017), 'Review of maritime transport'.

Velasco, N., Castagliola, P., Dejax, P., Guéret, C. & Prins, C. (2009), *A memetic algorithm for a pick-up and delivery problem by helicopter*, Springer Berlin Heidelberg, Berlin, Heidelberg, pp. 173–190.

Vidal, T. (2016), 'Technical note: split algorithm in o(n) for the capacitated vehicle routing problem', *Computers & Operations Research* **69**, 40–47.

Vidal, T., Crainic, T. G., Gendreau, M. & Prins, C. (2013), 'A hybrid genetic algorithm with adaptive diversity management for a large class of vehicle routing problems with time-windows', *Computers & Operations Research* **40**(1), 475 – 489.

Vidal, T., Crainic, T. G., Gendreau, M. & Prins, C. (2014), 'A unified solution framework for multi-attribute vehicle routing problems', *European Journal of Operational Research* **234**(3), 658 – 673.

Vidal, T., Crainic, T. G., Gendreau, M. & Prins, C. (2015*a*), 'Time-window relaxations in vehicle routing heuristics', *Journal of Heuristics* **21**(3), 329–358.

Vidal, T., Crainic, T. G., Gendreau, M. & Prins, C. (2015*b*), 'Timing problems and algorithms: time decisions for sequences of activities', *Networks* **65**(2), 102–128.

Vidal, T., Crainic, T. G., Gendreau, M., Lahrichi, N. & Rei, W. (2012), 'A hybrid genetic algorithm for multidepot and periodic vehicle routing problems', *Operations Research* **60**(3), 611–624.

Vidal, T., Gribel, D. & Jaillet, P. (2017), 'Separable convex optimization with nested lower and upper constraints', *ArXiv e-prints*.

Vidal, T., Maculan, N., Ochi, L. & Penna, P. (2016), 'Large neighborhoods with implicit customer selection for vehicle routing problems with profits', *Transportation Science* **50**(2), 720–734.

Vilhelmsen, C., Lusby, R. & Larsen, J. (2014), 'Tramp ship routing and scheduling with integrated bunker optimization', *EURO Journal on Transportation and Logistics* **3**(2), 143–175.

Wang, S. & Meng, Q. (2012), 'Sailing speed optimization for container ships in a liner shipping network', *Transportation Research Part E: Logistics and Transportation Review* **48**(3), 701–714.

Wen, M., Ropke, S., Petersen, H., Larsen, R. & Madsen, O. (2016), 'Full-shipload tramp ship routing and scheduling with variable speeds', *Computers & Operations Research* **70**, 1–8.

# A
# Appendix

Full HGS results on the ITSRSP instances are displayed in Tables A.1 to A.4. The best, average and worst travel cost found over 10 runs is reported in columns “Best”, “Avg” and “Worst”, respectively. Column “T” gives the average CPU time (in minutes).

Full B&P results are displayed in Tables A.5 to A.8. Columns “LB” and “UB” give respectively the lower and upper bounds. Column “T” gives the execution time (in seconds). Column “EN” gives the number of explored nodes, and column “HN” gives the number of hidden nodes.

Full results for the HGS-O and the HGS-J on the ITSRSPSO instances are displayed in Tables A.9 to A.12. Costs over five runs are reported in columns “Best”, “Avg” and “Worst”. Column “T” gives the average CPU time (in minutes).

Table A.1: Full results on Hemmati et al. (2014) for HGS-NO and HGS-SP.

| | **HGS-NO** | | | | **HGS-SP** | | | |
|---|---|---|---|---|---|---|---|---|
| Instance | Best | Avg | Worst | T | Best | Avg | Worst | T |
| SHORTSEA_MUN_C7_V3_HE_1 | 1476444 | 1476444.00 | 1476444 | 0.01 | 1476444 | 1476444.00 | 1476444 | 0.02 |
| SHORTSEA_MUN_C7_V3_HE_2 | 1134176 | 1134176.00 | 1134176 | 0.02 | 1134176 | 1134176.00 | 1134176 | 0.02 |
| SHORTSEA_MUN_C7_V3_HE_3 | 1196466 | 1196466.00 | 1196466 | 0.02 | 1196466 | 1196466.00 | 1196466 | 0.02 |
| SHORTSEA_MUN_C7_V3_HE_4 | 1256139 | 1256139.00 | 1256139 | 0.02 | 1256139 | 1256139.00 | 1256139 | 0.02 |
| SHORTSEA_MUN_C7_V3_HE_5 | 1160394 | 1160394.00 | 1160394 | 0.01 | 1160394 | 1160394.00 | 1160394 | 0.02 |
| SHORTSEA_MUN_C10_V3_HE_1 | 2083965 | 2083965.00 | 2083965 | 0.03 | 2083965 | 2083965.00 | 2083965 | 0.04 |
| SHORTSEA_MUN_C10_V3_HE_2 | 2012364 | 2012364.00 | 2012364 | 0.03 | 2012364 | 2012364.00 | 2012364 | 0.04 |
| SHORTSEA_MUN_C10_V3_HE_3 | 1986779 | 1986779.00 | 1986779 | 0.03 | 1986779 | 1986779.00 | 1986779 | 0.03 |
| SHORTSEA_MUN_C10_V3_HE_4 | 2125461 | 2125461.00 | 2125461 | 0.03 | 2125461 | 2125461.00 | 2125461 | 0.03 |
| SHORTSEA_MUN_C10_V3_HE_5 | 2162453 | 2162453.00 | 2162453 | 0.03 | 2162453 | 2162453.00 | 2162453 | 0.03 |
| SHORTSEA_MUN_C15_V4_HE_1 | 1959153 | 1959153.00 | 1959153 | 0.06 | 1959153 | 1959153.00 | 1959153 | 0.07 |
| SHORTSEA_MUN_C15_V4_HE_2 | 2560004 | 2560004.00 | 2560004 | 0.07 | 2560004 | 2560004.00 | 2560004 | 0.07 |
| SHORTSEA_MUN_C15_V4_HE_3 | 2582912 | 2582912.00 | 2582912 | 0.07 | 2582912 | 2582912.00 | 2582912 | 0.07 |
| SHORTSEA_MUN_C15_V4_HE_4 | 2265396 | 2265396.00 | 2265396 | 0.08 | 2265396 | 2265396.00 | 2265396 | 0.08 |
| SHORTSEA_MUN_C15_V4_HE_5 | 2230861 | 2230861.00 | 2230861 | 0.06 | 2230861 | 2230861.00 | 2230861 | 0.07 |
| SHORTSEA_MUN_C18_V5_HE_1 | 2374420 | 2374420.00 | 2374420 | 0.09 | 2374420 | 2374420.00 | 2374420 | 0.09 |
| SHORTSEA_MUN_C18_V5_HE_2 | 2987358 | 2987358.00 | 2987358 | 0.09 | 2987358 | 2987358.00 | 2987358 | 0.10 |
| SHORTSEA_MUN_C18_V5_HE_3 | 2301308 | 2301308.00 | 2301308 | 0.10 | 2301308 | 2301308.00 | 2301308 | 0.10 |
| SHORTSEA_MUN_C18_V5_HE_4 | 2400016 | 2410332.50 | 2428601 | 0.13 | 2400016 | 2401507.60 | 2414932 | 0.14 |
| SHORTSEA_MUN_C18_V5_HE_5 | 2813167 | 2813763.60 | 2816150 | 0.13 | 2813167 | 2813167.00 | 2813167 | 0.13 |
| SHORTSEA_MUN_C22_V6_HE_1 | 3928483 | 3928483.00 | 3928483 | 0.13 | 3928483 | 3928483.00 | 3928483 | 0.13 |
| SHORTSEA_MUN_C22_V6_HE_2 | 3683436 | 3683436.00 | 3683436 | 0.14 | 3683436 | 3683436.00 | 3683436 | 0.14 |
| SHORTSEA_MUN_C22_V6_HE_3 | 3264770 | 3264770.00 | 3264770 | 0.13 | 3264770 | 3264770.00 | 3264770 | 0.14 |
| SHORTSEA_MUN_C22_V6_HE_4 | 3228262 | 3228262.00 | 3228262 | 0.14 | 3228262 | 3228262.00 | 3228262 | 0.15 |
| SHORTSEA_MUN_C22_V6_HE_5 | 3770560 | 3770560.00 | 3770560 | 0.13 | 3770560 | 3770560.00 | 3770560 | 0.14 |
| SHORTSEA_MUN_C23_V13_HE_1 | 2276832 | 2276832.00 | 2276832 | 0.14 | 2276832 | 2276832.00 | 2276832 | 0.15 |
| SHORTSEA_MUN_C23_V13_HE_2 | 2255469 | 2261452.50 | 2305997 | 0.22 | 2255469 | 2255469.00 | 2255469 | 0.18 |
| SHORTSEA_MUN_C23_V13_HE_3 | 2362503 | 2362503.00 | 2362503 | 0.19 | 2362503 | 2362503.00 | 2362503 | 0.17 |
| SHORTSEA_MUN_C23_V13_HE_4 | 2250110 | 2250873.10 | 2257741 | 0.23 | 2250110 | 2250110.00 | 2250110 | 0.20 |
| SHORTSEA_MUN_C23_V13_HE_5 | 2325941 | 2325941.00 | 2325941 | 0.15 | 2325941 | 2325941.00 | 2325941 | 0.15 |
| SHORTSEA_MUN_C30_V6_HE_1 | 4958542 | 4958542.00 | 4958542 | 0.34 | 4958542 | 4958542.00 | 4958542 | 0.24 |
| SHORTSEA_MUN_C30_V6_HE_2 | 4549708 | 4550160.60 | 4554234 | 0.34 | 4549708 | 4549708.00 | 4549708 | 0.26 |
| SHORTSEA_MUN_C30_V6_HE_3 | 4098111 | 4098111.00 | 4098111 | 0.25 | 4098111 | 4098111.00 | 4098111 | 0.24 |
| SHORTSEA_MUN_C30_V6_HE_4 | 4449449 | 4449521.70 | 4449812 | 0.31 | 4449449 | 4449449.00 | 4449449 | 0.30 |
| SHORTSEA_MUN_C30_V6_HE_5 | 4528514 | 4528514.00 | 4528514 | 0.23 | 4528514 | 4528514.00 | 4528514 | 0.22 |
| SHORTSEA_MUN_C35_V7_HE_1 | 4893734 | 4920016.80 | 4957949 | 0.45 | 4893734 | 4894505.40 | 4897591 | 0.50 |
| SHORTSEA_MUN_C35_V7_HE_2 | 4533265 | 4540178.70 | 4548401 | 0.40 | 4533265 | 4533265.00 | 4533265 | 0.40 |
| SHORTSEA_MUN_C35_V7_HE_3 | 4433847 | 4433847.00 | 4433847 | 0.41 | 4433847 | 4433847.00 | 4433847 | 0.32 |
| SHORTSEA_MUN_C35_V7_HE_4 | 4580935 | 4599980.00 | 4629068 | 0.52 | 4580935 | 4580935.00 | 4580935 | 0.40 |
| SHORTSEA_MUN_C35_V7_HE_5 | 5542825 | 5562666.60 | 5595294 | 0.43 | 5511661 | 5512815.00 | 5523201 | 0.42 |
| SHORTSEA_MUN_C60_V13_HE_1 | 8150597 | 8168916.70 | 8193642 | 1.84 | 8133385 | 8136827.40 | 8150597 | 2.12 |
| SHORTSEA_MUN_C60_V13_HE_2 | 7971685 | 7991077.90 | 8008264 | 1.57 | 7971476 | 7971538.70 | 7971685 | 1.17 |
| SHORTSEA_MUN_C60_V13_HE_3 | 7633937 | 7659749.70 | 7700655 | 1.64 | 7604198 | 7620215.00 | 7636891 | 1.40 |
| SHORTSEA_MUN_C60_V13_HE_4 | 8508321 | 8553112.40 | 8627386 | 1.54 | 8505125 | 8505391.40 | 8505421 | 1.39 |
| SHORTSEA_MUN_C60_V13_HE_5 | 8921762 | 8965048.40 | 8996365 | 1.82 | 8921750 | 8921752.20 | 8921761 | 1.46 |
| SHORTSEA_MUN_C80_V20_HE_1 | 10312967 | 10410325.20 | 10629254 | 4.20 | 10289573 | 10292640.60 | 10296807 | 5.10 |
| SHORTSEA_MUN_C80_V20_HE_2 | 10289830 | 10326494.40 | 10377475 | 4.70 | 10240618 | 10241195.50 | 10246354 | 2.24 |
| SHORTSEA_MUN_C80_V20_HE_3 | 9625648 | 9666363.10 | 9739462 | 6.01 | 9606530 | 9606530.00 | 9606530 | 2.10 |
| SHORTSEA_MUN_C80_V20_HE_4 | 11444974 | 11554480.20 | 11699999 | 3.27 | 11302476 | 11302995.60 | 11305074 | 3.79 |
| SHORTSEA_MUN_C80_V20_HE_5 | 10915609 | 10988509.70 | 11037616 | 3.77 | 10862563 | 10862563.00 | 10862563 | 1.72 |
| SHORTSEA_MUN_C100_V30_HE_1 | 12686059 | 12782256.60 | 12894417 | 6.99 | 12626988 | 12626988.00 | 12626988 | 3.03 |
| SHORTSEA_MUN_C100_V30_HE_2 | 12842978 | 12936285.80 | 13045150 | 9.32 | 12774864 | 12775433.00 | 12776760 | 4.22 |
| SHORTSEA_MUN_C100_V30_HE_3 | 11973900 | 12034803.50 | 12090079 | 7.48 | 11935332 | 11935332.00 | 11935332 | 4.05 |
| SHORTSEA_MUN_C100_V30_HE_4 | 13702161 | 13799089.70 | 13966302 | 8.05 | 13605352 | 13605874.90 | 13610581 | 3.91 |
| SHORTSEA_MUN_C100_V30_HE_5 | 13326476 | 13408557.60 | 13628878 | 7.92 | 13240648 | 13240648.00 | 13240648 | 4.42 |
| SHORTSEA_MUN_C130_V40_HE_1 | 16419109 | 16512854.60 | 16667949 | 12.52 | 16316051 | 16316084.70 | 16316388 | 10.84 |
| SHORTSEA_MUN_C130_V40_HE_2 | 16510343 | 16568550.80 | 16806478 | 13.45 | 16260579 | 16260728.30 | 16262072 | 9.36 |
| SHORTSEA_MUN_C130_V40_HE_3 | 15707113 | 15771278.90 | 15858671 | 13.78 | 15537963 | 15541382.60 | 15546512 | 8.11 |
| SHORTSEA_MUN_C130_V40_HE_4 | 17159564 | 17191068.80 | 17265729 | 14.23 | 17011065 | 17012189.90 | 17014719 | 12.88 |
| SHORTSEA_MUN_C130_V40_HE_5 | 18567598 | 18660824.00 | 18740877 | 12.59 | 18273893 | 18275037.10 | 18281798 | 9.41 |

Table A.2: Full results on Hemmati et al. (2014) for HGS-NO and HGS-SP.

| | **HGS** | | | | **HGS-SP** | | | |
|---|---|---|---|---|---|---|---|---|
| Instance | Best | Avg | Worst | T | Best | Avg | Worst | T |
| SHORTSEA_FUN_C8_V3_HE_1 | 1391997 | 1391997.00 | 1391997 | 0.01 | 1391997 | 1391997.00 | 1391997 | 0.01 |
| SHORTSEA_FUN_C8_V3_HE_2 | 1246273 | 1246273.00 | 1246273 | 0.01 | 1246273 | 1246273.00 | 1246273 | 0.01 |
| SHORTSEA_FUN_C8_V3_HE_3 | 1698102 | 1698102.00 | 1698102 | 0.01 | 1698102 | 1698102.00 | 1698102 | 0.01 |
| SHORTSEA_FUN_C8_V3_HE_4 | 1777637 | 1777637.00 | 1777637 | 0.01 | 1777637 | 1777637.00 | 1777637 | 0.01 |
| SHORTSEA_FUN_C8_V3_HE_5 | 1636788 | 1636788.00 | 1636788 | 0.01 | 1636788 | 1636788.00 | 1636788 | 0.01 |
| SHORTSEA_FUN_C11_V4_HE_1 | 1052463 | 1052463.00 | 1052463 | 0.02 | 1052463 | 1052463.00 | 1052463 | 0.02 |
| SHORTSEA_FUN_C11_V4_HE_2 | 1067139 | 1067139.00 | 1067139 | 0.02 | 1067139 | 1067139.00 | 1067139 | 0.02 |
| SHORTSEA_FUN_C11_V4_HE_3 | 1212388 | 1212388.00 | 1212388 | 0.02 | 1212388 | 1212388.00 | 1212388 | 0.02 |
| SHORTSEA_FUN_C11_V4_HE_4 | 1185465 | 1185465.00 | 1185465 | 0.02 | 1185465 | 1185465.00 | 1185465 | 0.02 |
| SHORTSEA_FUN_C11_V4_HE_5 | 1310285 | 1310285.00 | 1310285 | 0.01 | 1310285 | 1310285.00 | 1310285 | 0.02 |
| SHORTSEA_FUN_C13_V5_HE_1 | 2034184 | 2034184.00 | 2034184 | 0.02 | 2034184 | 2034184.00 | 2034184 | 0.02 |
| SHORTSEA_FUN_C13_V5_HE_2 | 2043253 | 2043253.00 | 2043253 | 0.02 | 2043253 | 2043253.00 | 2043253 | 0.02 |
| SHORTSEA_FUN_C13_V5_HE_3 | 2378283 | 2378283.00 | 2378283 | 0.02 | 2378283 | 2378283.00 | 2378283 | 0.02 |
| SHORTSEA_FUN_C13_V5_HE_4 | 2707215 | 2707215.00 | 2707215 | 0.02 | 2707215 | 2707215.00 | 2707215 | 0.02 |
| SHORTSEA_FUN_C13_V5_HE_5 | 3011648 | 3011648.00 | 3011648 | 0.02 | 3011648 | 3011648.00 | 3011648 | 0.02 |
| SHORTSEA_FUN_C16_V6_HE_1 | 3577005 | 3577005.00 | 3577005 | 0.03 | 3577005 | 3577005.00 | 3577005 | 0.03 |
| SHORTSEA_FUN_C16_V6_HE_2 | 3560203 | 3560203.00 | 3560203 | 0.03 | 3560203 | 3560203.00 | 3560203 | 0.03 |
| SHORTSEA_FUN_C16_V6_HE_3 | 4081013 | 4081013.00 | 4081013 | 0.03 | 4081013 | 4081013.00 | 4081013 | 0.03 |
| SHORTSEA_FUN_C16_V6_HE_4 | 3667080 | 3667080.00 | 3667080 | 0.03 | 3667080 | 3667080.00 | 3667080 | 0.03 |
| SHORTSEA_FUN_C16_V6_HE_5 | 3438493 | 3438493.00 | 3438493 | 0.03 | 3438493 | 3438493.00 | 3438493 | 0.03 |
| SHORTSEA_FUN_C17_V13_HE_1 | 2265731 | 2265731.00 | 2265731 | 0.04 | 2265731 | 2265731.00 | 2265731 | 0.04 |
| SHORTSEA_FUN_C17_V13_HE_2 | 3154165 | 3154165.00 | 3154165 | 0.04 | 3154165 | 3154165.00 | 3154165 | 0.05 |
| SHORTSEA_FUN_C17_V13_HE_3 | 2699378 | 2699378.00 | 2699378 | 0.04 | 2699378 | 2699378.00 | 2699378 | 0.04 |
| SHORTSEA_FUN_C17_V13_HE_4 | 2806231 | 2806231.00 | 2806231 | 0.04 | 2806231 | 2806231.00 | 2806231 | 0.04 |
| SHORTSEA_FUN_C17_V13_HE_5 | 2910814 | 2910814.00 | 2910814 | 0.04 | 2910814 | 2910814.00 | 2910814 | 0.04 |
| SHORTSEA_FUN_C20_V6_HE_1 | 2973381 | 2973381.00 | 2973381 | 0.04 | 2973381 | 2973381.00 | 2973381 | 0.04 |
| SHORTSEA_FUN_C20_V6_HE_2 | 3206514 | 3206514.00 | 3206514 | 0.05 | 3206514 | 3206514.00 | 3206514 | 0.05 |
| SHORTSEA_FUN_C20_V6_HE_3 | 3197445 | 3197445.00 | 3197445 | 0.04 | 3197445 | 3197445.00 | 3197445 | 0.04 |
| SHORTSEA_FUN_C20_V6_HE_4 | 3342130 | 3342130.00 | 3342130 | 0.04 | 3342130 | 3342130.00 | 3342130 | 0.04 |
| SHORTSEA_FUN_C20_V6_HE_5 | 3156378 | 3156378.00 | 3156378 | 0.04 | 3156378 | 3156378.00 | 3156378 | 0.04 |
| SHORTSEA_FUN_C25_V7_HE_1 | 3833588 | 3833588.00 | 3833588 | 0.06 | 3833588 | 3833588.00 | 3833588 | 0.07 |
| SHORTSEA_FUN_C25_V7_HE_2 | 3673666 | 3673666.00 | 3673666 | 0.05 | 3673666 | 3673666.00 | 3673666 | 0.06 |
| SHORTSEA_FUN_C25_V7_HE_3 | 4238213 | 4238213.00 | 4238213 | 0.06 | 4238213 | 4238213.00 | 4238213 | 0.07 |
| SHORTSEA_FUN_C25_V7_HE_4 | 4260762 | 4260762.00 | 4260762 | 0.06 | 4260762 | 4260762.00 | 4260762 | 0.07 |
| SHORTSEA_FUN_C25_V7_HE_5 | 4069693 | 4069693.00 | 4069693 | 0.06 | 4069693 | 4069693.00 | 4069693 | 0.07 |
| SHORTSEA_FUN_C35_V13_HE_1 | 2986667 | 2986667.00 | 2986667 | 0.11 | 2986667 | 2986667.00 | 2986667 | 0.12 |
| SHORTSEA_FUN_C35_V13_HE_2 | 3002973 | 3003096.60 | 3004193 | 0.23 | 3002973 | 3002973.00 | 3002973 | 0.20 |
| SHORTSEA_FUN_C35_V13_HE_3 | 3084339 | 3084376.10 | 3084710 | 0.15 | 3084339 | 3084339.00 | 3084339 | 0.15 |
| SHORTSEA_FUN_C35_V13_HE_4 | 3952461 | 3952461.30 | 3952462 | 0.18 | 3952461 | 3952461.00 | 3952461 | 0.16 |
| SHORTSEA_FUN_C35_V13_HE_5 | 3293086 | 3293147.10 | 3293669 | 0.15 | 3293086 | 3293086.00 | 3293086 | 0.16 |
| SHORTSEA_FUN_C50_V20_HE_1 | 7258266 | 7261774.80 | 7274756 | 0.56 | 7258266 | 7258266.00 | 7258266 | 0.36 |
| SHORTSEA_FUN_C50_V20_HE_2 | 7458380 | 7466266.70 | 7469069 | 0.43 | 7452465 | 7452465.00 | 7452465 | 0.37 |
| SHORTSEA_FUN_C50_V20_HE_3 | 6929079 | 6949770.20 | 6969977 | 0.48 | 6922293 | 6922293.00 | 6922293 | 0.38 |
| SHORTSEA_FUN_C50_V20_HE_4 | 8933847 | 8945057.60 | 8958527 | 0.53 | 8933846 | 8933846.30 | 8933847 | 0.42 |
| SHORTSEA_FUN_C50_V20_HE_5 | 7322307 | 7324635.00 | 7330502 | 0.54 | 7322307 | 7322307.00 | 7322307 | 0.39 |
| SHORTSEA_FUN_C70_V30_HE_1 | 10064530 | 10079207.60 | 10099052 | 1.38 | 10051856 | 10051856.00 | 10051856 | 0.84 |
| SHORTSEA_FUN_C70_V30_HE_2 | 10464802 | 10481727.60 | 10506846 | 1.56 | 10455468 | 10455468.00 | 10455468 | 0.87 |
| SHORTSEA_FUN_C70_V30_HE_3 | 10273969 | 10288859.70 | 10315136 | 1.68 | 10172541 | 10172998.20 | 10174065 | 1.06 |
| SHORTSEA_FUN_C70_V30_HE_4 | 10864114 | 10911945.10 | 10946258 | 1.15 | 10854036 | 10854036.00 | 10854036 | 0.84 |
| SHORTSEA_FUN_C70_V30_HE_5 | 10902911 | 10926787.70 | 10951401 | 1.40 | 10886838 | 10886838.00 | 10886838 | 1.10 |
| SHORTSEA_FUN_C90_V40_HE_1 | 13413594 | 13437538.00 | 13460969 | 2.82 | 13361947 | 13362867.80 | 13371155 | 1.69 |
| SHORTSEA_FUN_C90_V40_HE_2 | 13856061 | 13891003.60 | 13920519 | 2.96 | 13828112 | 13828112.00 | 13828112 | 1.53 |
| SHORTSEA_FUN_C90_V40_HE_3 | 12660456 | 12695713.00 | 12739629 | 4.28 | 12627125 | 12627125.20 | 12627126 | 1.61 |
| SHORTSEA_FUN_C90_V40_HE_4 | 14440962 | 14478099.90 | 14503497 | 3.64 | 14406428 | 14406428.00 | 14406428 | 1.60 |
| SHORTSEA_FUN_C90_V40_HE_5 | 13619099 | 13660523.20 | 13721704 | 3.14 | 13560830 | 13560830.00 | 13560830 | 1.95 |
| SHORTSEA_FUN_C100_V50_HE_1 | 13813700 | 13821891.70 | 13832541 | 4.08 | 13800823 | 13800823.00 | 13800823 | 2.31 |
| SHORTSEA_FUN_C100_V50_HE_2 | 14682666 | 14698970.70 | 14722835 | 4.55 | 14644836 | 14644836.00 | 14644836 | 2.27 |
| SHORTSEA_FUN_C100_V50_HE_3 | 13152622 | 13182104.30 | 13210288 | 4.46 | 13135505 | 13135505.00 | 13135505 | 2.20 |
| SHORTSEA_FUN_C100_V50_HE_4 | 14877190 | 14894679.10 | 14917842 | 5.10 | 14841840 | 14841840.00 | 14841840 | 2.51 |
| SHORTSEA_FUN_C100_V50_HE_5 | 14050647 | 14075129.70 | 14096989 | 4.67 | 14009874 | 14009877.80 | 14009889 | 1.94 |

Table A.3: Full results on Hemmati et al. (2014) for HGS-NO and HGS-SP.

| | **HGS** | | | | **HGS-SP** | | | |
|---|---|---|---|---|---|---|---|---|
| Instance | Best | Avg | Worst | T | Best | Avg | Worst | T |
| DEEPSEA_MUN_C7_V3_HE_1 | 5233464 | 5233464.00 | 5233464 | 0.02 | 5233464 | 5233464.00 | 5233464 | 0.02 |
| DEEPSEA_MUN_C7_V3_HE_2 | 6053699 | 6053699.00 | 6053699 | 0.03 | 6053699 | 6053699.00 | 6053699 | 0.02 |
| DEEPSEA_MUN_C7_V3_HE_3 | 5888949 | 5888949.00 | 5888949 | 0.02 | 5888949 | 5888949.00 | 5888949 | 0.02 |
| DEEPSEA_MUN_C7_V3_HE_4 | 6510656 | 6510656.00 | 6510656 | 0.03 | 6510656 | 6510656.00 | 6510656 | 0.02 |
| DEEPSEA_MUN_C7_V3_HE_5 | 7220458 | 7220458.00 | 7220458 | 0.02 | 7220458 | 7220458.00 | 7220458 | 0.02 |
| DEEPSEA_MUN_C10_V3_HE_1 | 7986248 | 7986248.00 | 7986248 | 0.03 | 7986248 | 7986248.00 | 7986248 | 0.03 |
| DEEPSEA_MUN_C10_V3_HE_2 | 7754484 | 7754484.00 | 7754484 | 0.04 | 7754484 | 7754484.00 | 7754484 | 0.03 |
| DEEPSEA_MUN_C10_V3_HE_3 | 9499357 | 9499357.00 | 9499357 | 0.03 | 9499357 | 9499357.00 | 9499357 | 0.03 |
| DEEPSEA_MUN_C10_V3_HE_4 | 8617192 | 8617192.00 | 8617192 | 0.03 | 8617192 | 8617192.00 | 8617192 | 0.03 |
| DEEPSEA_MUN_C10_V3_HE_5 | 8653992 | 8653992.00 | 8653992 | 0.03 | 8653992 | 8653992.00 | 8653992 | 0.03 |
| DEEPSEA_MUN_C15_V4_HE_1 | 13467090 | 13467090.00 | 13467090 | 0.06 | 13467090 | 13467090.00 | 13467090 | 0.06 |
| DEEPSEA_MUN_C15_V4_HE_2 | 12457251 | 12457251.00 | 12457251 | 0.08 | 12457251 | 12457251.00 | 12457251 | 0.07 |
| DEEPSEA_MUN_C15_V4_HE_3 | 12567396 | 12567396.00 | 12567396 | 0.06 | 12567396 | 12567396.00 | 12567396 | 0.06 |
| DEEPSEA_MUN_C15_V4_HE_4 | 11764241 | 11764241.00 | 11764241 | 0.07 | 11764241 | 11764241.00 | 11764241 | 0.07 |
| DEEPSEA_MUN_C15_V4_HE_5 | 10833640 | 10833640.00 | 10833640 | 0.06 | 10833640 | 10833640.00 | 10833640 | 0.06 |
| DEEPSEA_MUN_C18_V5_HE_1 | 43054055 | 43054055.00 | 43054055 | 0.10 | 43054055 | 43054055.00 | 43054055 | 0.10 |
| DEEPSEA_MUN_C18_V5_HE_2 | 25068287 | 25068287.00 | 25068287 | 0.10 | 25068287 | 25068287.00 | 25068287 | 0.11 |
| DEEPSEA_MUN_C18_V5_HE_3 | 29211238 | 29211238.00 | 29211238 | 0.09 | 29211238 | 29211238.00 | 29211238 | 0.09 |
| DEEPSEA_MUN_C18_V5_HE_4 | 32281904 | 32281904.00 | 32281904 | 0.09 | 32281904 | 32281904.00 | 32281904 | 0.09 |
| DEEPSEA_MUN_C18_V5_HE_5 | 40718028 | 40718028.00 | 40718028 | 0.09 | 40718028 | 40718028.00 | 40718028 | 0.09 |
| DEEPSEA_MUN_C22_V6_HE_1 | 41176718 | 41176718.00 | 41176718 | 0.12 | 41176718 | 41176718.00 | 41176718 | 0.12 |
| DEEPSEA_MUN_C22_V6_HE_2 | 37236363 | 37236363.00 | 37236363 | 0.17 | 37236363 | 37236363.00 | 37236363 | 0.15 |
| DEEPSEA_MUN_C22_V6_HE_3 | 38215238 | 38215238.00 | 38215238 | 0.14 | 38215238 | 38215238.00 | 38215238 | 0.14 |
| DEEPSEA_MUN_C22_V6_HE_4 | 34129809 | 34129809.00 | 34129809 | 0.15 | 34129809 | 34129809.00 | 34129809 | 0.16 |
| DEEPSEA_MUN_C22_V6_HE_5 | 46379332 | 46379332.00 | 46379332 | 0.12 | 46379332 | 46379332.00 | 46379332 | 0.12 |
| DEEPSEA_MUN_C23_V13_HE_1 | 41002992 | 41002992.00 | 41002992 | 0.15 | 41002992 | 41002992.00 | 41002992 | 0.15 |
| DEEPSEA_MUN_C23_V13_HE_2 | 28014147 | 28014147.00 | 28014147 | 0.15 | 28014147 | 28014147.00 | 28014147 | 0.15 |
| DEEPSEA_MUN_C23_V13_HE_3 | 29090422 | 29090422.00 | 29090422 | 0.13 | 29090422 | 29090422.00 | 29090422 | 0.13 |
| DEEPSEA_MUN_C23_V13_HE_4 | 33685274 | 33685439.20 | 33686926 | 0.18 | 33685274 | 33685274.00 | 33685274 | 0.17 |
| DEEPSEA_MUN_C23_V13_HE_5 | 38664843 | 38664843.00 | 38664843 | 0.14 | 38664843 | 38664843.00 | 38664843 | 0.14 |
| DEEPSEA_MUN_C30_V6_HE_1 | 19227093 | 19227093.20 | 19227094 | 0.23 | 19227093 | 19227093.00 | 19227093 | 0.21 |
| DEEPSEA_MUN_C30_V6_HE_2 | 16784810 | 16807970.70 | 16904604 | 0.31 | 16784810 | 16784810.00 | 16784810 | 0.28 |
| DEEPSEA_MUN_C30_V6_HE_3 | 21298546 | 21309027.50 | 21402168 | 0.29 | 21183928 | 21193941.20 | 21208961 | 0.28 |
| DEEPSEA_MUN_C30_V6_HE_4 | 21076728 | 21076728.00 | 21076728 | 0.20 | 21076728 | 21076728.00 | 21076728 | 0.21 |
| DEEPSEA_MUN_C30_V6_HE_5 | 24490671 | 24493822.70 | 24509193 | 0.30 | 24490671 | 24490671.00 | 24490671 | 0.25 |
| DEEPSEA_MUN_C35_V7_HE_1 | 65359491 | 65440588.00 | 65570413 | 0.34 | 65082675 | 65082675.00 | 65082675 | 0.37 |
| DEEPSEA_MUN_C35_V7_HE_2 | 54810586 | 54867979.50 | 55016029 | 0.47 | 54810586 | 54810586.00 | 54810586 | 0.32 |
| DEEPSEA_MUN_C35_V7_HE_3 | 56182502 | 56182502.80 | 56182510 | 0.38 | 56182502 | 56182502.00 | 56182502 | 0.32 |
| DEEPSEA_MUN_C35_V7_HE_4 | 61354812 | 61368330.60 | 61489997 | 0.42 | 61354812 | 61354812.00 | 61354812 | 0.39 |
| DEEPSEA_MUN_C35_V7_HE_5 | 63904705 | 63904705.00 | 63904705 | 0.27 | 63904705 | 63904705.00 | 63904705 | 0.26 |
| DEEPSEA_MUN_C60_V13_HE_1 | 80779035 | 81179047.90 | 81602589 | 1.91 | 80649895 | 80661548.00 | 80708160 | 1.94 |
| DEEPSEA_MUN_C60_V13_HE_2 | 74881110 | 75244185.50 | 75847675 | 2.28 | 74881109 | 74881109.20 | 74881110 | 1.11 |
| DEEPSEA_MUN_C60_V13_HE_3 | 92362334 | 92657898.60 | 92870090 | 1.86 | 91766747 | 91766833.90 | 91767616 | 1.14 |
| DEEPSEA_MUN_C60_V13_HE_4 | 90323416 | 91162742.90 | 92201850 | 2.31 | 89702352 | 89702352.00 | 89702352 | 1.39 |
| DEEPSEA_MUN_C60_V13_HE_5 | 89109660 | 89301080.00 | 89766598 | 1.67 | 88486544 | 88486544.00 | 88486544 | 1.24 |
| DEEPSEA_MUN_C80_V20_HE_1 | 70859172 | 71341637.90 | 72265959 | 4.55 | 70718084 | 70738509.40 | 70922338 | 2.46 |
| DEEPSEA_MUN_C80_V20_HE_2 | 74444535 | 74740704.80 | 75681332 | 3.60 | 73558165 | 73584102.20 | 73603212 | 4.10 |
| DEEPSEA_MUN_C80_V20_HE_3 | 78615067 | 78996540.20 | 79407419 | 3.46 | 78250612 | 78250612.00 | 78250612 | 2.08 |
| DEEPSEA_MUN_C80_V20_HE_4 | 76108732 | 76586051.40 | 77653002 | 3.86 | 75962439 | 75993240.20 | 76061556 | 3.25 |
| DEEPSEA_MUN_C80_V20_HE_5 | 74351451 | 75540439.50 | 76727758 | 4.36 | 74162521 | 74162522.10 | 74162524 | 2.47 |
| DEEPSEA_MUN_C100_V30_HE_1 | 153939004 | 154825211.00 | 157456520 | 6.00 | 150481912 | 150497215.70 | 150522656 | 7.41 |
| DEEPSEA_MUN_C100_V30_HE_2 | 152382679 | 153649456.70 | 155340239 | 9.60 | 150826322 | 150837539.30 | 150902591 | 7.05 |
| DEEPSEA_MUN_C100_V30_HE_3 | 152433775 | 153482921.50 | 154433184 | 7.14 | 151027805 | 151031384.70 | 151038978 | 8.49 |
| DEEPSEA_MUN_C100_V30_HE_4 | 155586124 | 158301263.40 | 160614189 | 6.54 | 151193009 | 151204669.80 | 151256471 | 7.31 |
| DEEPSEA_MUN_C100_V30_HE_5 | 161289248 | 163809733.00 | 166560867 | 7.01 | 159789021 | 159790522.60 | 159800907 | 6.63 |
| DEEPSEA_MUN_C130_V40_HE_1 | 238775717 | 241008794.40 | 243960181 | 12.37 | 232625257 | 232634270.10 | 232637186 | 14.08 |
| DEEPSEA_MUN_C130_V40_HE_2 | 233033136 | 235230009.70 | 237753236 | 12.55 | 228058626 | 228184429.60 | 228240325 | 14.39 |
| DEEPSEA_MUN_C130_V40_HE_3 | 244438374 | 247157840.70 | 250071099 | 12.63 | 235666249 | 235742810.90 | 235949491 | 13.87 |
| DEEPSEA_MUN_C130_V40_HE_4 | 225692405 | 228146599.60 | 231896479 | 13.57 | 220357686 | 220419662.80 | 220762578 | 14.06 |
| DEEPSEA_MUN_C130_V40_HE_5 | 243557347 | 245724607.50 | 247919101 | 13.35 | 235381937 | 235586360.10 | 235752606 | 14.91 |

Table A.4: Full results on Hemmati et al. (2014) for HGS-NO and HGS-SP.

| | **HGS** | | | | **HGS-SP** | | | |
|---|---|---|---|---|---|---|---|---|
| Instance | Best | Avg | Worst | T | Best | Avg | Worst | T |
| DEEPSEA_FUN_C8_V3_HE_1 | 9584863 | 9584863.00 | 9584863 | 0.01 | 9584863 | 9584863.00 | 9584863 | 0.01 |
| DEEPSEA_FUN_C8_V3_HE_2 | 9369654 | 9369654.00 | 9369654 | 0.01 | 9369654 | 9369654.00 | 9369654 | 0.01 |
| DEEPSEA_FUN_C8_V3_HE_3 | 4596681 | 4596681.00 | 4596681 | 0.01 | 4596681 | 4596681.00 | 4596681 | 0.01 |
| DEEPSEA_FUN_C8_V3_HE_4 | 6899730 | 6899730.00 | 6899730 | 0.01 | 6899730 | 6899730.00 | 6899730 | 0.01 |
| DEEPSEA_FUN_C8_V3_HE_5 | 6815253 | 6815253.00 | 6815253 | 0.01 | 6815253 | 6815253.00 | 6815253 | 0.01 |
| DEEPSEA_FUN_C11_V4_HE_1 | 34854819 | 34854819.00 | 34854819 | 0.01 | 34854819 | 34854819.00 | 34854819 | 0.02 |
| DEEPSEA_FUN_C11_V4_HE_2 | 25454434 | 25454434.00 | 25454434 | 0.02 | 25454434 | 25454434.00 | 25454434 | 0.02 |
| DEEPSEA_FUN_C11_V4_HE_3 | 29627143 | 29627143.00 | 29627143 | 0.02 | 29627143 | 29627143.00 | 29627143 | 0.02 |
| DEEPSEA_FUN_C11_V4_HE_4 | 33111680 | 33111680.00 | 33111680 | 0.02 | 33111680 | 33111680.00 | 33111680 | 0.02 |
| DEEPSEA_FUN_C11_V4_HE_5 | 28175914 | 28175914.00 | 28175914 | 0.01 | 28175914 | 28175914.00 | 28175914 | 0.02 |
| DEEPSEA_FUN_C13_V5_HE_1 | 11629005 | 11629005.00 | 11629005 | 0.02 | 11629005 | 11629005.00 | 11629005 | 0.02 |
| DEEPSEA_FUN_C13_V5_HE_2 | 11820655 | 11820655.00 | 11820655 | 0.02 | 11820655 | 11820655.00 | 11820655 | 0.02 |
| DEEPSEA_FUN_C13_V5_HE_3 | 9992593 | 9992593.00 | 9992593 | 0.02 | 9992593 | 9992593.00 | 9992593 | 0.02 |
| DEEPSEA_FUN_C13_V5_HE_4 | 12819619 | 12819619.00 | 12819619 | 0.02 | 12819619 | 12819619.00 | 12819619 | 0.02 |
| DEEPSEA_FUN_C13_V5_HE_5 | 10534892 | 10534892.00 | 10534892 | 0.02 | 10534892 | 10534892.00 | 10534892 | 0.02 |
| DEEPSEA_FUN_C16_V6_HE_1 | 51127590 | 51127590.00 | 51127590 | 0.03 | 51127590 | 51127590.00 | 51127590 | 0.03 |
| DEEPSEA_FUN_C16_V6_HE_2 | 44342796 | 44342796.00 | 44342796 | 0.03 | 44342796 | 44342796.00 | 44342796 | 0.03 |
| DEEPSEA_FUN_C16_V6_HE_3 | 45391842 | 45391842.00 | 45391842 | 0.03 | 45391842 | 45391842.00 | 45391842 | 0.03 |
| DEEPSEA_FUN_C16_V6_HE_4 | 39687114 | 39687114.00 | 39687114 | 0.03 | 39687114 | 39687114.00 | 39687114 | 0.03 |
| DEEPSEA_FUN_C16_V6_HE_5 | 42855603 | 42855603.00 | 42855603 | 0.03 | 42855603 | 42855603.00 | 42855603 | 0.04 |
| DEEPSEA_FUN_C17_V13_HE_1 | 17316720 | 17316720.00 | 17316720 | 0.04 | 17316720 | 17316720.00 | 17316720 | 0.04 |
| DEEPSEA_FUN_C17_V13_HE_2 | 12194861 | 12194861.00 | 12194861 | 0.04 | 12194861 | 12194861.00 | 12194861 | 0.04 |
| DEEPSEA_FUN_C17_V13_HE_3 | 12091554 | 12091554.00 | 12091554 | 0.04 | 12091554 | 12091554.00 | 12091554 | 0.04 |
| DEEPSEA_FUN_C17_V13_HE_4 | 12847653 | 12847653.00 | 12847653 | 0.04 | 12847653 | 12847653.00 | 12847653 | 0.05 |
| DEEPSEA_FUN_C17_V13_HE_5 | 13213406 | 13213406.00 | 13213406 | 0.04 | 13213406 | 13213406.00 | 13213406 | 0.04 |
| DEEPSEA_FUN_C20_V6_HE_1 | 16406738 | 16406738.00 | 16406738 | 0.04 | 16406738 | 16406738.00 | 16406738 | 0.04 |
| DEEPSEA_FUN_C20_V6_HE_2 | 16079401 | 16079401.00 | 16079401 | 0.04 | 16079401 | 16079401.00 | 16079401 | 0.04 |
| DEEPSEA_FUN_C20_V6_HE_3 | 17342200 | 17342200.00 | 17342200 | 0.04 | 17342200 | 17342200.00 | 17342200 | 0.04 |
| DEEPSEA_FUN_C20_V6_HE_4 | 16529748 | 16529748.00 | 16529748 | 0.04 | 16529748 | 16529748.00 | 16529748 | 0.04 |
| DEEPSEA_FUN_C20_V6_HE_5 | 17449378 | 17449378.00 | 17449378 | 0.04 | 17449378 | 17449378.00 | 17449378 | 0.04 |
| DEEPSEA_FUN_C25_V7_HE_1 | 22773158 | 22773158.00 | 22773158 | 0.06 | 22773158 | 22773158.00 | 22773158 | 0.06 |
| DEEPSEA_FUN_C25_V7_HE_2 | 20206329 | 20206329.00 | 20206329 | 0.07 | 20206329 | 20206329.00 | 20206329 | 0.07 |
| DEEPSEA_FUN_C25_V7_HE_3 | 19108952 | 19108952.00 | 19108952 | 0.06 | 19108952 | 19108952.00 | 19108952 | 0.06 |
| DEEPSEA_FUN_C25_V7_HE_4 | 22668675 | 22668675.00 | 22668675 | 0.06 | 22668675 | 22668675.00 | 22668675 | 0.06 |
| DEEPSEA_FUN_C25_V7_HE_5 | 23036603 | 23036603.00 | 23036603 | 0.07 | 23036603 | 23036603.00 | 23036603 | 0.07 |
| DEEPSEA_FUN_C35_V13_HE_1 | 86951609 | 86951609.60 | 86951611 | 0.24 | 86951609 | 86951609.00 | 86951609 | 0.20 |
| DEEPSEA_FUN_C35_V13_HE_2 | 83422071 | 83422071.00 | 83422071 | 0.21 | 83422071 | 83422071.00 | 83422071 | 0.18 |
| DEEPSEA_FUN_C35_V13_HE_3 | 83898591 | 83898591.00 | 83898591 | 0.17 | 83898591 | 83898591.00 | 83898591 | 0.17 |
| DEEPSEA_FUN_C35_V13_HE_4 | 91970481 | 91970481.00 | 91970481 | 0.24 | 91970481 | 91970481.00 | 91970481 | 0.20 |
| DEEPSEA_FUN_C35_V13_HE_5 | 91123040 | 91159811.60 | 91216286 | 0.20 | 91123040 | 91123040.00 | 91123040 | 0.19 |
| DEEPSEA_FUN_C50_V20_HE_1 | 41313566 | 41326002.70 | 41381501 | 0.66 | 41310946 | 41310946.00 | 41310946 | 0.39 |
| DEEPSEA_FUN_C50_V20_HE_2 | 37825509 | 37888723.20 | 37947319 | 0.51 | 37784994 | 37784994.00 | 37784994 | 0.43 |
| DEEPSEA_FUN_C50_V20_HE_3 | 39844745 | 39897627.00 | 39943733 | 0.68 | 39841724 | 39841724.00 | 39841724 | 0.37 |
| DEEPSEA_FUN_C50_V20_HE_4 | 43941098 | 43986102.90 | 44011291 | 0.45 | 43941098 | 43941098.00 | 43941098 | 0.38 |
| DEEPSEA_FUN_C50_V20_HE_5 | 41947437 | 41984135.90 | 42143433 | 0.62 | 41947437 | 41947437.00 | 41947437 | 0.38 |
| DEEPSEA_FUN_C70_V30_HE_1 | 142680222 | 142723400.50 | 142799012 | 1.20 | 142679953 | 142679953.20 | 142679954 | 0.91 |
| DEEPSEA_FUN_C70_V30_HE_2 | 135342011 | 135738652.90 | 136013952 | 1.21 | 135031988 | 135031988.00 | 135031988 | 0.99 |
| DEEPSEA_FUN_C70_V30_HE_3 | 162773501 | 162905956.30 | 163268139 | 1.43 | 162759203 | 162759203.00 | 162759203 | 0.89 |
| DEEPSEA_FUN_C70_V30_HE_4 | 155964893 | 156117951.00 | 156254078 | 1.43 | 155855123 | 155855123.00 | 155855123 | 0.88 |
| DEEPSEA_FUN_C70_V30_HE_5 | 156704112 | 156872711.50 | 157041679 | 1.66 | 156557723 | 156557723.00 | 156557723 | 0.85 |
| DEEPSEA_FUN_C90_V40_HE_1 | 191055926 | 191192052.80 | 191435179 | 2.67 | 190627186 | 190628742.10 | 190642742 | 1.85 |
| DEEPSEA_FUN_C90_V40_HE_2 | 190028139 | 190249888.10 | 190725101 | 2.87 | 189770977 | 189771678.30 | 189777990 | 2.16 |
| DEEPSEA_FUN_C90_V40_HE_3 | 211265485 | 211436543.20 | 211600313 | 3.35 | 211038412 | 211038626.90 | 211040561 | 2.10 |
| DEEPSEA_FUN_C90_V40_HE_4 | 210564220 | 210704075.00 | 210868247 | 3.70 | 210449287 | 210449287.00 | 210449287 | 1.71 |
| DEEPSEA_FUN_C90_V40_HE_5 | 198084330 | 198352390.50 | 198672087 | 3.78 | 197804917 | 197804917.00 | 197804917 | 1.91 |
| DEEPSEA_FUN_C100_V50_HE_1 | 205965394 | 206152838.40 | 206399739 | 4.74 | 205826535 | 205826658.30 | 205827768 | 2.66 |
| DEEPSEA_FUN_C100_V50_HE_2 | 208251869 | 208472467.40 | 208737288 | 4.25 | 207809147 | 207809147.00 | 207809147 | 3.05 |
| DEEPSEA_FUN_C100_V50_HE_3 | 217551154 | 218077707.80 | 218927606 | 4.70 | 217000928 | 217000928.00 | 217000928 | 2.40 |
| DEEPSEA_FUN_C100_V50_HE_4 | 221017064 | 221273598.90 | 221508378 | 6.22 | 220879632 | 220880010.80 | 220882880 | 2.51 |
| DEEPSEA_FUN_C100_V50_HE_5 | 223346039 | 223606855.80 | 223876870 | 3.91 | 223265017 | 223265017.10 | 223265018 | 2.52 |

Table A.5: Full results on Hemmati et al. (2014) for B&P.

| | Root Node | | MIP | | B&P | | | | |
|---|---|---|---|---|---|---|---|---|---|
| Instance | LB | T | UB | T | LB | UB | T | EN | HN |
| SHORTSEA_MUN_C7_V3_HE_1 | 1476444.0 | 0.0 | 1476444 | 0.0 | 1476444.0 | 1476444 | 0.0 | 1 | 0 |
| SHORTSEA_MUN_C7_V3_HE_2 | 1134176.0 | 0.0 | 1134176 | 0.0 | 1134176.0 | 1134176 | 0.0 | 1 | 0 |
| SHORTSEA_MUN_C7_V3_HE_3 | 1196466.0 | 0.0 | 1196466 | 0.0 | 1196466.0 | 1196466 | 0.0 | 1 | 0 |
| SHORTSEA_MUN_C7_V3_HE_4 | 1256139.0 | 0.0 | 1256139 | 0.0 | 1256139.0 | 1256139 | 0.0 | 1 | 0 |
| SHORTSEA_MUN_C7_V3_HE_5 | 1160394.0 | 0.0 | 1160394 | 0.0 | 1160394.0 | 1160394 | 0.0 | 1 | 0 |
| SHORTSEA_MUN_C10_V3_HE_1 | 2083965.0 | 0.0 | 2083965 | 0.0 | 2083965.0 | 2083965 | 0.0 | 1 | 0 |
| SHORTSEA_MUN_C10_V3_HE_2 | 2012364.0 | 0.0 | 2012364 | 0.0 | 2012364.0 | 2012364 | 0.0 | 1 | 0 |
| SHORTSEA_MUN_C10_V3_HE_3 | 1986779.0 | 0.0 | 1986779 | 0.0 | 1986779.0 | 1986779 | 0.0 | 1 | 0 |
| SHORTSEA_MUN_C10_V3_HE_4 | 2125461.0 | 0.0 | 2125461 | 0.0 | 2125461.0 | 2125461 | 0.0 | 1 | 0 |
| SHORTSEA_MUN_C10_V3_HE_5 | 2162453.0 | 0.0 | 2162453 | 0.0 | 2162453.0 | 2162453 | 0.0 | 1 | 0 |
| SHORTSEA_MUN_C15_V4_HE_1 | 1959153.0 | 0.0 | 1959153 | 0.0 | 1959153.0 | 1959153 | 0.0 | 1 | 0 |
| SHORTSEA_MUN_C15_V4_HE_2 | 2538961.0 | 0.0 | 2560004 | 0.0 | 2560004.0 | 2560004 | 0.1 | 7 | 16 |
| SHORTSEA_MUN_C15_V4_HE_3 | 2484024.5 | 0.0 | 2587984 | 0.0 | 2582912.0 | 2582912 | 0.1 | 5 | 6 |
| SHORTSEA_MUN_C15_V4_HE_4 | 2252946.0 | 0.0 | 2265396 | 0.0 | 2265396.0 | 2265396 | 0.1 | 3 | 2 |
| SHORTSEA_MUN_C15_V4_HE_5 | 2230861.0 | 0.0 | 2230861 | 0.0 | 2230861.0 | 2230861 | 0.0 | 1 | 0 |
| SHORTSEA_MUN_C18_V5_HE_1 | 2329225.5 | 0.1 | 2416632 | 0.1 | 2374420.0 | 2374420 | 0.6 | 15 | 100 |
| SHORTSEA_MUN_C18_V5_HE_2 | 2987358.0 | 0.1 | 2987358 | 0.1 | 2987358.0 | 2987358 | 0.1 | 1 | 0 |
| SHORTSEA_MUN_C18_V5_HE_3 | 2301308.0 | 0.0 | 2301308 | 0.0 | 2301308.0 | 2301308 | 0.0 | 1 | 0 |
| SHORTSEA_MUN_C18_V5_HE_4 | 2400016.0 | 0.1 | 2400016 | 0.1 | 2400016.0 | 2400016 | 0.1 | 1 | 0 |
| SHORTSEA_MUN_C18_V5_HE_5 | 2789598.0 | 0.1 | 2816150 | 0.1 | 2813167.0 | 2813167 | 0.3 | 9 | 64 |
| SHORTSEA_MUN_C22_V6_HE_1 | 3928483.0 | 0.0 | 3928483 | 0.0 | 3928483.0 | 3928483 | 0.0 | 1 | 0 |
| SHORTSEA_MUN_C22_V6_HE_2 | 3487768.7 | 0.1 | 3774389 | 0.1 | 3683436.0 | 3683436 | 0.9 | 27 | 46 |
| SHORTSEA_MUN_C22_V6_HE_3 | 3231622.0 | 0.1 | 3308030 | 0.1 | 3264770.0 | 3264770 | 1.4 | 11 | 245 |
| SHORTSEA_MUN_C22_V6_HE_4 | 3222544.8 | 0.2 | 3228262 | 0.2 | 3228262.0 | 3228262 | 0.3 | 3 | 2 |
| SHORTSEA_MUN_C22_V6_HE_5 | 3763700.8 | 0.0 | 3771688 | 0.0 | 3770560.0 | 3770560 | 0.1 | 3 | 2 |
| SHORTSEA_MUN_C23_V13_HE_1 | 2249158.2 | 0.2 | 2293525 | 0.3 | 2276832.0 | 2276832 | 4.8 | 37 | 221 |
| SHORTSEA_MUN_C23_V13_HE_2 | 2255469.0 | 0.3 | 2255469 | 0.3 | 2255469.0 | 2255469 | 0.3 | 1 | 0 |
| SHORTSEA_MUN_C23_V13_HE_3 | 2362503.0 | 0.2 | 2362503 | 0.2 | 2362503.0 | 2362503 | 0.2 | 1 | 0 |
| SHORTSEA_MUN_C23_V13_HE_4 | 2231516.5 | 0.9 | 2253640 | 0.9 | 2250110.0 | 2250110 | 37.0 | 109 | 995 |
| SHORTSEA_MUN_C23_V13_HE_5 | 2325747.2 | 0.1 | 2325941 | 0.1 | 2325941.0 | 2325941 | 0.2 | 3 | 2 |
| SHORTSEA_MUN_C30_V6_HE_1 | 4958542.0 | 0.2 | 4958542 | 0.2 | 4958542.0 | 4958542 | 0.2 | 1 | 0 |
| SHORTSEA_MUN_C30_V6_HE_2 | 4495744.8 | 0.3 | 4549708 | 0.3 | 4549708.0 | 4549708 | 1.6 | 13 | 82 |
| SHORTSEA_MUN_C30_V6_HE_3 | 4034469.5 | 0.9 | 4159662 | 1.1 | 4098111.0 | 4098111 | 20.5 | 39 | 482 |
| SHORTSEA_MUN_C30_V6_HE_4 | 4410463.2 | 0.8 | 4616521 | 1.2 | 4449449.0 | 4449449 | 8.4 | 13 | 370 |
| SHORTSEA_MUN_C30_V6_HE_5 | 4528514.0 | 0.6 | 4528514 | 0.6 | 4528514.0 | 4528514 | 0.6 | 1 | 0 |
| SHORTSEA_MUN_C35_V7_HE_1 | 4866614.2 | 0.8 | 4985551 | 1.0 | 4893734.0 | 4893734 | 3.3 | 7 | 68 |
| SHORTSEA_MUN_C35_V7_HE_2 | 4460401.9 | 2.5 | 4718541 | 3.5 | 4533265.0 | 4533265 | 90.3 | 91 | 2161 |
| SHORTSEA_MUN_C35_V7_HE_3 | 4430107.9 | 2.2 | 4601192 | 2.7 | 4433847.0 | 4433847 | 5.5 | 3 | 70 |
| SHORTSEA_MUN_C35_V7_HE_4 | 4548437.7 | 2.5 | 4693288 | 2.9 | 4580935.0 | 4580935 | 22.3 | 19 | 394 |
| SHORTSEA_MUN_C35_V7_HE_5 | 5495244.0 | 0.7 | 5527520 | 0.8 | 5511661.0 | 5511661 | 4.1 | 5 | 148 |
| SHORTSEA_MUN_C60_V13_HE_1 | 8099191.6 | 33.3 | 8249940 | 50.8 | 8133385.0 | 8133385 | 1162.6 | 145 | 4226 |
| SHORTSEA_MUN_C60_V13_HE_2 | 7931646.5 | 38.9 | 8036756 | 47.4 | 7971476.0 | 7971476 | 1761.5 | 237 | 4247 |
| SHORTSEA_MUN_C60_V13_HE_3 | 7599147.4 | 43.8 | 7733822 | 62.2 | 7604198.0 | 7604198 | 94.8 | 3 | 57 |
| SHORTSEA_MUN_C60_V13_HE_4 | 8447115.5 | 19.5 | 8643183 | 37.8 | 8505125.0 | 8505125 | 1165.2 | 223 | 6336 |
| SHORTSEA_MUN_C60_V13_HE_5 | 8881967.7 | 10.3 | 8973580 | 12.7 | 8921750.0 | 8921750 | 266.1 | 57 | 1593 |
| SHORTSEA_MUN_C80_V20_HE_1 | 10255116.5 | 71.2 | 10326279 | 74.0 | 10289573.0 | 10289573 | 1279.1 | 51 | 1529 |
| SHORTSEA_MUN_C80_V20_HE_2 | 10211093.0 | 55.3 | 10292036 | 56.4 | 10240618.0 | 10240618 | 259.2 | 9 | 207 |
| SHORTSEA_MUN_C80_V20_HE_3 | 9596762.2 | 177.4 | 9627549 | 178.1 | 9606530.0 | 9606530 | 1282.1 | 19 | 522 |
| SHORTSEA_MUN_C80_V20_HE_4 | 11280736.1 | 24.7 | 11330979 | 25.6 | 11302476.0 | 11302476 | 173.4 | 15 | 31 |
| SHORTSEA_MUN_C80_V20_HE_5 | 10858161.5 | 23.2 | 10882782 | 23.6 | 10862563.0 | 10862563 | 54.1 | 5 | 59 |
| SHORTSEA_MUN_C100_V30_HE_1 | 12612920.4 | 128.2 | 12641227 | 129.8 | 12625185.1 | 12641227 | 3600.0 | 107 | 2710 |
| SHORTSEA_MUN_C100_V30_HE_2 | 12744751.8 | 115.9 | 12784951 | 116.8 | 12773692.8 | 12776760 | 3600.0 | 103 | 2987 |
| SHORTSEA_MUN_C100_V30_HE_3 | 11910321.0 | 345.2 | 11946818 | 347.6 | 11928269.6 | 11946818 | 3600.0 | 41 | 1125 |
| SHORTSEA_MUN_C100_V30_HE_4 | 13596484.5 | 107.5 | 13607851 | 107.8 | 13605352.0 | 13605352 | 1145.1 | 35 | 440 |
| SHORTSEA_MUN_C100_V30_HE_5 | 13225091.3 | 52.1 | 13251288 | 52.9 | 13240648.0 | 13240648 | 1263.7 | 55 | 930 |
| SHORTSEA_MUN_C130_V40_HE_1 | 16286675.8 | 369.3 | 16342248 | 456.0 | 16308671.9 | 16342248 | 3600.0 | 26 | 759 |
| SHORTSEA_MUN_C130_V40_HE_2 | 16243044.1 | 1324.0 | 16288691 | 1341.1 | 16246161.3 | 16288691 | 3600.0 | 8 | 73 |
| SHORTSEA_MUN_C130_V40_HE_3 | 15510595.3 | 793.5 | 15545580 | 795.4 | 15520539.8 | 15545580 | 3600.0 | 13 | 183 |
| SHORTSEA_MUN_C130_V40_HE_4 | 16998857.1 | 235.1 | 17020967 | 248.5 | 17007914.4 | 17020967 | 3600.0 | 55 | 1249 |
| SHORTSEA_MUN_C130_V40_HE_5 | 18251952.7 | 428.0 | 18275526 | 429.9 | 18264649.5 | 18275526 | 3600.0 | 34 | 483 |

Table A.6: Full results on Hemmati et al. (2014) for B&P.

| | Root Node | | MIP | | B&P | | | | |
|---|---|---|---|---|---|---|---|---|---|
| Instance | LB | T | UB | T | LB | UB | T | EN | HN |
| SHORTSEA_FUN_C8_V3_HE_1 | 1391997.0 | 0.0 | 1391997 | 0.0 | 1391997.0 | 1391997 | 0.0 | 1 | 0 |
| SHORTSEA_FUN_C8_V3_HE_2 | 1246273.0 | 0.0 | 1246273 | 0.0 | 1246273.0 | 1246273 | 0.0 | 1 | 0 |
| SHORTSEA_FUN_C8_V3_HE_3 | 1698102.0 | 0.0 | 1698102 | 0.0 | 1698102.0 | 1698102 | 0.0 | 1 | 0 |
| SHORTSEA_FUN_C8_V3_HE_4 | 1777637.0 | 0.0 | 1777637 | 0.0 | 1777637.0 | 1777637 | 0.0 | 1 | 0 |
| SHORTSEA_FUN_C8_V3_HE_5 | 1636788.0 | 0.0 | 1636788 | 0.0 | 1636788.0 | 1636788 | 0.0 | 1 | 0 |
| SHORTSEA_FUN_C11_V4_HE_1 | 1052463.0 | 0.0 | 1052463 | 0.0 | 1052463.0 | 1052463 | 0.0 | 1 | 0 |
| SHORTSEA_FUN_C11_V4_HE_2 | 1067139.0 | 0.0 | 1067139 | 0.0 | 1067139.0 | 1067139 | 0.0 | 1 | 0 |
| SHORTSEA_FUN_C11_V4_HE_3 | 1212388.0 | 0.0 | 1212388 | 0.0 | 1212388.0 | 1212388 | 0.0 | 1 | 0 |
| SHORTSEA_FUN_C11_V4_HE_4 | 1185465.0 | 0.0 | 1185465 | 0.0 | 1185465.0 | 1185465 | 0.0 | 1 | 0 |
| SHORTSEA_FUN_C11_V4_HE_5 | 1310285.0 | 0.0 | 1310285 | 0.0 | 1310285.0 | 1310285 | 0.0 | 1 | 0 |
| SHORTSEA_FUN_C13_V5_HE_1 | 2034184.0 | 0.0 | 2034184 | 0.0 | 2034184.0 | 2034184 | 0.0 | 1 | 0 |
| SHORTSEA_FUN_C13_V5_HE_2 | 2043253.0 | 0.0 | 2043253 | 0.0 | 2043253.0 | 2043253 | 0.0 | 1 | 0 |
| SHORTSEA_FUN_C13_V5_HE_3 | 2378283.0 | 0.0 | 2378283 | 0.0 | 2378283.0 | 2378283 | 0.0 | 1 | 0 |
| SHORTSEA_FUN_C13_V5_HE_4 | 2707215.0 | 0.0 | 2707215 | 0.0 | 2707215.0 | 2707215 | 0.0 | 1 | 0 |
| SHORTSEA_FUN_C13_V5_HE_5 | 3011648.0 | 0.0 | 3011648 | 0.0 | 3011648.0 | 3011648 | 0.0 | 1 | 0 |
| SHORTSEA_FUN_C16_V6_HE_1 | 3577005.0 | 0.0 | 3577005 | 0.0 | 3577005.0 | 3577005 | 0.0 | 1 | 0 |
| SHORTSEA_FUN_C16_V6_HE_2 | 3560203.0 | 0.0 | 3560203 | 0.0 | 3560203.0 | 3560203 | 0.0 | 1 | 0 |
| SHORTSEA_FUN_C16_V6_HE_3 | 4081013.0 | 0.0 | 4081013 | 0.0 | 4081013.0 | 4081013 | 0.0 | 1 | 0 |
| SHORTSEA_FUN_C16_V6_HE_4 | 3667080.0 | 0.0 | 3667080 | 0.0 | 3667080.0 | 3667080 | 0.0 | 1 | 0 |
| SHORTSEA_FUN_C16_V6_HE_5 | 3438493.0 | 0.0 | 3438493 | 0.0 | 3438493.0 | 3438493 | 0.0 | 1 | 0 |
| SHORTSEA_FUN_C17_V13_HE_1 | 2265329.0 | 0.0 | 2265731 | 0.0 | 2265731.0 | 2265731 | 0.0 | 3 | 2 |
| SHORTSEA_FUN_C17_V13_HE_2 | 3154165.0 | 0.0 | 3154165 | 0.0 | 3154165.0 | 3154165 | 0.0 | 1 | 0 |
| SHORTSEA_FUN_C17_V13_HE_3 | 2697988.7 | 0.0 | 2699378 | 0.0 | 2699378.0 | 2699378 | 0.0 | 3 | 2 |
| SHORTSEA_FUN_C17_V13_HE_4 | 2806231.0 | 0.0 | 2806231 | 0.0 | 2806231.0 | 2806231 | 0.0 | 1 | 0 |
| SHORTSEA_FUN_C17_V13_HE_5 | 2910814.0 | 0.0 | 2910814 | 0.0 | 2910814.0 | 2910814 | 0.0 | 1 | 0 |
| SHORTSEA_FUN_C20_V6_HE_1 | 2973381.0 | 0.0 | 2973381 | 0.0 | 2973381.0 | 2973381 | 0.0 | 1 | 0 |
| SHORTSEA_FUN_C20_V6_HE_2 | 3206514.0 | 0.0 | 3206514 | 0.0 | 3206514.0 | 3206514 | 0.0 | 1 | 0 |
| SHORTSEA_FUN_C20_V6_HE_3 | 3192228.6 | 0.0 | 3200652 | 0.0 | 3197445.0 | 3197445 | 0.1 | 3 | 30 |
| SHORTSEA_FUN_C20_V6_HE_4 | 3342117.5 | 0.0 | 3342130 | 0.0 | 3342130.0 | 3342130 | 0.0 | 3 | 4 |
| SHORTSEA_FUN_C20_V6_HE_5 | 3156378.0 | 0.0 | 3156378 | 0.0 | 3156378.0 | 3156378 | 0.0 | 1 | 0 |
| SHORTSEA_FUN_C25_V7_HE_1 | 3833588.0 | 0.0 | 3833588 | 0.0 | 3833588.0 | 3833588 | 0.0 | 1 | 0 |
| SHORTSEA_FUN_C25_V7_HE_2 | 3673666.0 | 0.0 | 3673666 | 0.0 | 3673666.0 | 3673666 | 0.0 | 1 | 0 |
| SHORTSEA_FUN_C25_V7_HE_3 | 4237512.0 | 0.0 | 4250780 | 0.0 | 4238213.0 | 4238213 | 0.1 | 3 | 34 |
| SHORTSEA_FUN_C25_V7_HE_4 | 4260762.0 | 0.0 | 4260762 | 0.0 | 4260762.0 | 4260762 | 0.0 | 1 | 0 |
| SHORTSEA_FUN_C25_V7_HE_5 | 4069693.0 | 0.0 | 4069693 | 0.0 | 4069693.0 | 4069693 | 0.0 | 1 | 0 |
| SHORTSEA_FUN_C35_V13_HE_1 | 2986667.0 | 0.1 | 2986667 | 0.1 | 2986667.0 | 2986667 | 0.1 | 1 | 0 |
| SHORTSEA_FUN_C35_V13_HE_2 | 3002595.7 | 0.1 | 3002974 | 0.1 | 3002973.0 | 3002973 | 0.2 | 3 | 2 |
| SHORTSEA_FUN_C35_V13_HE_3 | 3084339.0 | 0.1 | 3084339 | 0.1 | 3084339.0 | 3084339 | 0.1 | 1 | 0 |
| SHORTSEA_FUN_C35_V13_HE_4 | 3952461.0 | 0.1 | 3952461 | 0.1 | 3952461.0 | 3952461 | 0.1 | 1 | 0 |
| SHORTSEA_FUN_C35_V13_HE_5 | 3293086.0 | 0.1 | 3293086 | 0.1 | 3293086.0 | 3293086 | 0.1 | 1 | 0 |
| SHORTSEA_FUN_C50_V20_HE_1 | 7258266.0 | 0.2 | 7258266 | 0.2 | 7258266.0 | 7258266 | 0.2 | 1 | 0 |
| SHORTSEA_FUN_C50_V20_HE_2 | 7452465.0 | 0.2 | 7452465 | 0.2 | 7452465.0 | 7452465 | 0.2 | 1 | 0 |
| SHORTSEA_FUN_C50_V20_HE_3 | 6922293.0 | 0.2 | 6922293 | 0.2 | 6922293.0 | 6922293 | 0.2 | 1 | 0 |
| SHORTSEA_FUN_C50_V20_HE_4 | 8933721.0 | 0.2 | 8933847 | 0.2 | 8933846.0 | 8933846 | 0.8 | 3 | 41 |
| SHORTSEA_FUN_C50_V20_HE_5 | 7312328.5 | 0.2 | 7322307 | 0.2 | 7322307.0 | 7322307 | 0.5 | 3 | 4 |
| SHORTSEA_FUN_C70_V30_HE_1 | 10051856.0 | 1.0 | 10051856 | 1.0 | 10051856.0 | 10051856 | 1.0 | 1 | 0 |
| SHORTSEA_FUN_C70_V30_HE_2 | 10455468.0 | 0.7 | 10455468 | 0.7 | 10455468.0 | 10455468 | 0.7 | 1 | 0 |
| SHORTSEA_FUN_C70_V30_HE_3 | 10172541.0 | 0.6 | 10172541 | 0.7 | 10172541.0 | 10172541 | 0.7 | 1 | 0 |
| SHORTSEA_FUN_C70_V30_HE_4 | 10851222.8 | 0.5 | 10854037 | 0.6 | 10854036.0 | 10854036 | 4.7 | 11 | 24 |
| SHORTSEA_FUN_C70_V30_HE_5 | 10822672.0 | 0.6 | 10888089 | 0.6 | 10886838.0 | 10886838 | 3.2 | 13 | 12 |
| SHORTSEA_FUN_C90_V40_HE_1 | 13361849.5 | 1.9 | 13362182 | 2.0 | 13361947.0 | 13361947 | 51.2 | 11 | 196 |
| SHORTSEA_FUN_C90_V40_HE_2 | 13828112.0 | 1.4 | 13828112 | 1.4 | 13828112.0 | 13828112 | 1.4 | 1 | 0 |
| SHORTSEA_FUN_C90_V40_HE_3 | 12626910.5 | 2.0 | 12627125 | 2.1 | 12627125.0 | 12627125 | 3.6 | 3 | 2 |
| SHORTSEA_FUN_C90_V40_HE_4 | 14406428.0 | 1.6 | 14406428 | 1.6 | 14406428.0 | 14406428 | 1.6 | 1 | 0 |
| SHORTSEA_FUN_C90_V40_HE_5 | 13559110.5 | 1.8 | 13564406 | 2.1 | 13560830.0 | 13560830 | 8.5 | 3 | 61 |
| SHORTSEA_FUN_C100_V50_HE_1 | 13800823.0 | 1.8 | 13800823 | 1.8 | 13800823.0 | 13800823 | 1.8 | 1 | 0 |
| SHORTSEA_FUN_C100_V50_HE_2 | 14639802.3 | 1.9 | 14645667 | 2.1 | 14644836.0 | 14644836 | 90.6 | 27 | 331 |
| SHORTSEA_FUN_C100_V50_HE_3 | 13135505.0 | 2.6 | 13135505 | 2.6 | 13135505.0 | 13135505 | 2.6 | 1 | 0 |
| SHORTSEA_FUN_C100_V50_HE_4 | 14839249.5 | 2.7 | 14841841 | 3.0 | 14841840.0 | 14841840 | 192.8 | 55 | 669 |
| SHORTSEA_FUN_C100_V50_HE_5 | 14009079.2 | 2.0 | 14009874 | 2.1 | 14009874.0 | 14009874 | 18.1 | 15 | 22 |

Table A.7: Full results on Hemmati et al. (2014) for B&P.

| | Root Node | | MIP | | Branch-and-Price | | | | |
|---|---|---|---|---|---|---|---|---|---|
| Instance | LB | T | UB | T | LB | UB | T | EN | HN |
| DEEPSEA_MUN_C7_V3_HE_1 | 4950070.5 | 0.0 | 5233464 | 0.0 | 5233464.0 | 5233464 | 0.0 | 3 | 2 |
| DEEPSEA_MUN_C7_V3_HE_2 | 6053699.0 | 0.0 | 6053699 | 0.0 | 6053699.0 | 6053699 | 0.0 | 1 | 0 |
| DEEPSEA_MUN_C7_V3_HE_3 | 5888949.0 | 0.0 | 5888949 | 0.0 | 5888949.0 | 5888949 | 0.0 | 1 | 0 |
| DEEPSEA_MUN_C7_V3_HE_4 | 6510656.0 | 0.0 | 6510656 | 0.0 | 6510656.0 | 6510656 | 0.0 | 1 | 0 |
| DEEPSEA_MUN_C7_V3_HE_5 | 7220458.0 | 0.0 | 7220458 | 0.0 | 7220458.0 | 7220458 | 0.0 | 1 | 0 |
| DEEPSEA_MUN_C10_V3_HE_1 | 7986248.0 | 0.0 | 7986248 | 0.0 | 7986248.0 | 7986248 | 0.0 | 1 | 0 |
| DEEPSEA_MUN_C10_V3_HE_2 | 7754484.0 | 0.0 | 7754484 | 0.0 | 7754484.0 | 7754484 | 0.0 | 1 | 0 |
| DEEPSEA_MUN_C10_V3_HE_3 | 9295578.0 | 0.0 | 9499357 | 0.0 | 9499357.0 | 9499357 | 0.0 | 3 | 4 |
| DEEPSEA_MUN_C10_V3_HE_4 | 8602011.0 | 0.0 | 8617192 | 0.0 | 8617192.0 | 8617192 | 0.0 | 5 | 4 |
| DEEPSEA_MUN_C10_V3_HE_5 | 8070404.0 | 0.0 | 9702181 | 0.0 | 8653992.0 | 8653992 | 0.0 | 5 | 15 |
| DEEPSEA_MUN_C15_V4_HE_1 | 12812979.5 | 0.0 | 13467090 | 0.0 | 13467090.0 | 13467090 | 0.0 | 5 | 9 |
| DEEPSEA_MUN_C15_V4_HE_2 | 12457251.0 | 0.0 | 12457251 | 0.0 | 12457251.0 | 12457251 | 0.0 | 1 | 0 |
| DEEPSEA_MUN_C15_V4_HE_3 | 12567396.0 | 0.0 | 12567396 | 0.0 | 12567396.0 | 12567396 | 0.0 | 1 | 0 |
| DEEPSEA_MUN_C15_V4_HE_4 | 11764241.0 | 0.0 | 11764241 | 0.0 | 11764241.0 | 11764241 | 0.0 | 1 | 0 |
| DEEPSEA_MUN_C15_V4_HE_5 | 10833640.0 | 0.0 | 10833640 | 0.0 | 10833640.0 | 10833640 | 0.0 | 1 | 0 |
| DEEPSEA_MUN_C18_V5_HE_1 | 42480419.0 | 0.0 | 43054055 | 0.0 | 43054055.0 | 43054055 | 0.0 | 3 | 2 |
| DEEPSEA_MUN_C18_V5_HE_2 | 24770447.0 | 0.1 | 25528180 | 0.1 | 25068287.0 | 25068287 | 0.7 | 7 | 56 |
| DEEPSEA_MUN_C18_V5_HE_3 | 29211238.0 | 0.0 | 29211238 | 0.0 | 29211238.0 | 29211238 | 0.0 | 1 | 0 |
| DEEPSEA_MUN_C18_V5_HE_4 | 32281904.0 | 0.0 | 32281904 | 0.0 | 32281904.0 | 32281904 | 0.0 | 1 | 0 |
| DEEPSEA_MUN_C18_V5_HE_5 | 40718028.0 | 0.0 | 40718028 | 0.0 | 40718028.0 | 40718028 | 0.0 | 1 | 0 |
| DEEPSEA_MUN_C22_V6_HE_1 | 41176718.0 | 0.0 | 41176718 | 0.0 | 41176718.0 | 41176718 | 0.0 | 1 | 0 |
| DEEPSEA_MUN_C22_V6_HE_2 | 37236363.0 | 0.0 | 37236363 | 0.0 | 37236363.0 | 37236363 | 0.0 | 1 | 0 |
| DEEPSEA_MUN_C22_V6_HE_3 | 36724417.0 | 0.0 | 38215238 | 0.0 | 38215238.0 | 38215238 | 0.1 | 9 | 12 |
| DEEPSEA_MUN_C22_V6_HE_4 | 33070380.2 | 0.1 | 34364524 | 0.1 | 34129809.0 | 34129809 | 0.3 | 9 | 84 |
| DEEPSEA_MUN_C22_V6_HE_5 | 46379332.0 | 0.0 | 46379332 | 0.0 | 46379332.0 | 46379332 | 0.0 | 1 | 0 |
| DEEPSEA_MUN_C23_V13_HE_1 | 41002992.0 | 0.0 | 41002992 | 0.0 | 41002992.0 | 41002992 | 0.0 | 1 | 0 |
| DEEPSEA_MUN_C23_V13_HE_2 | 27814256.5 | 0.1 | 28014147 | 0.1 | 28014147.0 | 28014147 | 0.1 | 3 | 2 |
| DEEPSEA_MUN_C23_V13_HE_3 | 29090422.0 | 0.0 | 29090422 | 0.0 | 29090422.0 | 29090422 | 0.0 | 1 | 0 |
| DEEPSEA_MUN_C23_V13_HE_4 | 33471039.5 | 0.0 | 33685274 | 0.0 | 33685274.0 | 33685274 | 0.1 | 5 | 4 |
| DEEPSEA_MUN_C23_V13_HE_5 | 38664843.0 | 0.0 | 38664843 | 0.0 | 38664843.0 | 38664843 | 0.0 | 1 | 0 |
| DEEPSEA_MUN_C30_V6_HE_1 | 19227093.0 | 0.0 | 19227093 | 0.0 | 19227093.0 | 19227093 | 0.0 | 1 | 0 |
| DEEPSEA_MUN_C30_V6_HE_2 | 15950873.6 | 0.2 | 17642204 | 0.3 | 16784810.0 | 16784810 | 6.2 | 37 | 344 |
| DEEPSEA_MUN_C30_V6_HE_3 | 20917898.3 | 0.1 | 21431487 | 0.2 | 21183928.0 | 21183928 | 0.7 | 13 | 12 |
| DEEPSEA_MUN_C30_V6_HE_4 | 21076728.0 | 0.2 | 21076728 | 0.2 | 21076728.0 | 21076728 | 0.2 | 1 | 0 |
| DEEPSEA_MUN_C30_V6_HE_5 | 24177325.6 | 0.1 | 24513492 | 0.1 | 24490671.0 | 24490671 | 2.1 | 39 | 348 |
| DEEPSEA_MUN_C35_V7_HE_1 | 64451358.0 | 0.1 | 65119365 | 0.1 | 65082675.0 | 65082675 | 1.0 | 13 | 86 |
| DEEPSEA_MUN_C35_V7_HE_2 | 53980309.5 | 1.0 | 55025454 | 1.0 | 54810586.0 | 54810586 | 6.5 | 13 | 177 |
| DEEPSEA_MUN_C35_V7_HE_3 | 55814152.0 | 0.2 | 56182502 | 0.2 | 56182502.0 | 56182502 | 1.5 | 9 | 80 |
| DEEPSEA_MUN_C35_V7_HE_4 | 59887019.1 | 0.2 | 62723359 | 0.4 | 61354812.0 | 61354812 | 1.6 | 15 | 50 |
| DEEPSEA_MUN_C35_V7_HE_5 | 63904705.0 | 0.1 | 63904705 | 0.1 | 63904705.0 | 63904705 | 0.1 | 1 | 0 |
| DEEPSEA_MUN_C60_V13_HE_1 | 79933869.8 | 18.5 | 81972624 | 43.5 | 80649895.0 | 80649895 | 984.2 | 157 | 4174 |
| DEEPSEA_MUN_C60_V13_HE_2 | 73811018.5 | 6.3 | 78034376 | 7.4 | 74881109.0 | 74881109 | 138.0 | 47 | 1221 |
| DEEPSEA_MUN_C60_V13_HE_3 | 91718990.0 | 1.5 | 91766747 | 1.6 | 91766747.0 | 91766747 | 2.5 | 3 | 5 |
| DEEPSEA_MUN_C60_V13_HE_4 | 89702352.0 | 3.2 | 89702352 | 3.2 | 89702352.0 | 89702352 | 3.2 | 1 | 0 |
| DEEPSEA_MUN_C60_V13_HE_5 | 88056480.1 | 3.8 | 89071597 | 4.1 | 88486544.0 | 88486544 | 25.4 | 9 | 257 |
| DEEPSEA_MUN_C80_V20_HE_1 | 70345242.4 | 14.8 | 71448738 | 25.9 | 70718084.0 | 70718084 | 354.8 | 53 | 918 |
| DEEPSEA_MUN_C80_V20_HE_2 | 73068858.7 | 54.3 | 73921496 | 60.3 | 73463298.1 | 73601236 | 3600.0 | 247 | 6333 |
| DEEPSEA_MUN_C80_V20_HE_3 | 78104852.0 | 8.6 | 78268464 | 8.6 | 78250612.0 | 78250612 | 30.3 | 5 | 71 |
| DEEPSEA_MUN_C80_V20_HE_4 | 75749235.0 | 14.7 | 76486358 | 20.9 | 75962439.0 | 75962439 | 416.6 | 77 | 1118 |
| DEEPSEA_MUN_C80_V20_HE_5 | 73808271.6 | 11.3 | 75315334 | 13.1 | 74162521.0 | 74162521 | 127.0 | 27 | 464 |
| DEEPSEA_MUN_C100_V30_HE_1 | 150197055.9 | 29.7 | 150638897 | 39.1 | 150451783.0 | 150638897 | 3600.0 | 277 | 6775 |
| DEEPSEA_MUN_C100_V30_HE_2 | 150350415.5 | 25.4 | 150862914 | 25.6 | 150826322.0 | 150826322 | 697.3 | 79 | 935 |
| DEEPSEA_MUN_C100_V30_HE_3 | 149804321.2 | 23.5 | 151718112 | 65.3 | 150837352.8 | 151718112 | 3600.0 | 341 | 8198 |
| DEEPSEA_MUN_C100_V30_HE_4 | 150062944.5 | 46.7 | 151890429 | 55.1 | 150404783.5 | 151890429 | 3600.0 | 223 | 4821 |
| DEEPSEA_MUN_C100_V30_HE_5 | 158977634.6 | 40.5 | 160713609 | 42.2 | 159789021.0 | 159789021 | 1392.4 | 97 | 1954 |
| DEEPSEA_MUN_C130_V40_HE_1 | 232233375.9 | 200.2 | 232641884 | 205.1 | 232324965.2 | 232641884 | 3600.0 | 52 | 924 |
| DEEPSEA_MUN_C130_V40_HE_2 | 226590319.5 | 215.8 | 229307168 | 224.9 | 226683287.2 | 229307168 | 3600.0 | 69 | 683 |
| DEEPSEA_MUN_C130_V40_HE_3 | 234147177.2 | 170.6 | 235705442 | 174.4 | 235477285.1 | 235705442 | 3600.0 | 60 | 1059 |
| DEEPSEA_MUN_C130_V40_HE_4 | 219926810.8 | 270.6 | 220540075 | 277.7 | 220165826.8 | 220540075 | 3600.0 | 43 | 752 |
| DEEPSEA_MUN_C130_V40_HE_5 | 234436256.7 | 205.6 | 235661384 | 209.6 | 234727321.5 | 235661384 | 3600.0 | 74 | 590 |

Table A.8: Full results on Hemmati et al. (2014) for B&P.

| | Root Node | | MIP | | B&P | | | | |
|---|---|---|---|---|---|---|---|---|---|
| Instance | LB | T | UB | T | LB | UB | T | EN | HN |
| DEEPSEA_FUN_C8_V3_HE_1 | 9584863.0 | 0.0 | 9584863 | 0.0 | 9584863.0 | 9584863 | 0.0 | 1 | 0 |
| DEEPSEA_FUN_C8_V3_HE_2 | 9369654.0 | 0.0 | 9369654 | 0.0 | 9369654.0 | 9369654 | 0.0 | 1 | 0 |
| DEEPSEA_FUN_C8_V3_HE_3 | 4596681.0 | 0.0 | 4596681 | 0.0 | 4596681.0 | 4596681 | 0.0 | 1 | 0 |
| DEEPSEA_FUN_C8_V3_HE_4 | 6899730.0 | 0.0 | 6899730 | 0.0 | 6899730.0 | 6899730 | 0.0 | 1 | 0 |
| DEEPSEA_FUN_C8_V3_HE_5 | 6815253.0 | 0.0 | 6815253 | 0.0 | 6815253.0 | 6815253 | 0.0 | 1 | 0 |
| DEEPSEA_FUN_C11_V4_HE_1 | 34854819.0 | 0.0 | 34854819 | 0.0 | 34854819.0 | 34854819 | 0.0 | 1 | 0 |
| DEEPSEA_FUN_C11_V4_HE_2 | 25454434.0 | 0.0 | 25454434 | 0.0 | 25454434.0 | 25454434 | 0.0 | 1 | 0 |
| DEEPSEA_FUN_C11_V4_HE_3 | 29627143.0 | 0.0 | 29627143 | 0.0 | 29627143.0 | 29627143 | 0.0 | 1 | 0 |
| DEEPSEA_FUN_C11_V4_HE_4 | 33111680.0 | 0.0 | 33111680 | 0.0 | 33111680.0 | 33111680 | 0.0 | 1 | 0 |
| DEEPSEA_FUN_C11_V4_HE_5 | 28175914.0 | 0.0 | 28175914 | 0.0 | 28175914.0 | 28175914 | 0.0 | 1 | 0 |
| DEEPSEA_FUN_C13_V5_HE_1 | 11629005.0 | 0.0 | 11629005 | 0.0 | 11629005.0 | 11629005 | 0.0 | 1 | 0 |
| DEEPSEA_FUN_C13_V5_HE_2 | 11820655.0 | 0.0 | 11820655 | 0.0 | 11820655.0 | 11820655 | 0.0 | 1 | 0 |
| DEEPSEA_FUN_C13_V5_HE_3 | 9992593.0 | 0.0 | 9992593 | 0.0 | 9992593.0 | 9992593 | 0.0 | 1 | 0 |
| DEEPSEA_FUN_C13_V5_HE_4 | 12819619.0 | 0.0 | 12819619 | 0.0 | 12819619.0 | 12819619 | 0.0 | 1 | 0 |
| DEEPSEA_FUN_C13_V5_HE_5 | 10534892.0 | 0.0 | 10534892 | 0.0 | 10534892.0 | 10534892 | 0.0 | 1 | 0 |
| DEEPSEA_FUN_C16_V6_HE_1 | 51091999.5 | 0.0 | 51127590 | 0.0 | 51127590.0 | 51127590 | 0.0 | 3 | 2 |
| DEEPSEA_FUN_C16_V6_HE_2 | 44342796.0 | 0.0 | 44342796 | 0.0 | 44342796.0 | 44342796 | 0.0 | 1 | 0 |
| DEEPSEA_FUN_C16_V6_HE_3 | 45391842.0 | 0.0 | 45391842 | 0.0 | 45391842.0 | 45391842 | 0.0 | 1 | 0 |
| DEEPSEA_FUN_C16_V6_HE_4 | 39687114.0 | 0.0 | 39687114 | 0.0 | 39687114.0 | 39687114 | 0.0 | 1 | 0 |
| DEEPSEA_FUN_C16_V6_HE_5 | 42855603.0 | 0.0 | 42855603 | 0.0 | 42855603.0 | 42855603 | 0.0 | 1 | 0 |
| DEEPSEA_FUN_C17_V13_HE_1 | 17316720.0 | 0.0 | 17316720 | 0.0 | 17316720.0 | 17316720 | 0.0 | 1 | 0 |
| DEEPSEA_FUN_C17_V13_HE_2 | 12180956.5 | 0.0 | 12194861 | 0.0 | 12194861.0 | 12194861 | 0.0 | 3 | 4 |
| DEEPSEA_FUN_C17_V13_HE_3 | 12091554.0 | 0.0 | 12091554 | 0.0 | 12091554.0 | 12091554 | 0.0 | 1 | 0 |
| DEEPSEA_FUN_C17_V13_HE_4 | 12847653.0 | 0.0 | 12847653 | 0.0 | 12847653.0 | 12847653 | 0.0 | 1 | 0 |
| DEEPSEA_FUN_C17_V13_HE_5 | 13213406.0 | 0.0 | 13213406 | 0.0 | 13213406.0 | 13213406 | 0.0 | 1 | 0 |
| DEEPSEA_FUN_C20_V6_HE_1 | 16315682.5 | 0.0 | 16406738 | 0.0 | 16406738.0 | 16406738 | 0.0 | 5 | 6 |
| DEEPSEA_FUN_C20_V6_HE_2 | 16079401.0 | 0.0 | 16079401 | 0.0 | 16079401.0 | 16079401 | 0.0 | 1 | 0 |
| DEEPSEA_FUN_C20_V6_HE_3 | 17342200.0 | 0.0 | 17342200 | 0.0 | 17342200.0 | 17342200 | 0.0 | 1 | 0 |
| DEEPSEA_FUN_C20_V6_HE_4 | 16529748.0 | 0.0 | 16529748 | 0.0 | 16529748.0 | 16529748 | 0.0 | 1 | 0 |
| DEEPSEA_FUN_C20_V6_HE_5 | 17449378.0 | 0.0 | 17449379 | 0.0 | 17449378.0 | 17449378 | 0.0 | 3 | 16 |
| DEEPSEA_FUN_C25_V7_HE_1 | 22773158.0 | 0.0 | 22773158 | 0.0 | 22773158.0 | 22773158 | 0.0 | 1 | 0 |
| DEEPSEA_FUN_C25_V7_HE_2 | 20206329.0 | 0.0 | 20206329 | 0.0 | 20206329.0 | 20206329 | 0.0 | 1 | 0 |
| DEEPSEA_FUN_C25_V7_HE_3 | 19108952.0 | 0.0 | 19108952 | 0.0 | 19108952.0 | 19108952 | 0.0 | 1 | 0 |
| DEEPSEA_FUN_C25_V7_HE_4 | 22668675.0 | 0.0 | 22668675 | 0.0 | 22668675.0 | 22668675 | 0.0 | 1 | 0 |
| DEEPSEA_FUN_C25_V7_HE_5 | 23036603.0 | 0.0 | 23036603 | 0.0 | 23036603.0 | 23036603 | 0.0 | 1 | 0 |
| DEEPSEA_FUN_C35_V13_HE_1 | 86951609.0 | 0.1 | 86951609 | 0.1 | 86951609.0 | 86951609 | 0.1 | 1 | 0 |
| DEEPSEA_FUN_C35_V13_HE_2 | 83422071.0 | 0.1 | 83422071 | 0.1 | 83422071.0 | 83422071 | 0.1 | 1 | 0 |
| DEEPSEA_FUN_C35_V13_HE_3 | 83898591.0 | 0.1 | 83898591 | 0.1 | 83898591.0 | 83898591 | 0.1 | 1 | 0 |
| DEEPSEA_FUN_C35_V13_HE_4 | 91970481.0 | 0.1 | 91970481 | 0.1 | 91970481.0 | 91970481 | 0.1 | 1 | 0 |
| DEEPSEA_FUN_C35_V13_HE_5 | 91003609.7 | 0.1 | 91123040 | 0.1 | 91123040.0 | 91123040 | 0.6 | 13 | 30 |
| DEEPSEA_FUN_C50_V20_HE_1 | 41310946.0 | 0.1 | 41310946 | 0.1 | 41310946.0 | 41310946 | 0.1 | 1 | 0 |
| DEEPSEA_FUN_C50_V20_HE_2 | 37784994.0 | 0.1 | 37784994 | 0.1 | 37784994.0 | 37784994 | 0.1 | 1 | 0 |
| DEEPSEA_FUN_C50_V20_HE_3 | 39841724.0 | 0.1 | 39841724 | 0.1 | 39841724.0 | 39841724 | 0.1 | 1 | 0 |
| DEEPSEA_FUN_C50_V20_HE_4 | 43941098.0 | 0.1 | 43941098 | 0.1 | 43941098.0 | 43941098 | 0.1 | 1 | 0 |
| DEEPSEA_FUN_C50_V20_HE_5 | 41947437.0 | 0.1 | 41947437 | 0.1 | 41947437.0 | 41947437 | 0.1 | 1 | 0 |
| DEEPSEA_FUN_C70_V30_HE_1 | 142679953.0 | 0.4 | 142679953 | 0.4 | 142679953.0 | 142679953 | 0.4 | 1 | 0 |
| DEEPSEA_FUN_C70_V30_HE_2 | 135008299.5 | 0.5 | 135031990 | 0.6 | 135031988.0 | 135031988 | 1.8 | 3 | 35 |
| DEEPSEA_FUN_C70_V30_HE_3 | 162759203.0 | 0.3 | 162759203 | 0.3 | 162759203.0 | 162759203 | 0.3 | 1 | 0 |
| DEEPSEA_FUN_C70_V30_HE_4 | 155855123.0 | 0.3 | 155855123 | 0.3 | 155855123.0 | 155855123 | 0.3 | 1 | 0 |
| DEEPSEA_FUN_C70_V30_HE_5 | 156557723.0 | 0.3 | 156557723 | 0.3 | 156557723.0 | 156557723 | 0.3 | 1 | 0 |
| DEEPSEA_FUN_C90_V40_HE_1 | 190624194.5 | 1.0 | 190629225 | 1.1 | 190627186.0 | 190627186 | 23.9 | 9 | 164 |
| DEEPSEA_FUN_C90_V40_HE_2 | 189770977.0 | 0.9 | 189770977 | 0.9 | 189770977.0 | 189770977 | 0.9 | 1 | 0 |
| DEEPSEA_FUN_C90_V40_HE_3 | 211038412.0 | 0.7 | 211038412 | 0.8 | 211038412.0 | 211038412 | 0.8 | 1 | 0 |
| DEEPSEA_FUN_C90_V40_HE_4 | 210449287.0 | 0.8 | 210449287 | 0.8 | 210449287.0 | 210449287 | 0.8 | 1 | 0 |
| DEEPSEA_FUN_C90_V40_HE_5 | 197797793.0 | 0.9 | 197804918 | 0.9 | 197804917.0 | 197804917 | 4.2 | 3 | 45 |
| DEEPSEA_FUN_C100_V50_HE_1 | 205824545.5 | 1.0 | 205826535 | 1.1 | 205826535.0 | 205826535 | 2.1 | 3 | 2 |
| DEEPSEA_FUN_C100_V50_HE_2 | 207809147.0 | 1.3 | 207809147 | 1.4 | 207809147.0 | 207809147 | 1.4 | 1 | 0 |
| DEEPSEA_FUN_C100_V50_HE_3 | 217000928.0 | 1.0 | 217000928 | 1.0 | 217000928.0 | 217000928 | 1.0 | 1 | 0 |
| DEEPSEA_FUN_C100_V50_HE_4 | 220879530.5 | 1.1 | 220879632 | 1.2 | 220879632.0 | 220879632 | 2.4 | 3 | 2 |
| DEEPSEA_FUN_C100_V50_HE_5 | 223265017.0 | 0.9 | 223265017 | 0.9 | 223265017.0 | 223265017 | 0.9 | 1 | 0 |

Table A.9: Full results on ITSRSPSO SS_MUN instances.

| | HGS-O | | | | HGS-J | | | |
|---|---|---|---|---|---|---|---|---|
| Instance | Best | Avg | Worst | T | Best | Avg | Worst | T |
| SHORTSEA_MUN_C7_V3_HE_1 | 1166381.49 | 1167132.18 | 1168258.22 | 0.02 | 1166381.49 | 1166381.49 | 1166381.49 | 0.16 |
| SHORTSEA_MUN_C7_V3_HE_2 | 815775.78 | 818829.30 | 819592.68 | 0.02 | 782788.27 | 782788.27 | 782788.27 | 0.38 |
| SHORTSEA_MUN_C7_V3_HE_3 | 892411.55 | 892411.55 | 892411.55 | 0.02 | 892411.55 | 892411.55 | 892411.55 | 0.35 |
| SHORTSEA_MUN_C7_V3_HE_4 | 770921.80 | 773398.60 | 775049.80 | 0.02 | 750081.73 | 750081.73 | 750081.73 | 0.36 |
| SHORTSEA_MUN_C7_V3_HE_5 | 898921.62 | 898921.62 | 898921.62 | 0.02 | 883520.58 | 883520.58 | 883520.58 | 0.28 |
| SHORTSEA_MUN_C10_V3_HE_1 | 1592630.53 | 1593429.41 | 1596624.91 | 0.03 | 1445963.78 | 1445963.78 | 1445963.78 | 0.71 |
| SHORTSEA_MUN_C10_V3_HE_2 | 1426733.17 | 1426733.17 | 1426733.17 | 0.03 | 1373919.28 | 1373919.28 | 1373919.28 | 1.03 |
| SHORTSEA_MUN_C10_V3_HE_3 | 1512591.38 | 1512591.38 | 1512591.38 | 0.04 | 1496838.85 | 1496838.85 | 1496838.85 | 1.02 |
| SHORTSEA_MUN_C10_V3_HE_4 | 1613472.87 | 1613472.87 | 1613472.87 | 0.04 | 1597462.74 | 1597462.74 | 1597462.74 | 1.21 |
| SHORTSEA_MUN_C10_V3_HE_5 | 1399559.10 | 1401354.28 | 1404047.04 | 0.04 | 1399559.10 | 1399559.10 | 1399559.10 | 0.75 |
| SHORTSEA_MUN_C15_V4_HE_1 | 1211743.73 | 1211753.01 | 1211790.12 | 0.07 | 1199770.91 | 1199770.91 | 1199770.91 | 2.99 |
| SHORTSEA_MUN_C15_V4_HE_2 | 1927069.71 | 1937319.74 | 1943638.17 | 0.08 | 1867671.50 | 1867671.50 | 1867671.50 | 3.50 |
| SHORTSEA_MUN_C15_V4_HE_3 | 1926526.92 | 1945767.56 | 1950577.72 | 0.08 | 1777836.83 | 1777836.83 | 1777836.83 | 4.92 |
| SHORTSEA_MUN_C15_V4_HE_4 | 1753962.83 | 1769996.24 | 1780685.18 | 0.09 | 1446644.28 | 1446644.28 | 1446644.28 | 3.52 |
| SHORTSEA_MUN_C15_V4_HE_5 | 1704484.62 | 1706603.90 | 1709782.82 | 0.07 | 1632981.62 | 1632981.62 | 1632981.62 | 3.28 |
| SHORTSEA_MUN_C18_V5_HE_1 | 1740636.01 | 1740636.01 | 1740636.01 | 0.10 | 1644116.25 | 1644116.25 | 1644116.25 | 4.27 |
| SHORTSEA_MUN_C18_V5_HE_2 | 2502280.63 | 2507044.65 | 2508235.65 | 0.12 | 2339298.58 | 2339298.58 | 2339298.58 | 5.90 |
| SHORTSEA_MUN_C18_V5_HE_3 | 1767685.42 | 1770144.47 | 1779674.32 | 0.12 | 1663189.32 | 1663189.32 | 1663189.32 | 6.57 |
| SHORTSEA_MUN_C18_V5_HE_4 | 1833155.63 | 1843680.02 | 1846642.87 | 0.15 | 1724844.09 | 1724844.09 | 1724844.09 | 5.65 |
| SHORTSEA_MUN_C18_V5_HE_5 | 2202180.97 | 2202180.97 | 2202180.97 | 0.12 | 1845590.32 | 1845590.32 | 1845590.32 | 5.08 |
| SHORTSEA_MUN_C22_V6_HE_1 | 2483182.85 | 2483182.85 | 2483182.85 | 0.15 | 2378854.16 | 2378854.16 | 2378854.16 | 6.05 |
| SHORTSEA_MUN_C22_V6_HE_2 | 2631639.98 | 2631686.14 | 2631697.68 | 0.17 | 2198359.19 | 2198359.19 | 2198359.19 | 7.16 |
| SHORTSEA_MUN_C22_V6_HE_3 | 2250128.80 | 2250128.80 | 2250128.80 | 0.18 | 2041332.32 | 2041332.32 | 2041332.32 | 10.18 |
| SHORTSEA_MUN_C22_V6_HE_4 | 2181167.68 | 2181167.68 | 2181167.68 | 0.17 | 2053885.58 | 2053885.58 | 2053885.58 | 10.41 |
| SHORTSEA_MUN_C22_V6_HE_5 | 2221632.33 | 2234155.04 | 2245160.88 | 0.16 | 2217719.97 | 2217719.97 | 2217719.97 | 7.34 |
| SHORTSEA_MUN_C23_V13_HE_1 | 1591809.65 | 1591855.05 | 1591923.16 | 0.17 | 1526493.15 | 1526493.15 | 1526493.15 | 5.64 |
| SHORTSEA_MUN_C23_V13_HE_2 | 1564761.82 | 1564886.51 | 1565385.29 | 0.21 | 1536614.21 | 1536614.21 | 1536614.21 | 6.98 |
| SHORTSEA_MUN_C23_V13_HE_3 | 1875108.52 | 1886805.65 | 1889729.94 | 0.18 | 1770199.31 | 1770199.31 | 1770199.31 | 5.05 |
| SHORTSEA_MUN_C23_V13_HE_4 | 1675269.26 | 1678575.63 | 1683639.61 | 0.20 | 1526817.62 | 1526817.62 | 1526817.62 | 6.69 |
| SHORTSEA_MUN_C23_V13_HE_5 | 1631311.02 | 1633691.82 | 1643215.02 | 0.19 | 1573273.06 | 1573273.06 | 1573273.06 | 4.60 |
| SHORTSEA_MUN_C30_V6_HE_1 | 3465705.97 | 3467988.78 | 3471413.00 | 0.29 | 2950022.75 | 2950022.75 | 2950022.75 | 15.00 |
| SHORTSEA_MUN_C30_V6_HE_2 | 3280445.83 | 3280923.59 | 3281059.50 | 0.31 | 2936017.54 | 2958170.88 | 2998787.59 | 15.01 |
| SHORTSEA_MUN_C30_V6_HE_3 | 2982366.95 | 2988588.74 | 2998159.41 | 0.31 | 2702494.56 | 2702494.56 | 2702494.56 | 15.01 |
| SHORTSEA_MUN_C30_V6_HE_4 | 3236303.46 | 3237610.70 | 3238221.87 | 0.33 | 3034654.37 | 3034654.37 | 3034654.37 | 15.00 |
| SHORTSEA_MUN_C30_V6_HE_5 | 3066698.66 | 3081532.83 | 3096353.15 | 0.23 | 2945430.73 | 2945430.73 | 2945430.73 | 15.01 |
| SHORTSEA_MUN_C35_V7_HE_1 | 3480753.15 | 3503066.30 | 3528606.13 | 0.53 | 3264245.07 | 3288551.97 | 3325397.73 | 15.00 |
| SHORTSEA_MUN_C35_V7_HE_2 | 3467193.13 | 3468356.83 | 3472059.04 | 0.43 | 3043015.36 | 3043015.36 | 3043015.36 | 15.00 |
| SHORTSEA_MUN_C35_V7_HE_3 | 3182368.59 | 3186227.73 | 3191364.58 | 0.42 | 3008349.15 | 3028384.24 | 3059072.67 | 15.01 |
| SHORTSEA_MUN_C35_V7_HE_4 | 3327936.41 | 3328323.90 | 3328905.13 | 0.43 | 3094466.45 | 3099095.98 | 3117614.10 | 15.00 |
| SHORTSEA_MUN_C35_V7_HE_5 | 3948107.09 | 3972851.98 | 4071831.53 | 0.49 | 3784395.57 | 3785760.94 | 3791222.40 | 15.01 |
| SHORTSEA_MUN_C60_V13_HE_1 | 5878462.82 | 5931487.16 | 6013883.84 | 2.15 | 5215454.63 | 5238052.37 | 5259528.81 | 15.01 |
| SHORTSEA_MUN_C60_V13_HE_2 | 5443824.51 | 5455773.94 | 5465467.71 | 1.46 | 5127323.74 | 5182831.13 | 5217151.58 | 15.01 |
| SHORTSEA_MUN_C60_V13_HE_3 | 5452079.49 | 5488967.76 | 5533449.95 | 1.17 | 5019760.25 | 5046927.42 | 5072193.44 | 15.01 |
| SHORTSEA_MUN_C60_V13_HE_4 | 5731275.00 | 5795704.64 | 5858906.54 | 1.52 | 5282856.73 | 5371580.08 | 5433885.93 | 15.01 |
| SHORTSEA_MUN_C60_V13_HE_5 | 6225939.75 | 6246595.37 | 6284144.48 | 1.34 | 5578731.95 | 5649159.65 | 5720349.85 | 15.01 |
| SHORTSEA_MUN_C80_V20_HE_1 | 7228373.81 | 7244876.99 | 7253636.86 | 4.30 | 6940586.81 | 6966300.27 | 6980802.69 | 15.02 |
| SHORTSEA_MUN_C80_V20_HE_2 | 7183394.16 | 7232755.78 | 7271518.85 | 2.92 | 6768752.10 | 6798215.54 | 6847424.25 | 15.01 |
| SHORTSEA_MUN_C80_V20_HE_3 | 6917293.24 | 6937672.81 | 6961280.12 | 3.18 | 6492245.30 | 6541928.66 | 6560944.44 | 15.02 |
| SHORTSEA_MUN_C80_V20_HE_4 | 7907856.07 | 7932345.80 | 7962844.62 | 4.82 | 7516349.11 | 7604514.61 | 7674188.88 | 15.02 |
| SHORTSEA_MUN_C80_V20_HE_5 | 7543369.26 | 7606816.98 | 7653860.95 | 2.86 | 7003010.40 | 7117798.41 | 7258518.33 | 15.02 |
| SHORTSEA_MUN_C100_V30_HE_1 | 8691100.26 | 8716776.36 | 8730091.34 | 4.88 | 8370664.81 | 8381207.09 | 8398292.36 | 15.02 |
| SHORTSEA_MUN_C100_V30_HE_2 | 8802114.22 | 8824225.24 | 8849771.38 | 6.20 | 8446069.29 | 8472523.45 | 8496617.38 | 15.03 |
| SHORTSEA_MUN_C100_V30_HE_3 | 8355857.03 | 8392497.32 | 8409510.95 | 5.01 | 8052665.81 | 8068517.26 | 8084067.25 | 15.02 |
| SHORTSEA_MUN_C100_V30_HE_4 | 9190265.76 | 9218754.67 | 9249184.86 | 5.58 | 8648990.22 | 8689451.73 | 8728988.09 | 15.03 |
| SHORTSEA_MUN_C100_V30_HE_5 | 9282359.56 | 9321631.10 | 9364275.66 | 7.12 | 8527892.14 | 8551541.91 | 8588877.18 | 15.02 |
| SHORTSEA_MUN_C130_V40_HE_1 | 11410905.75 | 11472383.86 | 11566286.06 | 12.31 | 10767542.03 | 10827154.34 | 10856536.82 | 15.03 |
| SHORTSEA_MUN_C130_V40_HE_2 | 11176148.40 | 11239199.31 | 11321575.82 | 13.24 | 10871479.48 | 10911573.10 | 10941996.75 | 15.03 |
| SHORTSEA_MUN_C130_V40_HE_3 | 10943790.59 | 11086803.90 | 11208710.22 | 11.86 | 10535719.46 | 10548431.55 | 10563372.19 | 15.03 |
| SHORTSEA_MUN_C130_V40_HE_4 | 11615173.88 | 11657419.93 | 11765598.40 | 11.97 | 11028948.45 | 11041212.77 | 11054915.45 | 15.03 |
| SHORTSEA_MUN_C130_V40_HE_5 | 13574003.55 | 13636707.83 | 13709064.75 | 13.05 | 12915656.69 | 13083062.16 | 13242595.59 | 15.04 |

Table A.10: Full results on ITSRSPSO SS_FUN instances.

| | HGS-O | | | | HGS-J | | | |
|---|---|---|---|---|---|---|---|---|
| Instance | Best | Avg | Worst | T | Best | Avg | Worst | T |
| SHORTSEA_FUN_C8_V3_HE_1 | 1013289.87 | 1013289.87 | 1013289.87 | 0.01 | 973478.67 | 973478.67 | 973478.67 | 0.53 |
| SHORTSEA_FUN_C8_V3_HE_2 | 1000249.54 | 1000249.54 | 1000249.54 | 0.01 | 914798.06 | 914798.06 | 914798.06 | 0.31 |
| SHORTSEA_FUN_C8_V3_HE_3 | 1300323.30 | 1300323.30 | 1300323.30 | 0.01 | 1289904.93 | 1289904.93 | 1289904.93 | 0.34 |
| SHORTSEA_FUN_C8_V3_HE_4 | 1232379.84 | 1232379.84 | 1232379.84 | 0.01 | 1224374.01 | 1224374.01 | 1224374.01 | 0.58 |
| SHORTSEA_FUN_C8_V3_HE_5 | 1173813.43 | 1173813.43 | 1173813.43 | 0.01 | 1125733.15 | 1125733.15 | 1125733.15 | 0.52 |
| SHORTSEA_FUN_C11_V4_HE_1 | 846368.79 | 846368.79 | 846368.79 | 0.02 | 758817.86 | 758817.86 | 758817.86 | 1.10 |
| SHORTSEA_FUN_C11_V4_HE_2 | 823461.48 | 823461.48 | 823461.48 | 0.02 | 723187.10 | 723187.10 | 723187.10 | 1.19 |
| SHORTSEA_FUN_C11_V4_HE_3 | 855242.11 | 855242.11 | 855242.11 | 0.02 | 806121.58 | 806121.58 | 806121.58 | 1.17 |
| SHORTSEA_FUN_C11_V4_HE_4 | 845851.45 | 845851.45 | 845851.45 | 0.02 | 748443.91 | 748443.91 | 748443.91 | 1.01 |
| SHORTSEA_FUN_C11_V4_HE_5 | 976626.47 | 976626.47 | 976626.47 | 0.02 | 957044.76 | 957044.76 | 957044.76 | 1.52 |
| SHORTSEA_FUN_C13_V5_HE_1 | 1264843.54 | 1264843.54 | 1264843.54 | 0.02 | 1241876.60 | 1241876.60 | 1241876.60 | 1.46 |
| SHORTSEA_FUN_C13_V5_HE_2 | 1374567.90 | 1374567.90 | 1374567.90 | 0.03 | 1221025.27 | 1221025.27 | 1221025.27 | 1.48 |
| SHORTSEA_FUN_C13_V5_HE_3 | 1492717.07 | 1510461.57 | 1529961.66 | 0.03 | 1411874.93 | 1411874.93 | 1411874.93 | 1.56 |
| SHORTSEA_FUN_C13_V5_HE_4 | 1941350.40 | 1946564.64 | 1967421.62 | 0.03 | 1864784.67 | 1864784.67 | 1864784.67 | 1.52 |
| SHORTSEA_FUN_C13_V5_HE_5 | 2247100.91 | 2254073.99 | 2281966.33 | 0.03 | 2097682.01 | 2097682.01 | 2097682.01 | 1.04 |
| SHORTSEA_FUN_C16_V6_HE_1 | 2520852.41 | 2521742.57 | 2522336.01 | 0.04 | 2432112.71 | 2432112.71 | 2432112.71 | 1.53 |
| SHORTSEA_FUN_C16_V6_HE_2 | 2402558.15 | 2402558.15 | 2402558.15 | 0.04 | 2345680.37 | 2345680.37 | 2345680.37 | 2.32 |
| SHORTSEA_FUN_C16_V6_HE_3 | 2715354.36 | 2748771.74 | 2757126.08 | 0.04 | 2544664.54 | 2544664.54 | 2544664.54 | 2.58 |
| SHORTSEA_FUN_C16_V6_HE_4 | 2311830.40 | 2311830.40 | 2311830.40 | 0.04 | 2172664.53 | 2172664.53 | 2172664.53 | 2.21 |
| SHORTSEA_FUN_C16_V6_HE_5 | 2144846.58 | 2144846.58 | 2144846.58 | 0.04 | 2070448.97 | 2070448.97 | 2070448.97 | 2.08 |
| SHORTSEA_FUN_C17_V13_HE_1 | 1484383.43 | 1509429.37 | 1526126.66 | 0.06 | 1418052.45 | 1418052.45 | 1418052.45 | 1.26 |
| SHORTSEA_FUN_C17_V13_HE_2 | 2101437.31 | 2115572.82 | 2147307.15 | 0.06 | 2068527.68 | 2068527.68 | 2068527.68 | 1.51 |
| SHORTSEA_FUN_C17_V13_HE_3 | 1652308.55 | 1653046.50 | 1655998.31 | 0.05 | 1548716.17 | 1548716.17 | 1548716.17 | 1.72 |
| SHORTSEA_FUN_C17_V13_HE_4 | 1778348.98 | 1799932.55 | 1832569.03 | 0.05 | 1562165.70 | 1562165.70 | 1562165.70 | 2.40 |
| SHORTSEA_FUN_C17_V13_HE_5 | 2041369.29 | 2041369.29 | 2041369.29 | 0.06 | 1971929.46 | 1971929.46 | 1971929.46 | 1.35 |
| SHORTSEA_FUN_C20_V6_HE_1 | 2176655.70 | 2176655.70 | 2176655.70 | 0.05 | 1856108.50 | 1856108.50 | 1856108.50 | 4.06 |
| SHORTSEA_FUN_C20_V6_HE_2 | 2226828.87 | 2234747.95 | 2246626.56 | 0.06 | 1973277.96 | 1973277.96 | 1973277.96 | 4.63 |
| SHORTSEA_FUN_C20_V6_HE_3 | 2130394.19 | 2139900.95 | 2154161.10 | 0.05 | 1962909.07 | 1962909.07 | 1962909.07 | 5.43 |
| SHORTSEA_FUN_C20_V6_HE_4 | 2045942.46 | 2069750.50 | 2089906.33 | 0.05 | 1942215.44 | 1942215.44 | 1942215.44 | 5.11 |
| SHORTSEA_FUN_C20_V6_HE_5 | 2002612.98 | 2063346.18 | 2092530.58 | 0.05 | 1886265.64 | 1886265.64 | 1886265.64 | 3.51 |
| SHORTSEA_FUN_C25_V7_HE_1 | 2664460.06 | 2686684.32 | 2710395.16 | 0.07 | 2527108.03 | 2527108.03 | 2527108.03 | 7.63 |
| SHORTSEA_FUN_C25_V7_HE_2 | 2358286.89 | 2364818.22 | 2369172.44 | 0.07 | 2241254.72 | 2241254.72 | 2241254.72 | 7.80 |
| SHORTSEA_FUN_C25_V7_HE_3 | 2847843.27 | 2856833.10 | 2875043.61 | 0.08 | 2582543.73 | 2582543.73 | 2582543.73 | 7.22 |
| SHORTSEA_FUN_C25_V7_HE_4 | 2832202.83 | 2839502.66 | 2863351.15 | 0.09 | 2611673.70 | 2611673.70 | 2611673.70 | 9.79 |
| SHORTSEA_FUN_C25_V7_HE_5 | 2807022.62 | 2821260.57 | 2831948.04 | 0.09 | 2469514.09 | 2469514.09 | 2469514.09 | 8.40 |
| SHORTSEA_FUN_C35_V13_HE_1 | 2200360.92 | 2207006.45 | 2221151.82 | 0.16 | 2092392.83 | 2092392.83 | 2092392.83 | 14.08 |
| SHORTSEA_FUN_C35_V13_HE_2 | 2279906.46 | 2315559.33 | 2355640.32 | 0.22 | 2111122.32 | 2111122.32 | 2111122.32 | 15.06 |
| SHORTSEA_FUN_C35_V13_HE_3 | 2536809.15 | 2543970.57 | 2545760.93 | 0.22 | 2234685.10 | 2234685.10 | 2234685.10 | 15.00 |
| SHORTSEA_FUN_C35_V13_HE_4 | 3291681.46 | 3295385.33 | 3298136.24 | 0.23 | 3077623.47 | 3077623.47 | 3077623.47 | 14.52 |
| SHORTSEA_FUN_C35_V13_HE_5 | 2434970.93 | 2447699.44 | 2461520.01 | 0.21 | 2231281.65 | 2231281.65 | 2231281.65 | 14.29 |
| SHORTSEA_FUN_C50_V20_HE_1 | 4959478.95 | 4999437.15 | 5032759.81 | 0.52 | 4502621.25 | 4502621.25 | 4502621.25 | 15.00 |
| SHORTSEA_FUN_C50_V20_HE_2 | 4990335.19 | 5070756.86 | 5110144.29 | 0.55 | 4564505.62 | 4564745.17 | 4565609.84 | 15.00 |
| SHORTSEA_FUN_C50_V20_HE_3 | 4693164.11 | 4721783.05 | 4743111.04 | 0.59 | 4351682.23 | 4351682.23 | 4351682.23 | 15.10 |
| SHORTSEA_FUN_C50_V20_HE_4 | 6458898.80 | 6483047.13 | 6500138.52 | 0.59 | 5876803.03 | 5876803.03 | 5876803.03 | 15.08 |
| SHORTSEA_FUN_C50_V20_HE_5 | 5149788.77 | 5161885.27 | 5170384.62 | 0.52 | 4527908.94 | 4527908.94 | 4527908.94 | 15.01 |
| SHORTSEA_FUN_C70_V30_HE_1 | 6922089.49 | 6942086.49 | 6972014.05 | 1.36 | 6233127.33 | 6250942.88 | 6278152.90 | 15.01 |
| SHORTSEA_FUN_C70_V30_HE_2 | 7067457.12 | 7093249.37 | 7124892.98 | 1.47 | 6464719.94 | 6483800.13 | 6522069.90 | 15.01 |
| SHORTSEA_FUN_C70_V30_HE_3 | 6778673.86 | 6790545.00 | 6796925.13 | 1.61 | 6483064.25 | 6551648.95 | 6655441.64 | 15.01 |
| SHORTSEA_FUN_C70_V30_HE_4 | 7940062.91 | 7985227.79 | 8005660.04 | 1.23 | 6553797.05 | 6581736.08 | 6633379.10 | 15.01 |
| SHORTSEA_FUN_C70_V30_HE_5 | 7882155.82 | 7919219.25 | 7949740.66 | 1.49 | 6801570.31 | 6905173.32 | 7019870.11 | 15.01 |
| SHORTSEA_FUN_C90_V40_HE_1 | 9418198.92 | 9447534.34 | 9497374.31 | 2.71 | 8496852.28 | 8518492.33 | 8528574.21 | 15.02 |
| SHORTSEA_FUN_C90_V40_HE_2 | 9057498.26 | 9135539.33 | 9221395.46 | 2.63 | 8537822.35 | 8557264.25 | 8589997.87 | 15.01 |
| SHORTSEA_FUN_C90_V40_HE_3 | 9041295.16 | 9078245.42 | 9099256.84 | 2.83 | 7996465.96 | 8013130.22 | 8031810.71 | 15.01 |
| SHORTSEA_FUN_C90_V40_HE_4 | 10601100.81 | 10676039.78 | 10739927.11 | 2.95 | 9171325.93 | 9196158.20 | 9219990.44 | 15.01 |
| SHORTSEA_FUN_C90_V40_HE_5 | 9695996.12 | 9757978.89 | 9803165.26 | 2.80 | 8379441.43 | 8414307.00 | 8497138.05 | 15.01 |
| SHORTSEA_FUN_C100_V50_HE_1 | 9487678.62 | 9547498.68 | 9597817.06 | 3.97 | 8506548.72 | 8517760.95 | 8529036.29 | 15.01 |
| SHORTSEA_FUN_C100_V50_HE_2 | 10031729.20 | 10105446.30 | 10150788.35 | 3.81 | 8808023.39 | 8812980.50 | 8816819.45 | 15.02 |
| SHORTSEA_FUN_C100_V50_HE_3 | 9218124.18 | 9233991.02 | 9264852.02 | 3.66 | 8206895.30 | 8232574.42 | 8244493.73 | 15.01 |
| SHORTSEA_FUN_C100_V50_HE_4 | 10954492.57 | 10988571.45 | 11016373.07 | 3.56 | 8846071.93 | 8848678.06 | 8852706.66 | 15.01 |
| SHORTSEA_FUN_C100_V50_HE_5 | 10387434.04 | 10471780.86 | 10504360.80 | 3.66 | 8528096.62 | 8532430.54 | 8535903.75 | 15.01 |

Table A.11: Full results on ITSRSPSO DS_MUN instances.

| | HGS-O | | | | HGS-J | | | |
|---|---|---|---|---|---|---|---|---|
| Instance | Best | Avg | Worst | T | Best | Avg | Worst | T |
| DEEPSEA_MUN_C7_V3_HE_1 | 2832934.98 | 2837032.14 | 2843177.89 | 0.02 | 2796403.09 | 2796403.09 | 2796403.09 | 0.45 |
| DEEPSEA_MUN_C7_V3_HE_2 | 4343563.68 | 4343653.89 | 4343714.03 | 0.02 | 3791332.21 | 3791332.21 | 3791332.21 | 0.38 |
| DEEPSEA_MUN_C7_V3_HE_3 | 3959304.61 | 3971245.72 | 4019010.17 | 0.02 | 3907563.40 | 3907563.40 | 3907563.40 | 0.34 |
| DEEPSEA_MUN_C7_V3_HE_4 | 5419785.44 | 5420140.97 | 5420674.27 | 0.02 | 5380211.76 | 5380211.76 | 5380211.76 | 0.26 |
| DEEPSEA_MUN_C7_V3_HE_5 | 5433367.64 | 5433367.64 | 5433367.64 | 0.02 | 5318116.07 | 5318116.07 | 5318116.07 | 0.50 |
| DEEPSEA_MUN_C10_V3_HE_1 | 5329474.38 | 5332256.50 | 5336429.69 | 0.03 | 4837524.52 | 4837524.52 | 4837524.52 | 0.64 |
| DEEPSEA_MUN_C10_V3_HE_2 | 6025309.09 | 6033663.43 | 6046194.94 | 0.03 | 5857393.84 | 5857393.84 | 5857393.84 | 0.79 |
| DEEPSEA_MUN_C10_V3_HE_3 | 6862470.07 | 6862470.07 | 6862470.07 | 0.03 | 6700231.77 | 6700231.77 | 6700231.77 | 0.79 |
| DEEPSEA_MUN_C10_V3_HE_4 | 6879770.41 | 6891105.48 | 6893939.25 | 0.03 | 6729034.59 | 6729034.59 | 6729034.59 | 1.14 |
| DEEPSEA_MUN_C10_V3_HE_5 | 6434613.79 | 6436406.76 | 6443578.63 | 0.03 | 5925542.44 | 5925542.44 | 5925542.44 | 1.16 |
| DEEPSEA_MUN_C15_V4_HE_1 | 9928441.28 | 9933383.12 | 9940795.88 | 0.06 | 9556020.40 | 9556020.40 | 9556020.40 | 4.02 |
| DEEPSEA_MUN_C15_V4_HE_2 | 8499671.69 | 8505419.18 | 8522950.50 | 0.08 | 7261934.50 | 7261934.50 | 7261934.50 | 3.92 |
| DEEPSEA_MUN_C15_V4_HE_3 | 9459347.46 | 9459347.46 | 9459347.46 | 0.06 | 8935752.07 | 8935752.07 | 8935752.07 | 4.01 |
| DEEPSEA_MUN_C15_V4_HE_4 | 8116517.31 | 8119594.79 | 8124211.01 | 0.08 | 7815187.29 | 7815187.29 | 7815187.29 | 3.87 |
| DEEPSEA_MUN_C15_V4_HE_5 | 6986863.91 | 6990466.94 | 6995871.48 | 0.07 | 6451325.93 | 6451325.93 | 6451325.93 | 3.49 |
| DEEPSEA_MUN_C18_V5_HE_1 | 20861231.57 | 20865349.92 | 20881823.33 | 0.10 | 20397321.43 | 20397321.43 | 20397321.43 | 6.42 |
| DEEPSEA_MUN_C18_V5_HE_2 | 8622981.65 | 8624615.10 | 8625023.46 | 0.13 | 8524460.98 | 8524460.98 | 8524460.98 | 6.94 |
| DEEPSEA_MUN_C18_V5_HE_3 | 10534483.76 | 10534483.76 | 10534483.76 | 0.10 | 9598514.21 | 9598514.21 | 9598514.21 | 5.29 |
| DEEPSEA_MUN_C18_V5_HE_4 | 14338840.21 | 14341301.93 | 14344994.50 | 0.10 | 12172843.29 | 12172843.29 | 12172843.29 | 5.26 |
| DEEPSEA_MUN_C18_V5_HE_5 | 22799028.03 | 22805607.35 | 22809993.56 | 0.10 | 19109452.90 | 19109452.90 | 19109452.90 | 5.59 |
| DEEPSEA_MUN_C22_V6_HE_1 | 36556153.73 | 36567936.81 | 36615069.12 | 0.15 | 30899720.75 | 30899720.75 | 30899720.75 | 8.22 |
| DEEPSEA_MUN_C22_V6_HE_2 | 30286683.75 | 30291516.69 | 30300260.04 | 0.14 | 26662969.12 | 26662969.12 | 26662969.12 | 7.66 |
| DEEPSEA_MUN_C22_V6_HE_3 | 32898441.97 | 33054543.27 | 33111467.28 | 0.16 | 24188291.48 | 24188291.48 | 24188291.48 | 7.83 |
| DEEPSEA_MUN_C22_V6_HE_4 | 27576546.47 | 27658465.68 | 27794203.77 | 0.16 | 24883538.36 | 24883538.36 | 24883538.36 | 12.32 |
| DEEPSEA_MUN_C22_V6_HE_5 | 35778633.14 | 35778633.14 | 35778633.14 | 0.17 | 33173180.68 | 33173180.68 | 33173180.68 | 9.39 |
| DEEPSEA_MUN_C23_V13_HE_1 | 31816765.90 | 32018195.88 | 32144681.38 | 0.18 | 28622900.41 | 28622900.41 | 28622900.41 | 3.48 |
| DEEPSEA_MUN_C23_V13_HE_2 | 19402202.24 | 19427239.32 | 19441961.05 | 0.21 | 17646501.30 | 17646501.30 | 17646501.30 | 7.40 |
| DEEPSEA_MUN_C23_V13_HE_3 | 17807535.83 | 17809510.87 | 17810827.57 | 0.16 | 17081323.45 | 17081323.45 | 17081323.45 | 4.76 |
| DEEPSEA_MUN_C23_V13_HE_4 | 24119863.21 | 24415740.53 | 24612992.08 | 0.22 | 19896624.07 | 19896624.07 | 19896624.07 | 5.25 |
| DEEPSEA_MUN_C23_V13_HE_5 | 26285987.03 | 26285987.03 | 26285987.03 | 0.16 | 23880887.01 | 23880887.01 | 23880887.01 | 5.98 |
| DEEPSEA_MUN_C30_V6_HE_1 | 13192750.87 | 13411379.10 | 13735707.64 | 0.22 | 11545020.82 | 11545020.82 | 11545020.82 | 15.04 |
| DEEPSEA_MUN_C30_V6_HE_2 | 11853569.65 | 11880631.49 | 11916539.42 | 0.30 | 10562790.91 | 10583661.56 | 10667144.15 | 15.12 |
| DEEPSEA_MUN_C30_V6_HE_3 | 15520766.33 | 15520766.33 | 15520766.33 | 0.28 | 14401537.42 | 14401537.42 | 14401537.42 | 15.00 |
| DEEPSEA_MUN_C30_V6_HE_4 | 15122149.17 | 15443682.33 | 15664433.86 | 0.26 | 12523728.83 | 12523728.83 | 12523728.83 | 15.00 |
| DEEPSEA_MUN_C30_V6_HE_5 | 17865635.85 | 17871757.09 | 17888381.21 | 0.29 | 17130423.34 | 17158645.50 | 17200978.74 | 15.13 |
| DEEPSEA_MUN_C35_V7_HE_1 | 41120911.34 | 41453693.45 | 41936142.87 | 0.40 | 39110149.15 | 39187684.61 | 39497826.46 | 15.01 |
| DEEPSEA_MUN_C35_V7_HE_2 | 36730160.86 | 36770874.11 | 36798016.27 | 0.38 | 32997272.90 | 33674825.87 | 33967631.63 | 15.00 |
| DEEPSEA_MUN_C35_V7_HE_3 | 37198284.64 | 37474462.10 | 37560042.28 | 0.39 | 36024002.98 | 36142317.79 | 36615577.01 | 15.01 |
| DEEPSEA_MUN_C35_V7_HE_4 | 41887364.89 | 42072301.94 | 42208105.88 | 0.39 | 36177521.34 | 36313285.78 | 36612779.43 | 15.01 |
| DEEPSEA_MUN_C35_V7_HE_5 | 42408663.93 | 42451876.38 | 42570002.50 | 0.29 | 38869404.09 | 39057832.16 | 39811544.43 | 15.00 |
| DEEPSEA_MUN_C60_V13_HE_1 | 57788220.34 | 58059969.50 | 58380187.51 | 2.20 | 55344983.98 | 55996020.49 | 56639990.39 | 15.03 |
| DEEPSEA_MUN_C60_V13_HE_2 | 52606575.13 | 52705610.26 | 52812781.57 | 1.28 | 49163913.78 | 49947632.96 | 50567023.14 | 15.03 |
| DEEPSEA_MUN_C60_V13_HE_3 | 66271207.88 | 66682884.54 | 67257653.16 | 1.40 | 57034176.35 | 58199470.04 | 59761093.98 | 15.02 |
| DEEPSEA_MUN_C60_V13_HE_4 | 66808214.00 | 66986290.33 | 67159088.18 | 1.60 | 60354499.70 | 62698383.07 | 64274583.20 | 15.02 |
| DEEPSEA_MUN_C60_V13_HE_5 | 68076353.64 | 68816238.94 | 71604688.80 | 1.63 | 65084662.89 | 65905176.95 | 67368482.75 | 15.03 |
| DEEPSEA_MUN_C80_V20_HE_1 | 88731911.69 | 89499990.91 | 90097013.44 | 3.76 | 80853704.69 | 81918794.69 | 83193236.49 | 15.02 |
| DEEPSEA_MUN_C80_V20_HE_2 | 89415537.11 | 91843621.09 | 94471756.56 | 5.85 | 74673119.13 | 75673065.80 | 76664095.35 | 15.02 |
| DEEPSEA_MUN_C80_V20_HE_3 | 95689409.99 | 98072618.73 | 99353638.44 | 3.33 | 84216362.73 | 85548557.28 | 86445952.57 | 15.01 |
| DEEPSEA_MUN_C80_V20_HE_4 | 91546061.61 | 94373568.12 | 97370988.15 | 2.08 | 82647679.72 | 83723994.02 | 84633747.02 | 15.01 |
| DEEPSEA_MUN_C80_V20_HE_5 | 100242467.77 | 100651999.05 | 100857270.25 | 2.67 | 78081248.74 | 79502070.84 | 80795403.87 | 15.01 |
| DEEPSEA_MUN_C100_V30_HE_1 | 100967995.27 | 103497858.13 | 105170530.57 | 8.24 | 87494720.89 | 88677707.26 | 89500878.47 | 15.03 |
| DEEPSEA_MUN_C100_V30_HE_2 | 107732715.23 | 107966781.37 | 108454325.09 | 8.57 | 92825444.90 | 93326242.30 | 94079234.97 | 15.03 |
| DEEPSEA_MUN_C100_V30_HE_3 | 101893212.69 | 102036471.57 | 102169144.54 | 8.29 | 89011667.61 | 90576660.31 | 92795125.32 | 15.04 |
| DEEPSEA_MUN_C100_V30_HE_4 | 103325308.70 | 104373270.20 | 105588295.97 | 7.97 | 95812819.93 | 96578411.48 | 97982469.21 | 15.02 |
| DEEPSEA_MUN_C100_V30_HE_5 | 103828287.57 | 104070943.93 | 104563902.77 | 8.74 | 95707451.07 | 96429315.55 | 97842987.40 | 15.04 |
| DEEPSEA_MUN_C130_V40_HE_1 | 81394029.76 | 82263721.18 | 83176959.82 | 15.08 | 85810122.92 | 89150385.88 | 92330083.81 | 15.10 |
| DEEPSEA_MUN_C130_V40_HE_2 | 76417396.46 | 77244364.56 | 78908852.60 | 15.00 | 79391700.04 | 80317914.50 | 81728734.24 | 15.03 |
| DEEPSEA_MUN_C130_V40_HE_3 | 82243158.53 | 83086879.83 | 83811672.90 | 15.00 | 89057313.32 | 91532007.87 | 95685020.58 | 15.05 |
| DEEPSEA_MUN_C130_V40_HE_4 | 61769933.71 | 62234530.43 | 62859635.41 | 15.01 | 69758667.83 | 73609751.57 | 76665599.06 | 15.06 |
| DEEPSEA_MUN_C130_V40_HE_5 | 80097964.48 | 80840382.64 | 83149927.99 | 15.30 | 90786248.30 | 94424777.94 | 98578728.72 | 15.06 |

Table A.12: Full results on ITSRSPSO DS_FUN instances.

| | HGS-O | | | | HGS-J | | | |
|---|---|---|---|---|---|---|---|---|
| Instance | Best | Avg | Worst | T | Best | Avg | Worst | T |
| DEEPSEA_FUN_C8_V3_HE_1 | 7053629.77 | 7053629.77 | 7053629.77 | 0.01 | 5176264.79 | 5176264.79 | 5176264.79 | 0.55 |
| DEEPSEA_FUN_C8_V3_HE_2 | 7633883.10 | 7633883.10 | 7633883.10 | 0.01 | 7411131.41 | 7411131.41 | 7411131.41 | 0.40 |
| DEEPSEA_FUN_C8_V3_HE_3 | 2603121.04 | 2603121.04 | 2603121.04 | 0.01 | 2603121.04 | 2603121.04 | 2603121.04 | 0.27 |
| DEEPSEA_FUN_C8_V3_HE_4 | 5608794.59 | 5608794.59 | 5608794.59 | 0.01 | 5468590.60 | 5468590.60 | 5468590.60 | 0.72 |
| DEEPSEA_FUN_C8_V3_HE_5 | 4715457.02 | 4715457.02 | 4715457.02 | 0.01 | 4633069.90 | 4633069.90 | 4633069.90 | 0.85 |
| DEEPSEA_FUN_C11_V4_HE_1 | 20239020.95 | 20239020.95 | 20239020.95 | 0.02 | 20239020.95 | 20239020.95 | 20239020.95 | 0.74 |
| DEEPSEA_FUN_C11_V4_HE_2 | 12208695.13 | 12208695.13 | 12208695.13 | 0.02 | 11874556.52 | 11874556.52 | 11874556.52 | 1.50 |
| DEEPSEA_FUN_C11_V4_HE_3 | 13026718.56 | 13026718.56 | 13026718.56 | 0.02 | 13026718.56 | 13026718.56 | 13026718.56 | 1.19 |
| DEEPSEA_FUN_C11_V4_HE_4 | 16582971.92 | 16582971.92 | 16582971.92 | 0.02 | 11270464.22 | 11270464.22 | 11270464.22 | 0.93 |
| DEEPSEA_FUN_C11_V4_HE_5 | 14498736.72 | 14498736.72 | 14498736.72 | 0.02 | 11408712.87 | 11408712.87 | 11408712.87 | 1.45 |
| DEEPSEA_FUN_C13_V5_HE_1 | 8039849.57 | 8039849.57 | 8039849.57 | 0.03 | 7953555.54 | 7953555.54 | 7953555.54 | 1.93 |
| DEEPSEA_FUN_C13_V5_HE_2 | 8435738.12 | 8435738.12 | 8435738.12 | 0.03 | 8232260.88 | 8232260.88 | 8232260.88 | 1.44 |
| DEEPSEA_FUN_C13_V5_HE_3 | 7136618.66 | 7136618.66 | 7136618.66 | 0.03 | 6856436.04 | 6856436.04 | 6856436.04 | 1.87 |
| DEEPSEA_FUN_C13_V5_HE_4 | 9741715.84 | 9741715.84 | 9741715.84 | 0.03 | 9286602.75 | 9286602.75 | 9286602.75 | 1.33 |
| DEEPSEA_FUN_C13_V5_HE_5 | 6793423.45 | 6825675.34 | 6874053.17 | 0.02 | 6689508.72 | 6689508.72 | 6689508.72 | 1.55 |
| DEEPSEA_FUN_C16_V6_HE_1 | 29871927.48 | 29871927.48 | 29871927.48 | 0.04 | 24627424.31 | 24627424.31 | 24627424.31 | 2.61 |
| DEEPSEA_FUN_C16_V6_HE_2 | 18846052.77 | 18846052.77 | 18846052.77 | 0.04 | 18374891.10 | 18374891.10 | 18374891.10 | 3.12 |
| DEEPSEA_FUN_C16_V6_HE_3 | 25639454.55 | 25651324.60 | 25659237.97 | 0.04 | 19778140.50 | 19778140.50 | 19778140.50 | 2.26 |
| DEEPSEA_FUN_C16_V6_HE_4 | 12020651.76 | 12115488.93 | 12200672.06 | 0.04 | 11601030.22 | 11601030.22 | 11601030.22 | 2.33 |
| DEEPSEA_FUN_C16_V6_HE_5 | 18186300.47 | 18186300.47 | 18186300.47 | 0.04 | 17184445.98 | 17184445.98 | 17184445.98 | 2.59 |
| DEEPSEA_FUN_C17_V13_HE_1 | 14178294.59 | 14178294.59 | 14178294.59 | 0.06 | 13222105.46 | 13222105.46 | 13222105.46 | 1.77 |
| DEEPSEA_FUN_C17_V13_HE_2 | 7072317.27 | 7072546.78 | 7073464.81 | 0.05 | 6115054.90 | 6115054.90 | 6115054.90 | 2.03 |
| DEEPSEA_FUN_C17_V13_HE_3 | 8511082.46 | 8535559.27 | 8551877.14 | 0.05 | 7371359.05 | 7371359.05 | 7371359.05 | 2.00 |
| DEEPSEA_FUN_C17_V13_HE_4 | 7565230.47 | 7573754.57 | 7586540.71 | 0.06 | 6978841.51 | 6978841.51 | 6978841.51 | 1.79 |
| DEEPSEA_FUN_C17_V13_HE_5 | 8228314.78 | 8335527.39 | 8365885.37 | 0.06 | 7675819.79 | 7675819.79 | 7675819.79 | 2.76 |
| DEEPSEA_FUN_C20_V6_HE_1 | 12334463.96 | 12338383.33 | 12344262.39 | 0.05 | 10726291.11 | 10726291.11 | 10726291.11 | 4.09 |
| DEEPSEA_FUN_C20_V6_HE_2 | 11465951.24 | 11465951.24 | 11465951.24 | 0.06 | 10532603.30 | 10532603.30 | 10532603.30 | 4.97 |
| DEEPSEA_FUN_C20_V6_HE_3 | 13194245.08 | 13246779.68 | 13259913.33 | 0.05 | 12539855.50 | 12539855.50 | 12539855.50 | 5.09 |
| DEEPSEA_FUN_C20_V6_HE_4 | 11245339.50 | 11433961.14 | 11488426.10 | 0.05 | 10582247.98 | 10582247.98 | 10582247.98 | 6.57 |
| DEEPSEA_FUN_C20_V6_HE_5 | 13155920.32 | 13155920.32 | 13155920.32 | 0.06 | 11495942.21 | 11495942.21 | 11495942.21 | 4.42 |
| DEEPSEA_FUN_C25_V7_HE_1 | 16443589.66 | 16600861.22 | 16734299.10 | 0.08 | 14551679.99 | 14551679.99 | 14551679.99 | 8.51 |
| DEEPSEA_FUN_C25_V7_HE_2 | 14444533.33 | 14444533.33 | 14444533.33 | 0.08 | 13818829.77 | 13818829.77 | 13818829.77 | 10.15 |
| DEEPSEA_FUN_C25_V7_HE_3 | 12715248.95 | 13019002.95 | 13141212.27 | 0.08 | 11462608.41 | 11462608.41 | 11462608.41 | 7.33 |
| DEEPSEA_FUN_C25_V7_HE_4 | 15055615.59 | 15100939.54 | 15193891.95 | 0.08 | 13531763.52 | 13531763.52 | 13531763.52 | 11.25 |
| DEEPSEA_FUN_C25_V7_HE_5 | 17578324.75 | 17632385.27 | 17668425.61 | 0.08 | 16916916.83 | 16916916.83 | 16916916.83 | 12.05 |
| DEEPSEA_FUN_C35_V13_HE_1 | 34091943.46 | 34187730.92 | 34361554.67 | 0.24 | 32190876.48 | 32190876.48 | 32190876.48 | 15.00 |
| DEEPSEA_FUN_C35_V13_HE_2 | 34979535.48 | 34985948.91 | 34987552.27 | 0.29 | 32340250.02 | 32340250.02 | 32340250.02 | 15.00 |
| DEEPSEA_FUN_C35_V13_HE_3 | 36367935.91 | 36407859.64 | 36473267.83 | 0.26 | 31250194.55 | 31250194.55 | 31250194.55 | 15.00 |
| DEEPSEA_FUN_C35_V13_HE_4 | 38326874.77 | 38358190.68 | 38391696.40 | 0.26 | 34362295.26 | 34362295.26 | 34362295.26 | 15.21 |
| DEEPSEA_FUN_C35_V13_HE_5 | 38982034.94 | 38997536.90 | 39007871.54 | 0.24 | 36601759.93 | 36601759.93 | 36601759.93 | 15.05 |
| DEEPSEA_FUN_C50_V20_HE_1 | 31714106.40 | 31722174.05 | 31744213.40 | 0.65 | 26868909.98 | 26868909.98 | 26868909.98 | 15.19 |
| DEEPSEA_FUN_C50_V20_HE_2 | 29780153.21 | 29847181.62 | 29891070.44 | 0.61 | 24148564.29 | 24189961.67 | 24284477.25 | 15.00 |
| DEEPSEA_FUN_C50_V20_HE_3 | 30485469.66 | 30487184.25 | 30489756.13 | 0.61 | 25726501.72 | 25726501.72 | 25726501.72 | 15.00 |
| DEEPSEA_FUN_C50_V20_HE_4 | 32341061.45 | 32479423.06 | 32532799.55 | 0.65 | 27960578.46 | 27961127.15 | 27963321.90 | 15.01 |
| DEEPSEA_FUN_C50_V20_HE_5 | 31327248.97 | 31596551.41 | 31845446.44 | 0.62 | 27224627.19 | 27224627.19 | 27224627.19 | 15.01 |
| DEEPSEA_FUN_C70_V30_HE_1 | 96776778.48 | 96994180.55 | 97318603.01 | 1.62 | 84940529.78 | 85185022.67 | 85510551.59 | 15.01 |
| DEEPSEA_FUN_C70_V30_HE_2 | 101233577.26 | 101390265.72 | 101513036.32 | 1.55 | 78563704.63 | 79386397.42 | 80093285.14 | 15.01 |
| DEEPSEA_FUN_C70_V30_HE_3 | 119659725.92 | 120426620.47 | 120986171.23 | 1.46 | 104515448.02 | 104975140.31 | 105241833.49 | 15.01 |
| DEEPSEA_FUN_C70_V30_HE_4 | 120159116.50 | 120200867.22 | 120265334.01 | 1.44 | 98372657.52 | 98802378.04 | 99322610.04 | 15.01 |
| DEEPSEA_FUN_C70_V30_HE_5 | 116358602.13 | 116495270.59 | 116555689.96 | 1.32 | 92954769.67 | 93108353.19 | 93218243.17 | 15.01 |
| DEEPSEA_FUN_C90_V40_HE_1 | 135458583.60 | 136344656.25 | 136926558.29 | 3.55 | 113501619.49 | 114461536.19 | 115128848.64 | 15.03 |
| DEEPSEA_FUN_C90_V40_HE_2 | 139376523.52 | 139751577.58 | 140496167.11 | 3.17 | 122916831.37 | 123669276.57 | 124164156.64 | 15.01 |
| DEEPSEA_FUN_C90_V40_HE_3 | 158592379.92 | 158837939.94 | 158932796.87 | 3.41 | 139473007.91 | 140391743.60 | 141452184.68 | 15.01 |
| DEEPSEA_FUN_C90_V40_HE_4 | 163114981.16 | 163654646.82 | 163974917.73 | 2.77 | 133915724.73 | 134045556.85 | 134128397.72 | 15.01 |
| DEEPSEA_FUN_C90_V40_HE_5 | 146077540.41 | 146563253.47 | 146768867.44 | 3.27 | 124320546.16 | 125537789.39 | 126606396.12 | 15.02 |
| DEEPSEA_FUN_C100_V50_HE_1 | 149978246.96 | 150115446.68 | 150271245.82 | 4.54 | 123098500.67 | 124657435.94 | 125566932.64 | 15.03 |
| DEEPSEA_FUN_C100_V50_HE_2 | 149807415.88 | 150236003.32 | 151136510.96 | 4.78 | 129416636.97 | 130157542.63 | 130484081.45 | 15.02 |
| DEEPSEA_FUN_C100_V50_HE_3 | 161528601.40 | 161717042.37 | 161835645.19 | 4.42 | 133268424.23 | 133856208.44 | 134367773.97 | 15.03 |
| DEEPSEA_FUN_C100_V50_HE_4 | 166670427.42 | 167209515.85 | 167754655.36 | 4.19 | 133445916.93 | 133723245.09 | 134016416.15 | 15.02 |
| DEEPSEA_FUN_C100_V50_HE_5 | 166410544.91 | 166646811.27 | 166735760.17 | 4.22 | 144175327.73 | 144268272.80 | 144451106.78 | 15.02 |